AN EXPERIMENTAL STUDY OF THE SLOWING DOWN OF NEUTRONS IN SOME MODERATING MATERIALS

A Thesis Submitted for the
University of London for the Degree of
Doctor of Philosophy
in the
Faculty of Science

by

NASEER HAIDER
M.Sc., M.A.

Nuclear Power Group
Department of Mechanical Engineering
Imperial College of Science and Technology
London. S.W.7.

May 1975

ABSTRACT.

Neutron age determinations have been made in some materials and moderating conditions. The spatial distribution of the neutron resonance flux is measured by the change in the counting rate produced when a neutron sensitive scintillation counter is covered with an appropriate resonance neutron 'filter' for that energy. measurements in graphite are made to the indium resonance energy from different source energies. Details are given of the experiments and the technique of determining the ages of the fission neutrons in water to, indium, rhodium and gold resonances, using finite plane fission sources and essentially a point scintillation detector in conjunction with a resonance absorber. Evaluation for a point source is made by extrapolation, from the measured values obtained with different source sizes. Some details of the technique of analysis are provided. The results obtained with the present method agree well with the theoretical calculations and the best of the previous experimental age values measured with the foil-activation method. The ages of the fission neutrons to the indium resonance energy were also measured in water containing regular arrays of simulated cavities in the horizontal and the vertical directions, the diameter of the cavities and the dimensions of the cell of moderator round it, exceeds the mean free path of the neutrons in water. The results obtained are compared with the theoretical predictions of Behrens and Benoist.

ACKNOWLEDGEMENTS.

The author wishes to express his deep gratitude to his supervisor, Professor P.J. Grant, for his guidance, encouragement and intrest at every stage and throughout the couse of this research. The author is also grateful to him for many fruitful discussions and suggestions.

Many thanks, to the Technical Staff of the Nuclear Power Group for their assistance during the construction of the equipments, and to Miss E.M. Archer for her assistance in the library work.

The author also wishes to express his thanks to Mr. M. Kerridge, the Manager of the University of London Research Reactor and also to the entire staff there for their co-operation and kindness throughout the course of experiments, particularly in providing extra reactor time during the crucial stages of the experimental work.

It is with gratitude that the author acknowledges the support of the Scientific Research Council under the auspices of whom a major part of the present work was performed.

Finally, the author is very deeply grateful to his parents for their devotion and very generous financial

help for his education. Last but by no means least, a special thanks to his wife, Nusrat, for her devotion and patient understanding during this work.

DEDICATION.

The author wishes to dedicate this thesis to the loving memory of his father who died during the later stages of this research work.

TABLE OF CONTENTS.

LIST OF TABLES. Page

LIST OF FIGURES.

CHAPTER 1.

INTRODUCTION.

In a host of thermal reactors, graphite has been in use as a moderating material and a variety of reactors' use water as a coolant or as a moderator or both. It is therefore very much desirable that a sufficient amount of information may be available for these materials with a great degree of accuracy to facilitate improvements on the design of the reactors which may have a significant impact on the cost of the nuclear energy produced. The information sought, of the neutron interactions with the nuclei of the moderators, is the amount of energy a fast neutron loses in collision with these nuclei. A correct knowledge of the process of the slowing down of neutrons is important in establishing critical size of a reactor. Neutron age which is a measure of an average distance a neutron may travel from its emission as a fast neutron to its attainment of a lower energy approaching the thermal region, has attracted the attention of many scientists, both in its theory and the experimental determination of this parameter.

The theoretical calculation of neutron slowing down is a subject of considerable interest in view of its practical applications and the engineering importance

in reactor technology. With the improvements achieved in the performance of the various reactors, a detailed and more comprehensive knowledge of the spatial distribution of the slowing down neutron flux becomes necessary. The neutron age can be calculated by a number of methods, i.e., the Monte Carlo technique, the Fourier transformed Boltzmann equation and the moments method. In these rigorous solutions no physical assumptions or approximations are made to the Boltzmann transport equation. All these methods are briefly described in the second chapter along with some of the calculated results quoted for each.

The experimental determination of the neutron age is made by obtaining the spatial distribution of the slowing down flux of the required, (detector), low energy neutrons approaching the thermal region, about the source of fast neutrons. The most common method adopted has been by foil activation. This, however, suffers inherently from being an involved and cumbersome technique requiring a detailed inter-calibration of the foils if more than one are to be irradiated at the same time, and the effect of self-shielding has to be taken into account. In the present method, indium and also other resonance absorbers such as rhodium and gold have been used as resonance neutron filters in conjunction with a scintillation counter. The neutron flux measurements were made with and then without the resonance neutron filters using a neutron sensitive

scintillation counter protected from the thermal neutrons by a cadmium covering. The difference of the two fluxes result in the resonance neutron fluxes appropriate to the absorbers in use. The indium and rhodium resonances being conveniently close to the thermal region, are ideally suited for such measurements, gold being useful as well.

The neutron age determinations in the present case comprise three series. These are in reactor grade graphite, in demineralised water, and also in water moderator containing regular arrays of cylindrical voids simulated by immersing perspex tubes, in the horizontal (transverse) and the vertical (axial) directions.

When fast neutrons are emitted from a source in a moderator having an atomic weight much larger than that of the neutron, the slowing down occurs in such a way as to give the spatial distribution of the low energy neutrons which is approximately Gaussian. The slowing down process in such moderators being very gradual and continuous, the Fermi age solution is applicable. Placzek (R.3.3), and Marshak (R.3.4) obtained theoretically the next approximation to the spatial distribution taking into account the higher moments of this distribution. The equation (3.3.E9) which is a point source expression incorporating the above mentioned approximation, was further modified for the age evaluation, to equation (4.4.E1)

to carry out integration over the source and the detector geometries. In the case of a lighter hydrogenous moderator like water, for example, the above treatment of age is not applicable as in hydrogen, $\alpha = 0$, gives rise to quite a large average change of energy of a neutron in a single collision. The age evaluation in water involves the determination of the mean square slowing down distance, $\overline{r^2}$, given by the equation (6.4.E1). The neutron age 'τ' is obtained as one-sixth of this quantity.

The experimental determination of the neutron slowing down flux in graphite is made in a large stack of reactor grade graphite and using several different radio-active neutron sources. The measurements in water were carried out in a large water tank. A laminar fission source was triggered by the thermal neutrons from the vertical access of the reactor thermal column. The fission source was capable of being converted to different source diameters by the use of cadmium screens with appropriate apertures. In graphite the flux measurements were made using indium resonance filter. In water these were extended to other resonance filters like rhodium and gold in addition to indium. A high precision of the traversing mechanism of the counter ensured exact source-detector separation measurements. Procedures and techniques of a multi-stage data analysis are detailed out in chapter six. The age evaluation which is based on equation (6.6.E1), the various

modifications that lead upto this equation are also given in that chapter. The results obtained using different source diameters permit, by extrapolation, the evaluation of the age of fission neutrons in point geometry. The present values of the ages in graphite and in water are compared with the experimental and the theoretical estimates in each category where available.

One of the troublesome problems in reactor physics is to take into account the effect of cavities in the moderator. The presence of the holes causes loss of reactivity. The neutrons stream away from the regions of higher flux to the regions of lower flux. Thus a lattice of voids would disturb or alter the flux distribution. Behrens (R.8.1 to R.8.4) proposed a statistical way of evaluating this effect by calculating the mean square free path. His theory contains the use of certain conventional hypotheses such as isotropic scattering which lead to an overestimation of his radial streaming factor. Physically, one can see that if a neutron which has just crossed a void, has a greater chance of travelling a greater distance on its next track if it scatters backwards into a cavity than if it is scattered forwards into moderator. This leads to significant decrease of the radial streaming but it does not affect the axial streaming. Grant (R.8.8), studied the problem of neutron streaming in gas cooled reactors and showed by physical

arguments that Behrens theory was overestimating the radial streaming factor. Benoist (R.8.5 to R.8.7), gave a detailed treatment of neutron transport in a heterogeneous medium. Carter's theory (R.8.9) show agreement with the above. Some experimental evaluations and Monte Carlo estimations (R.8.10 to R.8.13) show rather better agreement with the later theories as compared to that of Behrens. In the present experimental work, ages of fission neutrons to indium resonance in water, and also in water with cavities in the axial direction and in water with cavities in the transverse direction were measured and used to evaluate the streaming ratios in the axial and the transverse directions. These values are compared with Behrens and Benoist theoretical predictions.

CHAPTER 2.

THE SLOWING DOWN AND THE CALCULATIONS OF NEUTRON AGE.

The neutron age is a measure of spatial dispersion of the slowing down neutrons about the initial source. The age of the fission neutrons in water does not pose any major analytical problems as the scattering of the neutrons against hydrogen nuclei can be taken spherically symmetric in the centre of mass system. The calculations for the slowing down density, or the second moment of it, are made by treating water as free hydrogen gas and any perturbing effect due to oxygen is considered to be very small and can be accurately known. Neutron age is of a considerable importance as this parameter dictates the size of a particular thermal reactor. So from the reactor design point of view it is essential that the values of the ages be made available for a variety of materials and sources. The main intrest, however, centres round the age of fission neutrons to indium resonance energy as it affords a direct comparison with the measured values. Some of the calculated values will be quoted for water for the above mentioned energy range, in the next three sections.

For an isotropic source in an infinite homogeneous medium, neutron age can be calculated in a rigorous manner by a number of methods. In these techniques which make

use of the Boltzmann equation, no physical assumptions or approximations are made to it. Following are some of the methods employed for these calculations.

(a) Moments solution of the Boltzmann equation.

(b) Monte Carlo variations of the Boltzmann equation.

(c) Fourier transformed Boltzmann equation.

These methods will be briefly described and some of the calculated results be quoted for each.

2.1. MOMENTS SOLUTION OF THE BOLTZMANN EQUATION.

This is an expansion technique for solving the transport equation in infinite media. Here, in this semi-analytic nature of operation, the angle, the space and energy variations are treated by polynomial expansion. The solutions is then obtained from the series by truncation.

The spatial moments for the neutron distribution function $\Phi(z,E)$ for a plane source (in plane z=0) are defined by,

$$\Phi_{nl}(E) = \frac{1}{n!} \int_0^\infty z^n \Phi_l(z,E)\, dz$$

$$= \frac{2\pi}{n!} \int_{-\infty}^{\infty} \int_{-1}^{1} z^n P_l(\Omega)\, \Phi(z,E,\Omega)\, dz\, d\Omega \qquad \text{.....(2.1.E1)}$$

The angle between the normal to the source plane and the direction of motion of neutrons is $\cos^{-1}\Omega$ and the angular number flux is represented by $\Phi(z,E,\Omega)$. The moments $\Phi_{nl}(E)$ satisfy an infinite sequence of integral equations which are obtained from Boltzmann equation by multiplying it by $z^nP(\Omega)/n!$ and integrating over the solid angle and z. The result is,

$$\Sigma_T(E)\ \Phi_{nl}(E) = \frac{(l+1)\Phi_{n-1,l+1}\ (E) + l\Phi_{n-1,l-1}\ (E)}{(2l+1)}$$

$$+ 2\pi\Sigma \left\{ \frac{2c}{1-\alpha} \int_{E}^{E/\alpha} \sigma_s(E')\ P(E',\mu') \right\}$$

$$\cdot P_l(\mu)\ \Phi_{nl}(E')\ \frac{dE'}{E'} + S(E)\delta_{no}\delta_{lo}$$

.....(2.1.E2)

Where Σ_T represents the total macroscopic cross section, c and σ_s the concentration and microscopic cross section of the individual elements, $P(E',\mu')$ the probability per unit solid angle in the centre of mass system, with $\alpha = ((A-1)^2/(A+1)^2)$, and $S(E)\delta_{no}\delta_{lo}$ is the source term.

The first few equations which are obtained from the equation (2.1.E2) are,

$$\Sigma(E)\,\Phi_{oo}(E) = \int \Sigma_s^o\,(E' \longrightarrow E)\,\Phi_{oo}(E')\,dE' + S(E) \qquad \text{.....(2.1.E3)}$$

$$\Sigma(E)\,\Phi_{11}(E) = \frac{1}{3}\int \Sigma_s^1\,(E' \longrightarrow E)\,\Phi_{11}(E')\,dE' + \Phi_{oo}(E) \qquad \text{.....(2.1.E4)}$$

$$\Sigma(E)\,\Phi_{2o}(E) = \int \Sigma_s^o\,(E' \longrightarrow E)\,\Phi_{2o}(E')\,dE' + \frac{1}{3}\,\Phi_{11}(E) \qquad \text{.....(2.1.E5)}$$

The neutron age is given by,

$$\tau(E) = \frac{\Phi_{2o}(E)}{\Phi_{oo}(E)} \qquad \text{.....(2.1.E6)}$$

In the evaluation of the scattering integral for water constituents, hydrogen poses no problems as the scattering here is isotropic in the centre of mass system, α being zero, the scattering integral is very much simple and the necessity of any particular treatment does not arise. In the case of oxygen however various ways can be adopted. In a more rigorous method of treating oxygen, no physical assumptions are made. This obviously yields very accurate results. But with the approximations of treating either the slowing down of oxygen by expanding the oxygen scattering integral as a linear function of m^{-1} or by considering no energy loss upon collision with the oxygen nuclei, are quite adequate as the difference

of the value obtained by these methods and that obtained by the exact method is insignificant in view of the uncertainties in the cross section data.

TABLE (T.2.1).

Theoretical values of the neutrons age to indium resonance energy calculated by moments method.

Authors - Year	Reference	Age (cm^2)	Remarks
Hurwitz, H., Zweifel, P.F. (1955)	(R.2.1)	25.8	(a),(b).
Certaine, J. (1957)	(R.2.2)	26.0	(a),(c), (d).
Goldstein, H., Certaine, J. (1957)	(R.2.3)	26.5	(e).
Joanou, G.D., Goodjohn, A.J., Wikner. (1961)	(R.2.4)	26.4	(f).

(a) Oxygen cross section from reference (R.2.12)

(b) The computed values of age has been corrected from 2.03 e.v. to 1.46 e.v.

(c) With slight revision of hydrogen cross sections.

(d) Oxygen slowing down treated exactly.

(e) Revised oxygen cross sections used (1)- upto

3 M.e.v. from reference (R.2.13) and (2)-above
3 M.e.v. from reference (R.2.12).

(f) Angular distribution data used.

The moments method is particularly useful in obtaining flux at large distances from the source and has therefore found considerable application in the shielding calculations. This method also offers a great advantage over the spherical harmonics method as it is possible to determine a finite number of moments Φ_{nl} exactly without making any assumptions as to the behavior of the neglected moments.

2.2. MONTE CARLO VARIATIONS OF THE BOLTZMANN EQUATION

This method is based on obtaining statistical estimates of certain quantities. A particular problem dictates its set of rules and set of probabilities governing the occurrence for the estimations of these quantities. Reactor Physics problems being probabilistic in nature offers the application of Monte Carlo methods. It is used in estimating the statistical behavior of a large number of neutrons directly to obtain their individual characteristics, such as their energy, position and direction of motion etc. These properties are then averaged over a large number of neutron histories. In order to reduce error down to about 1 % , as many as 10,000 neutron histories are required.

This method is generally used to its best advantage in solving problems that are difficult to solve analytically. The examples of such problems in Reactor Physics being those, for example, involving heterogeneous media, anisotropic scattering or irregularity or variation of the cross-sections with energy.

Monte Carlo technique is usefully employed for the calculation of neutron age in water as the cross-section of hydrogen increases strongly with decreasing energy down to about 200 K.e.v. A number of calculations for water have been made (R.2.5 to R.2.8) by this method. The basic procedure consists in obtaining the spatial distribution analytically but the slowing down energy is followed by Monte Carlo technique.

For a plane isotropic source in an infinite and homogeneous medium the expansion of the Fourier transform of the Boltzmann equation in Legendre Polynomial result in the following.

$$D_{nl}(u) = \Sigma_T \, D_{nl}(u') \, \Phi_i(u') \, k_{il}(u' \longrightarrow u) \, du' + \delta_{no}\delta_{lo}\delta(u)$$

$$+ \lambda(u) \left\{ \frac{n(l+1)}{2l+1} D_{n-1,l+1}(u) + \frac{nl}{2l+1} D_{n-1,l-1}(u) \right\}$$

.....(2.2.E1)

Where $D_{nl}(u)$ represents the spatial moments of the collision density at lethergy u, $\lambda(u)$ - the mean free path at lethergy u, $\Phi_i(u)$ - the probability that a neutron of lethergy u will scatter by a nucleus of element 'i', and $k(u' \rightarrow u)$ the probability that a neutron of lethergy u' scattered by a nucleus 'i' will assume lethergy u.

To fix second spatial moment we would require the following three equations obtained from the expression (2.2.E1)

$$D_{oo}(u) = \Sigma_i \int D_{oo}(u')\, \Phi_i(u')\, k_{io}(u' \rightarrow u)du' + \delta(u) \qquad \ldots\ldots(2.2.E2)$$

$$D_{11}(u) = \Sigma_i \int D_{11}(u')\, \Phi_i(u')\, k_{i1}(u' \rightarrow u)du' + \frac{\lambda(u)}{3} D_{oo}(u) \qquad \ldots\ldots(2.2.E3)$$

$$D_{2o}(u) = \Sigma_i \int D_{2o}(u')\, \Phi_i(u')\, k_{io}(u' \rightarrow u)du' + 2\lambda(u)\, D_{11}(u) \qquad \ldots\ldots(2.2.E4)$$

The above three equations provide the sets of rule and probabilities for the estimation of neutron age.

Considering a newly born neutron with zero lethergy. Upon its collision with the nucleus of element 'i', it scatters with a probability $\Phi_i(o)$ or gets absorbed with a probability $1-\Sigma_i\Phi_i(u)$. If however the neutron survives at this stage it is scattered by the nucleus i_1 and it

assumes lethergy u_1 with a probability $k_i(o \rightarrow u_1)$. The neutron continues this way untill it is finally absorbed. The behavior of group of such neutrons is given by the equation (2.2.E2). As regards D_{11} and D_{2o}, initially both are zero, but at each collision D_{11} is increased by an amount $\lambda(u)/3$ and at each scattering D_{11} is multiplied by $k_{i1}(u' \rightarrow u)/ k_{io}(u' \rightarrow u)$. D_{2o} at each collision is increased by $2\lambda(u)\ D_{11}$.

If a very large number of neutron histories are followed from its birth to its terminal energy then the average of D_{2o} over such histories is an estimate of the second spatial moment of the slowing down distribution at the termal energy.

In this process, the slowing down calculations do not stop at 1.46 e.v. but include all neutrons which scatter past this energy. Therefore the age value here refers to the slowing down density 'q' rather than flux 'Φ'. The correction for flux age can be obtained using the relationship,

$$\tau_\Phi = \tau_q + \frac{1}{3\bar{\xi}\Sigma_s\Sigma_{tr}} \qquad \text{.....(2.2.E5)}$$

In the case of water the correction $(\tau_\Phi - \tau_q)$ amounts to be 0.43 cm^2.

Some of the values of age of fission neutrons in water calculated by Monte Carlo method are displayed below in the table (T.2.2).

TABLE (T.2.2)

Neutron age estimations to Indium resonance energy using Monte Carlo technique.

Authors	Year	Reference	Age (cm^2)	Remarks
Coveyou, R.R.	(1956)	(R.2.5)	25.6 $\pm$0.3	(a),(b), (c).
Brown, H.D.	(1957)	(R.2.6)	26.7	(a),(c).
Coveyou, R.R., Sullivan, J.G.	(1958)	(R.2.7)	25.9 $\pm$0.3	(b),(c), (d).
Goldstein, H., Sullivan, J.G., Coveyou, R.R., Kinney, W.E., Bates, R.D.	(1961)	(R.2.8)	26.0 $\pm$0.3	(b),(e).
Alter, H.	(1965)	(R.2.9)	26.07 $\pm$0.09	(b),(f), (g).

(a) Oxygen cross-section from reference (R.2.12)

(b) Corrected for flux age.

(c) Slowing down in oxygen treated exactly.

(d) Revised oxygen cross-sections used from reference (R.2.13).

(e) Anisotropic scattering assumed for oxygen.

(f) Hydrogen cross-sections used from references (R.3.1) and (R.2.14).

(g) Following oxygen cross-sections used.

(1) 1 eV to 200 KeV from reference (R.2.15).

(2) 200 KeV to 700 KeV from reference (R.2.16).

(3) 700 Kev to 1400 KeV from reference (R.2.17).

(4) Upto 3.4 MeV from reference (R.2.18).

(5) Through to 10 MeV from reference (R.2.19).

Monte Carlo technique, due to its nature, requires a digital computer of large capacity and consumes lot of computer time for its operation. This method is applied to its best use where more conventional methods are very difficult to apply or are unmanageable.

2.3. FOURIER TRANSFORMED BOLTZMANN EQUATION.

The spatial moments of the flux distribution may be found by expanding the transform of flux in the power series with respect to 'k', the second spatial moment being $(-1)^n(2n+1)!$ times the co-efficient of k^{2n} in the expansion. This method of age calculation is based upon expanding the transforms N(k,u,w) and J(k,u,w), the angular

dependent flux and degradation integral in the series of Legendre Polynomials. This yields in an infinite set of simultaneous integral equations for the Legendre component of N. Thus,

$$\Sigma_T(u)\, N_l(k,u) = \sum_{l=o}^{l=\infty} (2l+1)\, A_{jl}\, \Sigma_{ALL}\, Jl^{ALL}(k,u) + S_l(k,u) \qquad \ldots\ldots(2.3.E1)$$

Where 'ALL' refers for all the moderator components present, S_l is the Legendre component of the transform of the source, where for an isotropic source $S_l(k,u)$ is equal to $S_o(k,u)\delta_{lo}$, and A_{jl} are the co-efficients.

The equation (2.3.E1) can be solved either by P_L or by B_L approximations. $N_l(k,u)$ can be expressed as,

$$N_l(k,u) = \Sigma_{j=l,l+2} \frac{(ik)^j}{j!} N_l^{(j)}(u) \qquad \ldots\ldots(2.3.E2)$$

Both P_L and B_L approximations give the correct value of $N_l^{(j)}(u)$ for all values of j upto and including j = 2L. For L = 1, both methods yield correct second moments of neutron flux from an isotropic point source. The neutron age is then given by,

$$\tau = \frac{1}{2} \frac{N_o^{(2)}(u)}{N_o^{(o)}(u)} \qquad \ldots\ldots(2.3.E3)$$

The tables (T.2.3) and (T.2.4) give some of the values calculated by the Fourier transformed Boltzmann equation and with the use of B_1 and P_1 methods. Reference may be made to Hurwitz and Zweifel (R.2.1) for the details of the theory.

TABLE (T.2.3)

Theoretical values of neutron age to indium resonance energy calculated by Fourier transformed Boltzmann equation.

Authors	Year	Reference	Age (cm^2)	Remarks
Certaine, J., Aronson, R.	(1954)	(R.2.10)	25.3	(a),(b).
Reier, M., Obenshaine, F., Hellens, R.L.	(1957)	(R.2.11)	25.9	(b).

(a) Oxygen cross-section as in reference (R.2.12)

(b) Oxygen slowing down treated exactly.

TABLE (T.2.4)

Neutron age calculations to indium resonance energy using P_1 and B_1 methods.

Age (cm^2)	Remarks
25.3	Oxygen slowing down treated exactly.
24.8	

For small values of 'k', B_L and P_L cases give similar results, in particular B_1 and P_1 both give correct values of the second moment of flux but as 'k' is increased the discrepency between these methods become large.

CHAPTER 3.

THE SLOWING DOWN OF NEUTRONS.

3.1. INTRODUCTION

The slowing down of fast neutrons in a moderator is a matter of considerable importance in the theory of the thermal reactors as it has a direct bearing on critical size of a reactor. The aim of the slowing down theory is to determine the space and the energy distribution of the neutron flux about the source which is producing the fast neutrons.

In this chapter attention is focussed on the problem of the slowing down in moderators of comparatively heavy elements such as graphite which has a direct application in the first experimental series of the present work.

3.2. SLOWING DOWN IN HEAVY MODERATORS (FERMI AGE TREATMENT)

Fast neutrons lose their energy upon collision with the nuclei of the moderators. The earliest successful method of treating the slowing down problem is due to Amaldi (R.3.1) and Fermi. In this model, the collision

between the neutrons and the nuclei of the moderator are treated as free particle collisions. In heavy moderator like graphite, neutrons suffer a large number of collisions, losing energy in small steps. The phenomenon of slowing down in a moderator like this conveniently approximates to continuous slowing down. Fermi age treatment is based on such a process of slowing down in a gradual way affords a simplified approach to establish relationship between neutron energy and the distance from the emitting source, during the process of slowing down. The simplifying assumptions made are that the moderator basically contains a single type of element which has a large mass as compared to that of neutron. It is also assumed that inelastic scattering and absorption are negligible and the energy-angle correlation (R.3.2) and the chemical binding effects are ignorable. Fermi's differential equation of age is then given by,

$$\frac{\partial q(\bar{x},\tau)}{\partial \tau} = \nabla^2 q(\bar{x},\tau) + S(\bar{x},\tau) \qquad \ldots\ldots (3.2.E1)$$

where the Fermi age 'τ' is given by,

$$\tau = \int_{E_o}^{E} \frac{D}{\xi \Sigma_t} \frac{dE}{E} \qquad \ldots\ldots (3.2.E2)$$

and $S(\bar{x},\tau)$ represents the number of neutrons produced by the source in unit volume per unit time and 'τ' intervals.

The solution of the Fermi age equation (3.2.E1) for the case of fast mono-energetic neutrons in an infinite medium, derived for a point source is given by

$$q_{point}(r,\tau) = \frac{c}{(4\pi\tau)^{3/2}} \exp(-r^2/4\tau) \qquad \ldots\ldots \text{(3.2.E3)}$$

where 'c' is a constant depending upon the source strength and $q(r,\tau)$ represents the slowing down density. Equation (3.2.E3) is valid upto a distance of $\tau\Sigma_t$. At greater distances the approximation does not hold. At large distances from the source the neutron flux is largely determined by the neutrons that have undergone only a few collisions and whose energy and direction have not changed much and whose angular distribution is very anisotropic.

In the age approximation there is no difference between the 'flux age' and the 'slowing down density age'. The Fermi age $\tau(E)$ refers to a quantity that increases as the slowing down process progresses.

Fermi age is not applicable in light moderators like hydrogen as $\alpha=0$ which gives rise to large average change in

energy in a single collision.

3.3. MODIFICATION OF AGE EQUATION.

Placzek (R.3.3) obtained an asymptotic formula for all moments for the case of constant mean free path. Assuming $u \gg \log(1/\alpha)$, where $\alpha = (A-1)^2/(A+1)^2$, he worked out an expression, going upto two highest powers of u. The expression arrived at, for a moderator containing a single element and for a plane neutron source is given by,

$$\left[x^{2m}(u)\right]_{\text{average}} = \frac{(2m)!}{m!}(\tau)^m\left[1 + \frac{m(mN_{11}+N_{10}) + \cdots}{u}\right] \quad \ldots\ldots (3.3.E1)$$

where $N_{11} = \Omega_1 + \Omega_2 + \Omega_3$ ..... (3.3.E2)

$N_{10} = \Omega_1 - \Omega_3$ ..... (3.3.E3)

with $\Omega_1 = \dfrac{8A+(A-1)^2\log\alpha(2-\log\alpha)}{8A+2(A-1)^2\log\alpha}$ ..... (3.3.E4)

$\Omega_2 = \dfrac{1}{6}\left[\dfrac{12A^2-20+3(A-1)^2(A+2)\log\alpha}{3A-2}\right]$ ..... (3.3.E5)

and $\Omega_3 = \dfrac{32}{15}\left[\dfrac{4A+(A-1)^2\log\alpha}{4A(A^2+1)+(A^2-1)^2\log\alpha}\right]$ ..... (3.3.E6)

The values of N_{11} and N_{10} for a moderator element, using respectively the equations (3.3.E2) and (3.3.E3), can be obtained with appropriate values of Ω_1, Ω_2 and Ω_3. These values for graphite are $N_{11} = 0.28666$ and $N_{10} = -0.017671$. The equation (3.3.E1) could also be applied in the case of mixtures provided the scattering mean free path for all component elements are constant, independent of energy.

Using expression (3.3.E1), Marshak (R.3.4) obtained the slowing down density distribution function for a plane source of neutrons as,

$$q_{plane}(x,\tau) = \frac{c}{(4\pi\tau)^{1/2}} \exp\left(\frac{-x^2}{4\tau}\right) \cdot \left[1 + \frac{1}{4u} \left\{ (N_{11}-2N_{10}) - (2N_{11}-N_{10}) \left(\frac{x^2}{\tau}\right) + \frac{N_{11}}{4} \left(\frac{x^2}{\tau}\right)^2 \right\} \right] \qquad \ldots\ldots (3.3.E7)$$

The expression for the slowing down density due to a point source can be had directly from the equation,

$$q_{point}(r,\tau) = - \frac{1}{2\pi r} \frac{\partial q_{plane}}{\partial x} \frac{(x,\tau)}{\partial x} \Bigg|^{x=r} \qquad \ldots\ldots (3.3.E8)$$

Thus,

$$q_{point}(r,\tau) = \frac{c}{(4\pi\tau)^{3/2}} \exp\left(\frac{-r^2}{4\tau}\right)$$

$$\cdot\left[\, 1 + \frac{1}{4u}\left\{3(3N_{11}-2N_{10}) - (4N_{11}-N_{10})\left(\frac{r^2}{\tau}\right)\right.\right.$$

$$\left.\left. + \frac{N_{11}}{4}\left(\frac{r^2}{\tau}\right)^2 \right\}\right] \qquad \ldots\ldots\ (3.3.E9)$$

here 'u' is the lethergy change from the source energy to the detector energy.

Equation (3.3.E9) is modified further for the finite sizes of the sources and detector, which forms the basis of analysis of the experimental work on age evaluation in graphite to be described in chapter 4.

CHAPTER 4.

THE MEASUREMENTS OF NEUTRON AGE IN GRAPHITE.

4.1. THE TECHNIQUE

The age to indium resonance energy is found by measuring the spatial distribution about the source of neutron flux at that energy. The resonance flux is obtained (R.4.6) by measuring the fall in the counting rate of an epi-cadmium neutron sensitive scintillation counter, produced when covered with an additional indium foil. This method is simple, quick and requires less elaborate techniques. The more traditional method of age evaluation is by foil irradiation and measuring the activity produced in the cadmium covered indium foils as a function of distance from the source. If accurate results are to be obtained, a careful attention has to be given to the inter-calibrations of the foils used, avoidance of mutual interference if more than one foils are irradiated at the same time. The reproducibility of geometric and intrinsic detection efficiencies of foil counting apparatus is vital. In addition to these effects, allowence must be given for the effects of the higher energy resonances in indium. The present method offers a much better counting statistics for the same strength

of the neutron source. Hence, particularly strong sources are not altogether essential for obtaining good accuracy of results. As for the disturbing effects of the higher resonances in indium, the present method also helps to minimise it as the efficiency of the scintillator used, goes down very rapidly with the increase in neutron energy. This method however stringently requires a very high degree of counter stability as a difference of measurements is involved.

4.2. THE EQUIPMENT.

4.2.1. THE NEUTRON SOURCES.

Three (α,n) neutron sources, Po^{216}-Be, Ra^{226}-Be, Am^{241}-Be and one photo-neutron, (γ,n), Sb^{124}-Be source were used in this series of age measurements in graphite moderator. All these sources were obtained from the United Kingdom Atomic Energy Authority, Radio-chemical centre, Amersham. With the exception of Ra^{226}-Be source, which was of 500-millicurie strength, the rest had the nominal strength of one curie. Some further details of these sources, regarding their constitution and physical features etc., are provided in Appendix (A.4.1).

4.2.2. THE SCINTILLATORS.

The measurements for Po^{216}-Be neutron source were carried out using Nuclear Enterprises NE 905 lithium-

glass scintillator. This contained 7.3 % lithium which is enriched to 96 % in Li^6. The scintillator has diameter of 1.75" and thickness 1/8" with alumina reflector on the outer face and along the circumference. The reaction of neutron with Li^6 is given by,

$$n + Li^6 = T^3 + \alpha + 4.78 \text{ Mev.}$$

The cross-section for this reaction is 945 barns at the neutron energy of 0.025 e.v. This cross-section varies as 1/V above this energy. The scintillator used has a calculated efficiency of 75 % for 1.46 e.v. neutrons. NE 905 offers excellent pulse height discrimination against the gammas especially if the gamma backgraound is not too high. The gamma dose per 10^6n/sec, from a one curie Po-Be source at one metre distance is less than 0.1 mR/h. This low gamma background from the source is easily baised off by the pulse height selection, from the neutron peak, at a loss of less than 1 % neutron counts. A typical pulse height discrimination curve for the Po-Be neutron source is shown in the fig (F.4.1). The curves 'A', 'B' and 'C' are respectively for the bare, for the cadmium covered and for cadmium + indium covered counter. (The thicknesses used for cadmium and indium are respectively 0.015" and 0.010".) The curve 'D' shows the response to Co^{60}gammas.

For the measurements of neutrons from Sb-Be and Ra-Be sources, NE 905, lithium glass scintillator was rendered quite unsuitable as a very high gamma background completely

FIG(F.4.1) PULSE HEIGHT DISTRIBUTION FOR LITHIUM-GLASS SCINTILLATOR NE905 FOR PO-Be SOURCE IN GRAPHITE

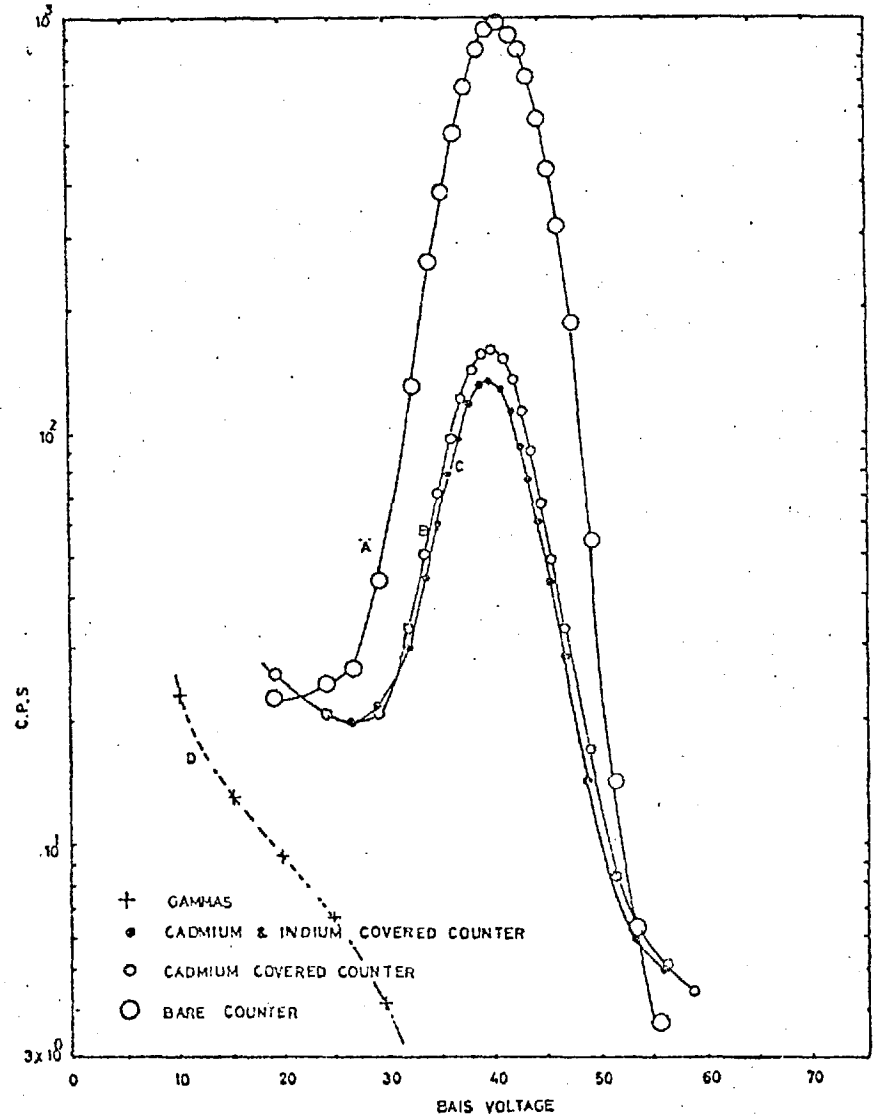

FIG(F.4.2) RESPONSE CURVES OF BORON POLYESTER DETECTOR WITH ZnS(Ag) ACTIVATOR, NE 401, FOR Sb-Be SOURCE IN GRAPHITE.

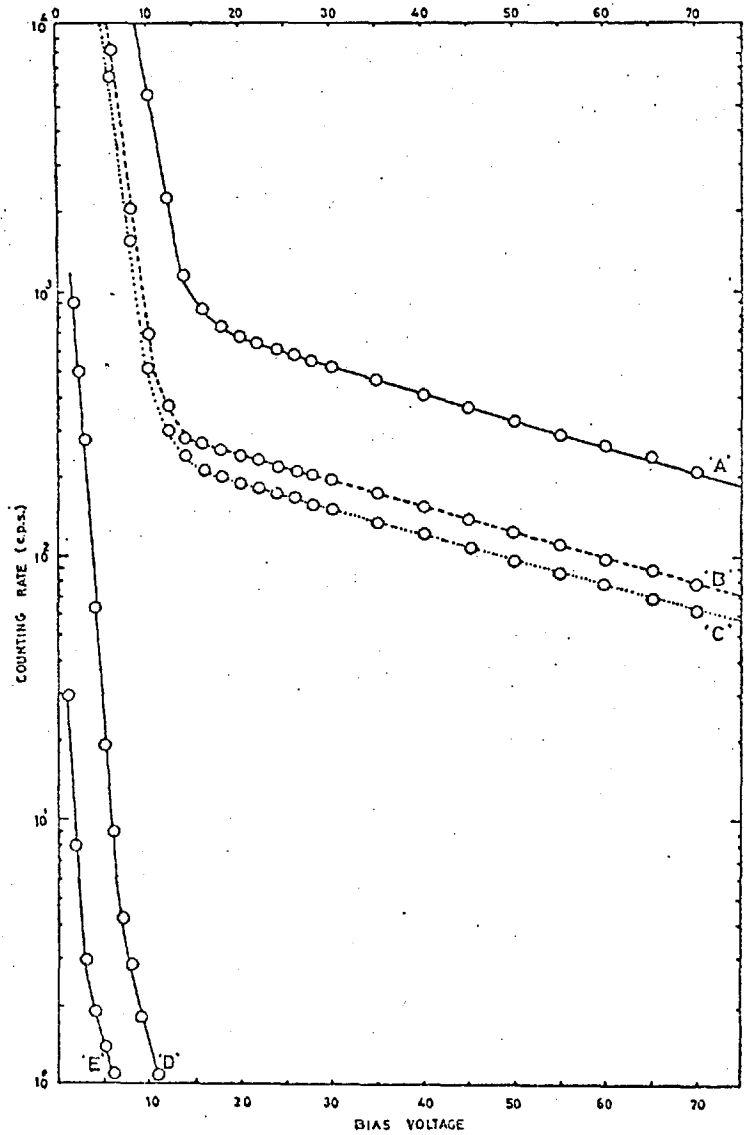

drowns the neutron peak. It was however possible to eliminate the gammas by the use of lead. The source was positioned accurately in a lead barrel and the thicknesses of lead in front of the counter was varied. It was found that a considerable lead thickness was needed to cut off gammas almost completely. This arrangement was not very satisfactory as apart from being cumbersome, it introduced ambiguity in the source-detector distance measurement. The above arrangement was abandoned for this reason. For the neutron age measurements from these sources another Nuclear Enterprises scintillator type NE 401, Boron polyester detector with Zns(Ag) activator was used. This scintillator provided means of effectively discriminating against the high gamma emission from some of these sources. A high neutron to gamma response is easily obtained by a higher bias setting with relatively little loss of neutron detection efficiency. The scintillator was 1" in diameter and of 0.125" in thickness and contained Boron enriched to 96 % in B^{10}. Figure (F.4.2) shows the response curves taken for Sb-Be source. These curves represent a typical response for this scintillator. The curves 'A', 'B' and 'C' are respectively for the bare, for the cadmium coved and for cadmium + indium covered counter. The curve 'D' is the response to a one curie Sb^{124} source of gamma rays and the curve 'E' represents the noise of the electronics used.

For Am^{241}-Be neutron source both NE 905 as well as

NE401 were equally suitable as the gamma emission from this source although more than that from Po-Be source, (see Appendix (A.4.1)), is still manageable and could easily be biased off by a proper pulse height selection using NE905 scintillator. But since NE401 was already set for the Ra-Be and Sb-Be sources so the same was used for this source also.

4.2.3. THE NEUTRON COUNTING SYSTEM

The lithium glass scintillator or the boron polyester detector, in the respective cases, were used with a 0.5" thick perspex light guide and an E.M.I. eleven stage photomultiplier tube type 6097B, and an ECKO scintillation assembly type N559B. The pulses from the photo-multiplier tube after passing through the cathode follower type NE5202A were amplified by a non-overloading linear pulse amplifier type NE5202 and were analysed by a differential pulse height selector type NE5102. These pulses were then counted by a Philips scaler type PW4032 via a Philips timer type PW4062.

4.2.4. THE MODERATING MEDIUM

In practice it is not possible to obtain an infinite size of the moderating medium. The dimensions of this medium are chosen that there is no measureable flux distortion. For the neutron flux in a finite size moderator to fall off in the same fashion as it does in an

infinite medium the length, suggested by Grant (R.4.1), of the finite moderator block should be at least $10\tau^{1/2}$. (Where 'τ' is the neutron age from the source energy to the detector energy.). In a simple Fermi age treatment the lateral dimensions has no effect on the shape of the axial flux distribution, only on the magnitude of the flux. For a point source in a medium of finite lateral dimensions the fractional depression would be constant along the long axis but it has been shown by Davy (R.4.2) that for an insufficient moderator dimensions, the flux depression increases at large distances from the source. To minimise this depression, taking higher moments into consideration Davy suggested that the minimum lateral dimensions as $6\tau^{1/2}$ in order to have flux measurements without depression.

The moderating medium used in the present series consists of a stack of graphite 4' x 4' x 7'-3". This was erected from grade 'A' reactor graphite blocks each 8" sq. and 29" long. The graphite had density of 1.75 gm cm^{-3}. Each block contained an axial channel 3.90" diameter which was fitted with graphite sleeve and plug. The clearance between the graphite plug, sleeve and the channel did not exceed 0.004". The overall dimensions of the graphite stack were above the minimum suggested size.

4.3. THE EXPERIMENTAL PROCEDURES.

4.3.1. THE STABILITY CHECKS.

The accuracy of the present method of measurements of the indium resonance flux, which involves difference of measurements, put a condition of very high standard of the counter stability. This aspect was stringently checked from time to time. This involved checking of the pulse height distribution or the response curves in the appropriate cases. This was done before and after each experiment and also at appropriate intervals, during the course of the experiment if needed. During the course of the flux measurements, observations for same points were repeated in random selection to check the reproducibility of the measurements. No counter drift was observed and the individual points of the spatial distribution were found to be reproducible within the statistical accuracy of the counting apparatus.

4.3.2. INDIUM RESONANCE FLUX MEASUREMENTS.

The neutron source in each case, were positioned 29" from one of the central channel of the graphite stack. The detector was placed in the same channel and the space between the source and the detector was filled with very accurately machined discs of graphite of the same diameter as the channel within the sleeve. The device which was used to position the graphite discs ensured the expulsion of air between them. The distance between the source and the detector being determined by thickness of interposed

discs and were known accurately to better than 1 mm. Countrates were obtained for a series of measurements taken at various source-detector distances along the axis of the source, with the counter cadmium covered and then with an additional Indium foil in front of the detector. The difference of the two give the spatial distribution of Indium resonance flux for a given neutron source.

4.4. CORRECTIONS FOR SOURCE AND DETECTOR SIZES.

The equation (3.3.E9) for the evaluation of neutron age is for a point source and detector, but the sources and the detectors in the present series were not of the point geometries. See figure (F.4.3) below.

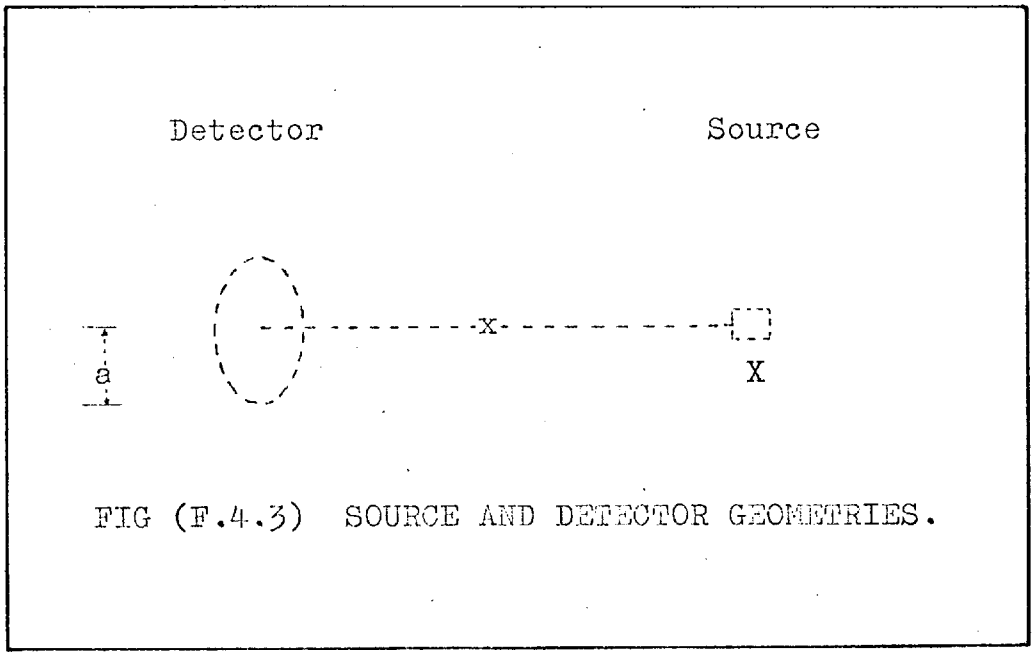

FIG (F.4.3) SOURCE AND DETECTOR GEOMETRIES.

The detectors used were discs of diameters 1.75" and 1" - respectively and the neutron sources were of cylindrical shape of varying sizes, see Appendix (A.3.1). The effect due to their finite sizes is taken into computations by carrying out integration over the source and detector sizes. The equation (3.3.E9) thus assumes the form,

$$\Phi(r,\tau) = B \int_0^a da \int_x^{x+X} dx \exp\left(-\left(\frac{a^2 + x^2}{4\tau}\right)\right) \cdot \left[1 + \frac{1}{4u} \left\{ A_o - A_1 \left(\frac{a^2 + x^2}{\tau} \right) + A_2 \left(\frac{a^2 + x^2}{\tau} \right)^2 \right\} \right] \quad \ldots\ldots(4.4.E1)$$

where

$$A_o = 3 \left(3N_{11} - 2N_{10} \right) \quad \ldots\ldots(4.4.E2)$$

$$A_1 = \left(4N_{11} - N_{10} \right) \quad \ldots\ldots(4.4.E3)$$

$$A_2 = \left(N_{11} / 4 \right) \quad \ldots\ldots(4.4.E4)$$

$$B = \frac{c}{\left(4\pi\tau \right)^{1.5}} \quad \ldots\ldots(4.4.E5)$$

and $$u = \log \left(\frac{E_s}{E_d} \right) \quad \ldots\ldots(4.4.E6)$$

'E_s' and 'E_d' here refered to the source and 1.46 e.v.

4.5. THE METHOD OF DATA ANALYSIS.

The measured resonance neutron flux as a function of distance 'r' in graphite from Po^{216}-Be, Sb^{124}-Be, Ra^{226}-Be and Am^{241}-Be sources in successive experiments should be proportional to the theoretical expression for the slowing down flux given by the equation (4.4.E1).

A computer programme 'CIAFFP' was written by the present author using the college IBM 7090/7094 computer. This programme was based on the equation (4.4.E1) which also allows for the finite sizes of the source and the detector used. A method of least squares is used for fitting the resonance neutron flux data to the theoretical expression. A block diagram of the programme 'CIAFFP' is given in the figure (F.4.4). To evaluate the integrals occurring in the fitting equation and its derivatives with respect to the parameters, numerical integration was carried out in the programme. The finally corrected results are given in Table (T.4.6).

4.6. RESULTS AND DISCUSSION

Tables (T.4.1), (T.4.2), (T.4.3) and (T.4.4) give the observed spatial distribution of indium resonance flux along with the calculated fluxes of the fitted curves, for each point corresponding to the observed data. The

FIG(F.4.4) A BLOCK DIAGRAM OF PROGRAMME "CIAFFP"

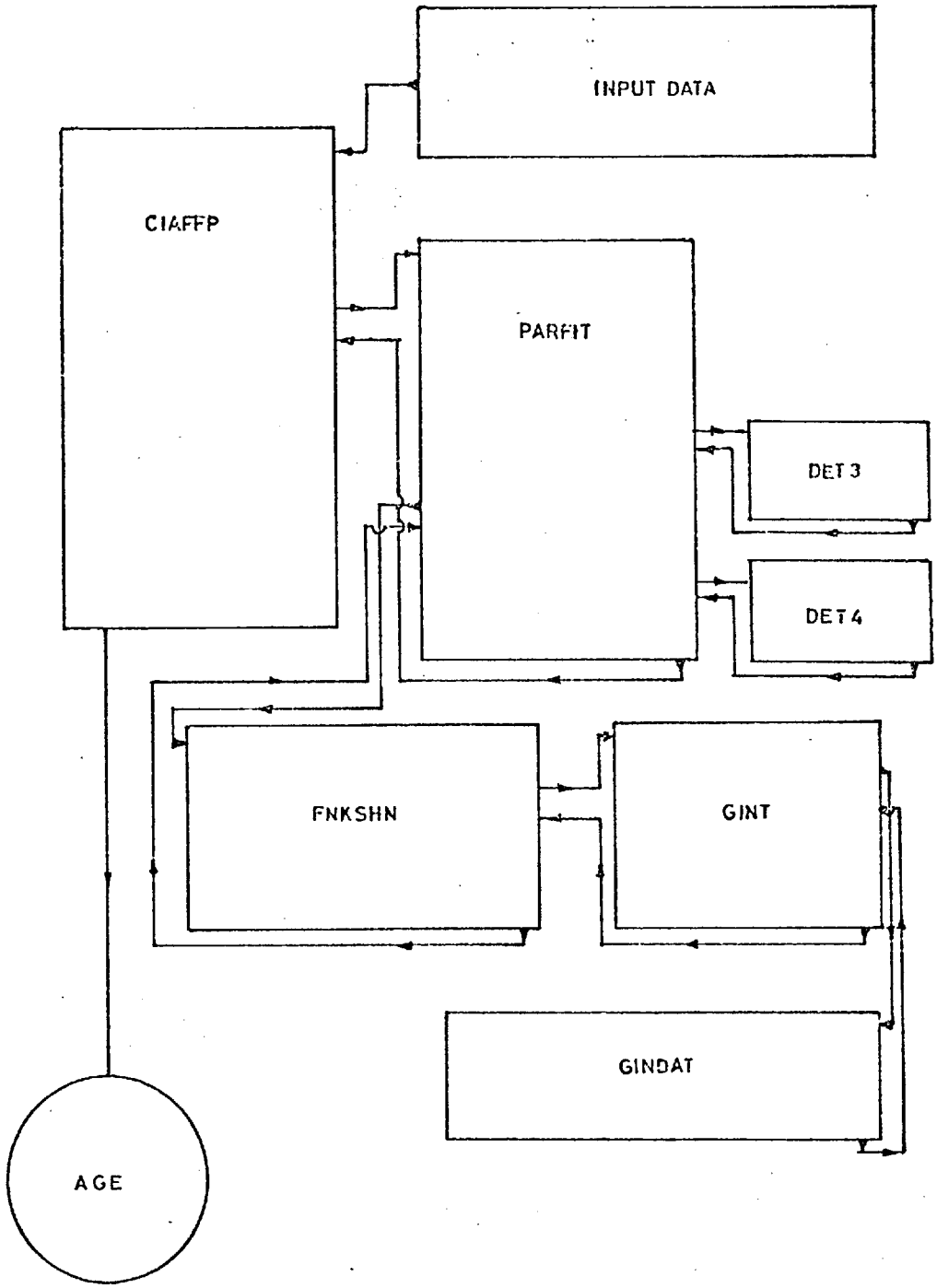

TABLE (T.4.1).

Spatial distributions (observed and calculated) of 1.46 e.v. neutrons from a Po^{216}-Be source in graphite.

(Density of graphite = 1.751 gm cm^{-3})

Source-detector distance (cms) (observed)	Indium resonance flux (cps) (observed)	Indium resonance flux (cps) (calculated)
3.00	349.54	322.05
8.00	299.64	308.94
13.00	286.31	275.65
18.05	230.41	235.53
23.00	186.21	193.88
27.00	160.23	159.37
32.25	116.82	121.37
37.25	90.74	89.20
42.30	61.44	62.97
47.25	42.31	43.23
52.55	29.75	27.87
56.50	20.28	19.64
61.50	12.39	12.28
66.50	7.99	7.46
71.50	4.65	4.41

FIG(F4.5) SPATIAL DISTRIBUTION OF 1.46 ev NEUTRONS FROM Po-Be SOURCE IN GRAPHITE ($\rho = 1.751$)

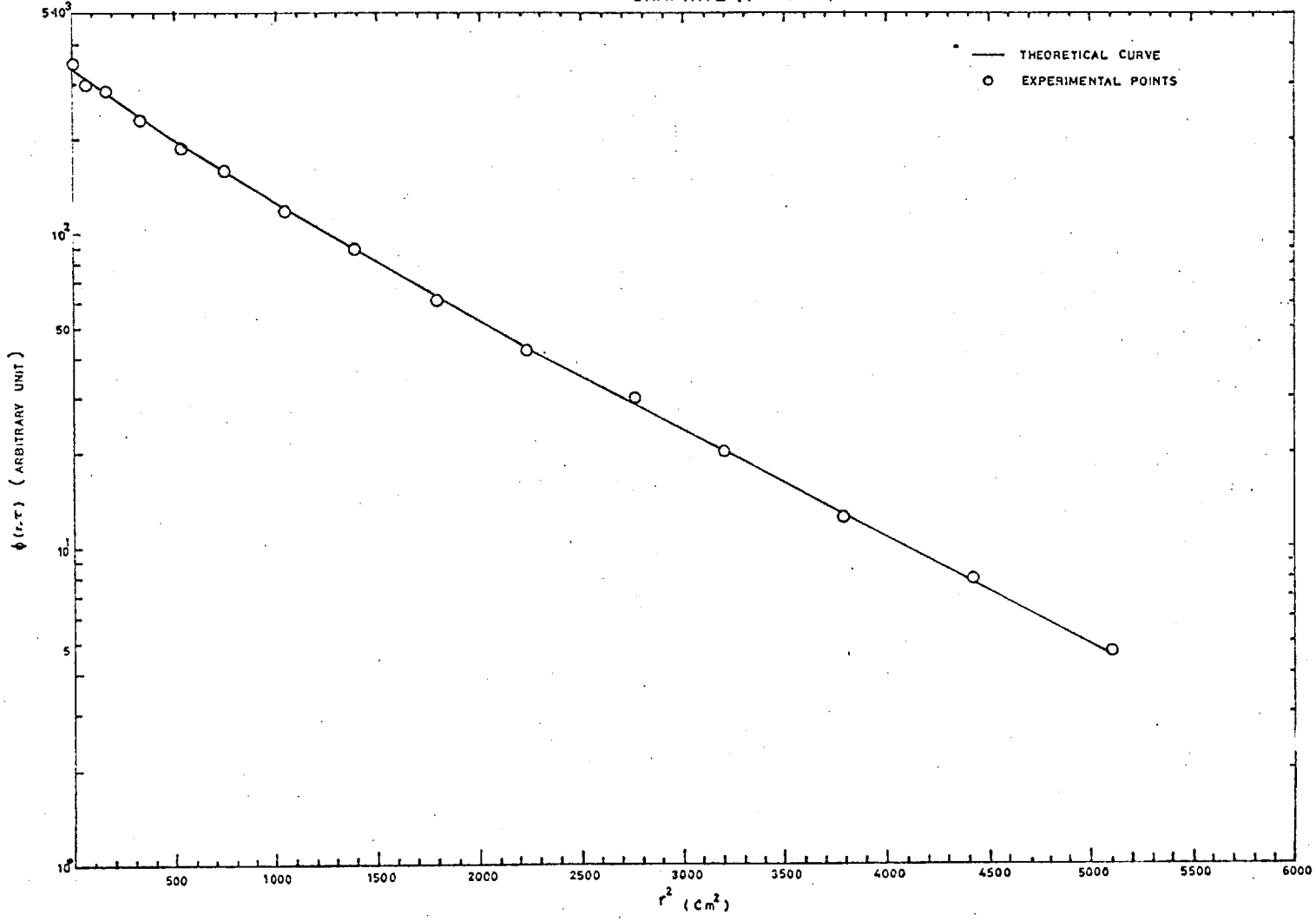

TABLE (T.4.2)

Spatial distributions (observed and calculated) of 1.46 e.v. neutron from Sb^{124}-Be source in graphite.

(Density of graphite = 1.751 gm cm^{-3})

Source-detector distance (cms) (observed)	Indium resonance flux (cps) (observed)	Indium resonance flux (cps) (calculated)
21.00	3.928	3.963
22.00	3.523	3.596
23.00	3.211	3.250
24.00	2.798	2.927
25.00	2.601	2.626
26.00	2.341	2.348
27.00	2.193	2.093
28.00	1.856	1.859
29.00	1.635	1.646
30.00	1.455	1.454
31.00	1.357	1.279
32.00	1.092	1.122
33.00	1.048	0.982
34.00	0.888	0.857
35.00	0.747	0.746
36.00	0.662	0.647
37.00	0.569	0.560
38.00	0.477	0.484
39.00	0.409	0.417
40.00	0.355	0.358
41.00	0.301	0.308
42.00	0.239	0.263

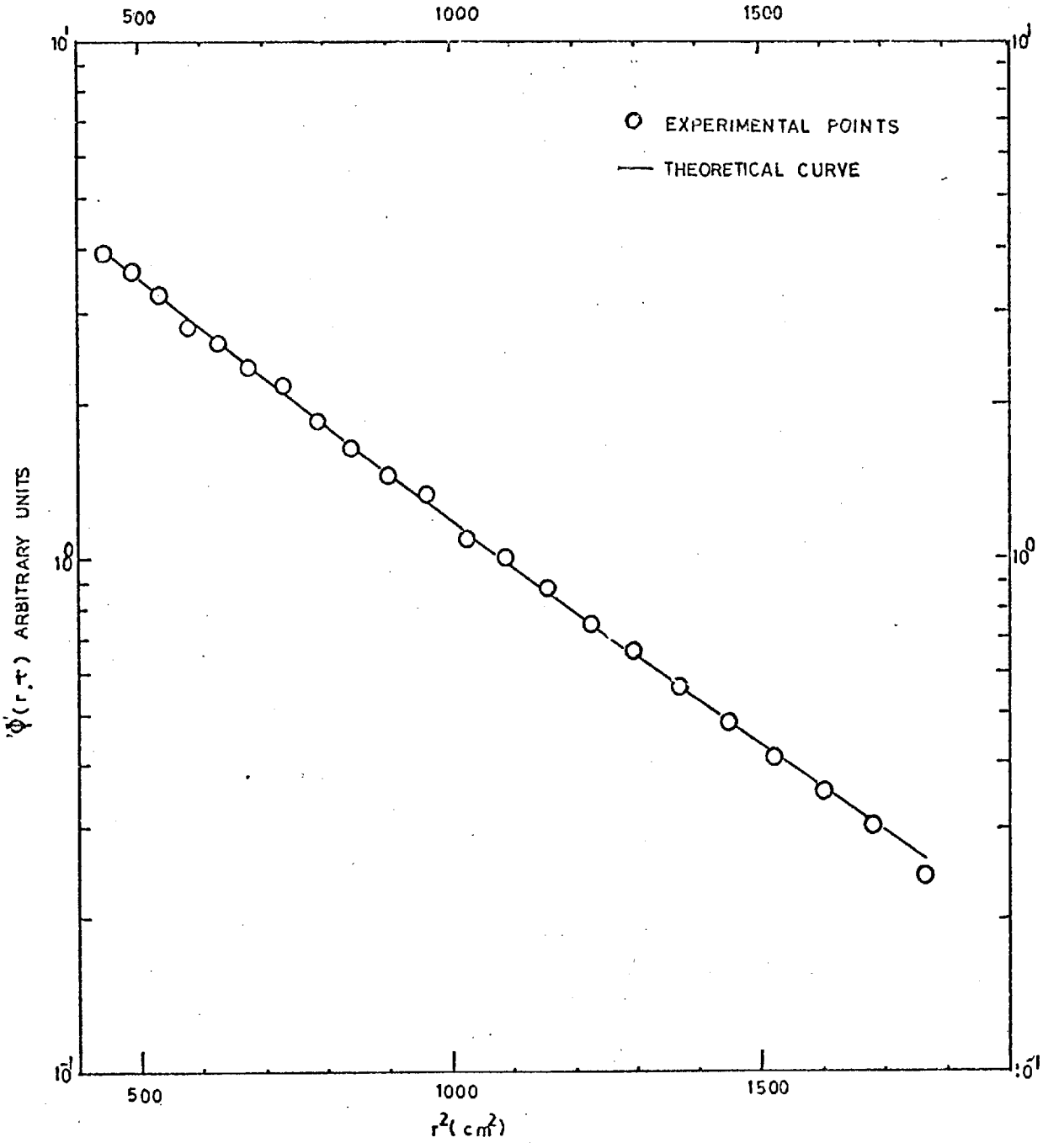

FIG(F.4.6) SPATIAL DISTRIBUTION OF 1.46ev. NEUTRONS FROM Sb-Be SOURCE IN GRAPHITE. ($\rho = 1.751$ gm cm^{-3})

TABLE (T.4.3)

Spatial distributions (observed and calculated) of 1.46 e.v. neutrons from a Ra^{226}-Be source in graphite.

(Density of graphite = 1.751 gm cm^{-3})

Source-detector distance (cms) (observed)	Indium resonance flux (cps) (observed)	Indium resonance flux (cps) (calculated)
14.50	18.803	17.712
17.50	16.252	16.017
20.50	14.751	14.262
23.50	12.745	12.507
26.50	10.565	10.803
29.50	8.978	9.194
32.50	7.590	7.711
35.50	6.484	6.375
38.50	5.441	5.198
41.50	3.980	4.180
44.50	3.227	3.318
47.50	2.470	2.600
50.50	2.009	2.012
53.50	1.494	1.539
56.50	1.149	1.163
59.50	0.887	0.870
62.50	0.645	0.643
67.50	0.442	0.380

FIG.(F.4.7). SPATIAL DISTRIBUTION OF 1.46 e.v. NEUTRONS FROM Ra-Be SOURCE IN GRAPHITE ($P = 1.751$ gm cm^{-3}).

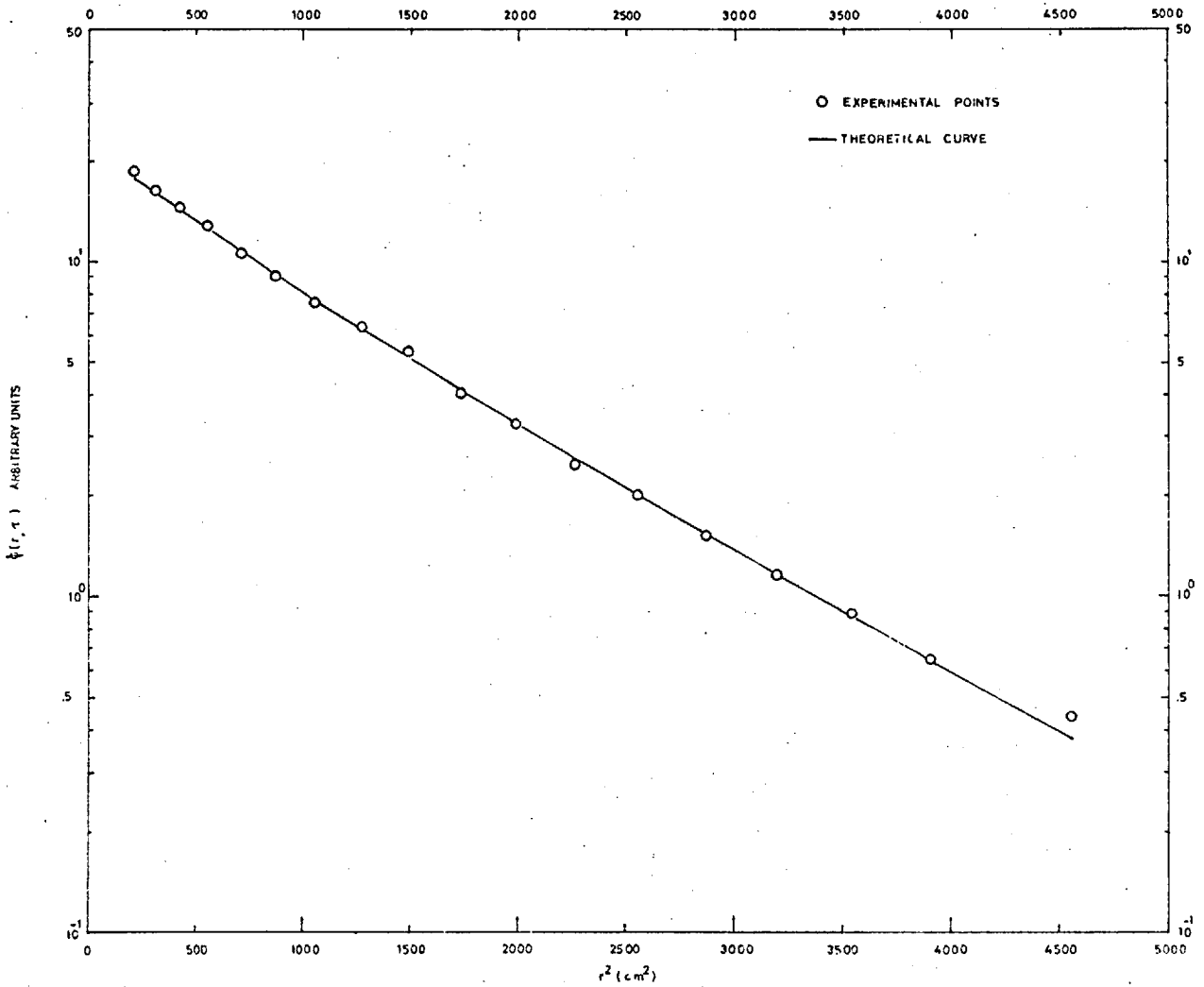

TABLE (T.4.4)

Spatial distributions (observed and calculated) of 1.46 e.v. neutrons from a Am^{241}-Be source in graphite.

(Density of graphite = 1.751 gm cm^{-3})

Source-detector distance (cms) (observed)	Indium resonance flux (cps) (observed)	Indium resonance flux (cps) (calculated)
11.00	17.313	16.033
14.00	15.266	14.833
17.00	14.055	13.522
20.00	11.704	12.146
23.00	11.278	10.754
26.00	9.167	9.386
29.00	7.866	8.076
32.00	6.850	6.854
35.00	5.381	5.737
38.00	4.882	4.739
41.00	3.595	3.864
44.00	3.012	3.110
47.00	2.542	2.473
50.00	1.925	1.943
53.00	1.590	1.509
56.00	1.153	1.159
61.00	0.719	0.729
66.00	0.478	0.445
71.00	0.320	0.265

FIG(F.4.8) SPATIAL DISTRIBUTION OF 1.46 e.v. NEUTRONS FROM Am-Be SOURCE IN GRAPHITE. (P=1.751)

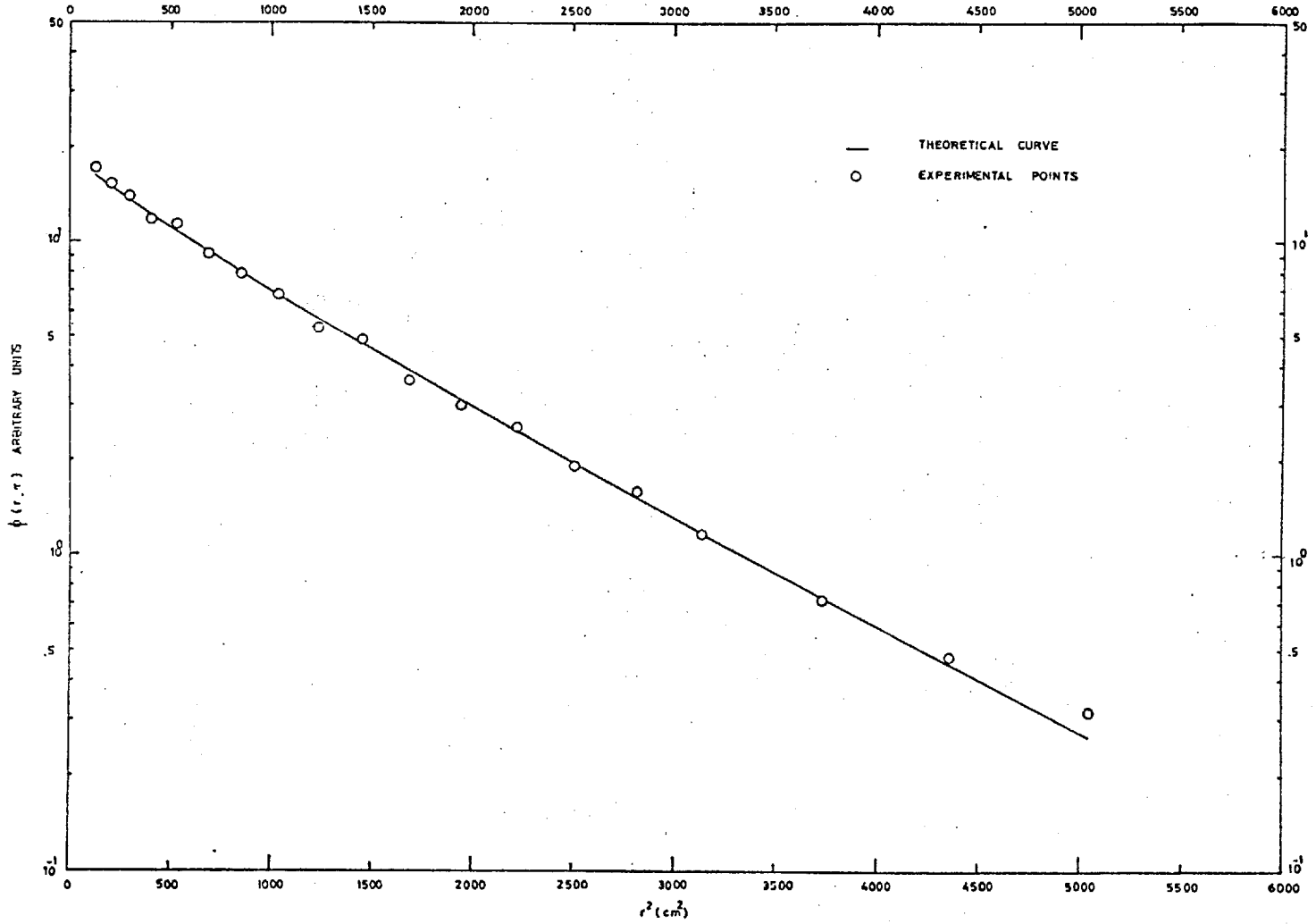

figures (F.4.5), (F.4.6), (F.4.7) and (F.4.8) show the observed points with the fitted curves in each case. Table (T.4.5) gives the summary of the values of neutron ages obtained in graphite of density 1.751 gm cm^{-3}

TABLE (T.4.5).

Experimental values of ages to 1.46 e.v. of neutrons from different sources in graphite. (density ρ = 1.751 gm cm^{-3}).

Source	Scintillators	Age (cm^2) (uncorrected)
Po^{210}-α-Be	NE 905	315.94 $\pm$ 4.19
Sb^{124}-γ-Be	NE 401	124.95 $\pm$ 1.36
Ra^{226}-α-Be	NE 401	300.67 $\pm$ 4.23
Am^{241}-α-Be	NE 401	322.69 $\pm$ 8.29

The effect of the random errors in the observations have been determined by the least-square fitting procedure. Systematic errors however could arise from the following.

(a) Error of distance measurements.

(b) Error from the neutron streaming along the cracks in graphite stack.

(c) Error from an inadequate moderator size.

and (d) Error from the effect of the non-1.46 e.v. energy resonances in indium.

The uncertainty in the source-detector distance amounts to less than 1mm, which contributes a possible error of less than 0.25 % in the value of τ.

The graphite blocks making up the stack were very accurately machined and carefully positioned. Any gap between them did not exceed 0.005". The clearance between the graphite sleeves and the plugs in the channels was within 0.004". This at worst, gives a fractional voidage of 0.002" and thus the experimental results could be too high by 0.4 % .

The effect of the finite moderator size was estimated by comparing the infinite medium and finite medium expressions for a simple Fermi theory. It was concluded that the value could be too high by not more than 0.5 % .

The thickness of the indium foils used was 0.010". In an activation experiment in a 1/E energy spectrum, as much as 15 % of the activation could be due to non-1.46 ev neutrons. In the slowing down experiment of this type

TABLE (T.4.6).

Ages to 1.46 e.v., of the neutrons from different sources in graphite. (Density ρ = 1.60 gm cm^{-3}).

Source	Present values Age. (cm^2).	Published values Age. (cm^2).Reference
Po^{210}-α-Be	381.5 $\pm$ 5	370 $\pm$ 20 (R.4.3) 416.1 (R.4.4)
Sb^{124}-γ-Be	151 $\pm$ 2	156.5 (R.4.5)
Ra^{226}-α-Be	363 $\pm$ 5	360 $\pm$ 10 (R.4.3) 380 (R.3.1)
Am^{241}-α-Be	389.5 $\pm$ 10	- -

the effect is considerably reduced because of the more rapid attenuation of the higher energy neutrons as the distance from the source increases. In the present method as the detector efficiency falls off quite swiftly with the increase of the neutron energy, the effect is further reduced. The additions of the distributions of the ages corresponding to non-1.46 e.v. and having the intensity of about 2 % of the main distribution would contribute to

the error on the measured value by about 1.1 % . Taking all these effect into consideration and the final values optimised to the standard graphite density of 1.60 gm cm^{-3}, are summarised (above) in the Table (T.4.6), along with other published results in each category.

CHAPTER 5.

EXPERIMENTAL DETERMINATION OF THE SPATIAL DISTRIBUTION OF THE RESONANCE ENERGY NEUTRONS IN WATER.

The age of fission neutrons in light water to energies close to the thermal region, is from the practical Reactor Physics point of view an important parameter. A discrepency of upto 20 % existed between very carefully computed values (R.2.1 to R.2.11) and its early experimental determinations (R.7.1 to R.7.5). The subsequent experimental values, (R.7.6 to R.7.12), of age in water seems to narrow down the gap between the experimental values and its theoretical estimates. The present determinations are undertaken to investigate it from a different experimental approach.

An account is given in this chapter of the equipmental details and some of the preliminary experiments done towards the measurement of neutron ages, using the University of London Research Reactor, CONSORT II. The purpose of the present series of experiments is determination of ages of fission neutrons to indium, rhodium, and gold resonance energies by a method (R.4.6) in which the measured quantity is the change in the counting rate produced due to the absorption of the neutrons of that resonance energy, when an epi-cadmium neutron sensitive

scintillation counter is covered with foil of the resonance absorber. The experiments also aim at proving the usefulness and validity of this method for a wide range of age measurements and thus establishing its status as an alternative technique which is quicker and positively less cumbersome than the foil activation method.

5.1. GENERAL EQUIPMENTAL DETAILS

The principle underlying the equipmental design is to eliminate as far as possible for the corrections to the spatial distribution measurements such as the considerations of size of the moderating medium, the intensity and the dimensions of the fission source, detector size etc. These aspects together with other considerations are dealt in greater detail later in this thesis.

The experiments to be described were done using the vertical access of the dual faced thermal column of CONSORT II. The experimental tank was placed inside the 'cave' formed in concrete biological shield of reactor. The thermal column is partially filled in design (R.5.1) and the face of the vertical access is square 36"x 36" with the nominal thermal flux of $10^9 n/cm^2/sec.$, at full power (100 kw), and the fast flux about 5 % of this value. In order to improve thermal to fast ratio, a ducted slab of paraffin wax 4" thick and of same lateral dimensions as

the face of the thermal column, contained in an aluminium can, on an aluminium base-plate which supports the weight of the entire equipment over the concrete ledges of the thermal column.

The equipment basically consists of a large aluminium tank 36"x 36" and 52" high, containing demineralised water upto a height of 45". The tank is covered on all sides and the bottom with cadmium sheet 0.020 inch thick, except for a 10" diameter aperture in the centre of the cadmium covering the bottom of the tank. An aluminium framework is provided to support the tank and also to house the cadmium shutter arrangement. Figure (F.5.1), gives some idea of the setting of apparatus in the cave.

5.2. THE FISSION SOURCE

A fission source was constructed from twelve foils of Uranium-Aluminium alloy 0.010" thick containing 25 % Uranium by weight. The uranium content was enriched to 80 % in U^{235}. The foils were obtained from the United Kingdom Atomic Energy Authority, Risley. These were available in 2" wide strips. Twelve such strips were used in two layers of 12"x12" each 0.010" thick placed one on top of the other. The strips were laid side by side in each layer but the direction of the strip in the top layer was made at right angles to the lower one,

(in a parallel plane) to provide the maximum uniformity possible as regards the number of uranium atoms per unit volume. The total weight of uranium was 39.88 gms in the alloy.

The fission source is housed in a water-tight can of aluminium. This consists essentially of three aluminium plates each 14" square. The can has two compartments, each one individually water-tight and independent of the other. The top compartment contained the fission source (described above) and a cadmium sheet 0.020" thick covering the fission source on top. The lower compartment contained a cadmium sheet 12" x 12" and having a central circular aperture of 10" in diameter. The lower compartment of the can could be openned without dislodging the upper compartment. The arrangement is shown in figure (F.5.2). Different cadmium sheets having circular apertures successively of 8" and 6" diameter concentric with the first one (10" dia.), were used for different observations for changed effective source sizes. The source could only be triggered by the neutrons comming from the thermal column via the circular aperture as the fission source is screened off from the slowed down neutrons from within the experimental tank. The canned fission source was fixed to a light rectangular framework constructed from aluminium T-section, which secures the source at the bottom of the experimental tank.

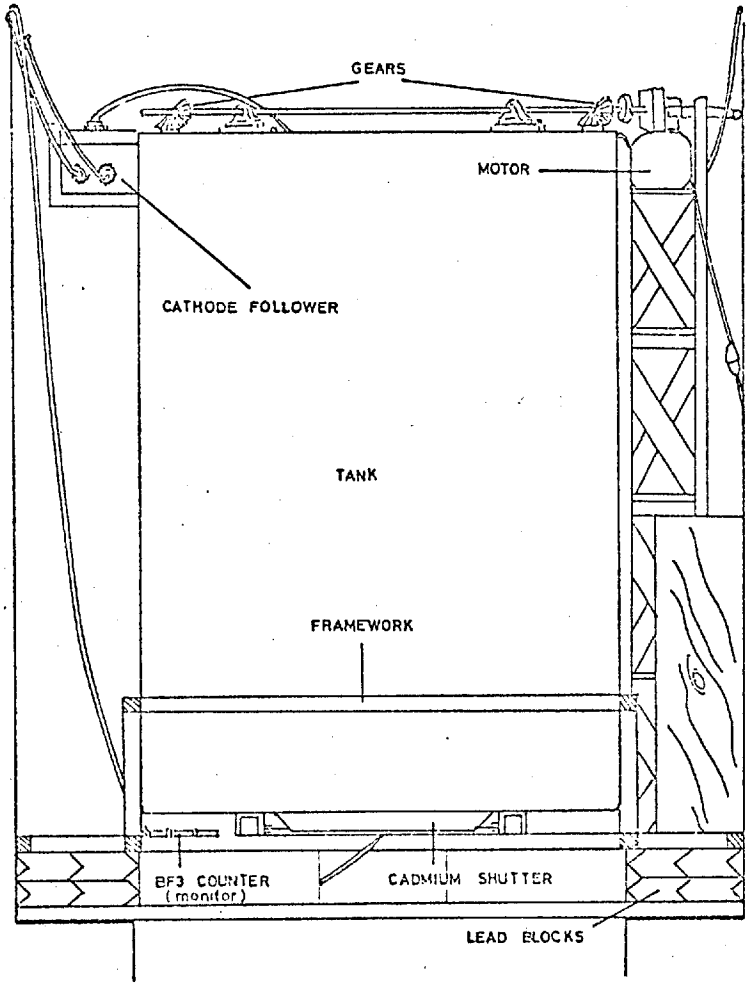

FIG (F.5.1) VERTICAL ACCESS OF THE THERMAL COLUMN AND THE EXPERIMENTAL EQUIPMENT.(elevation)

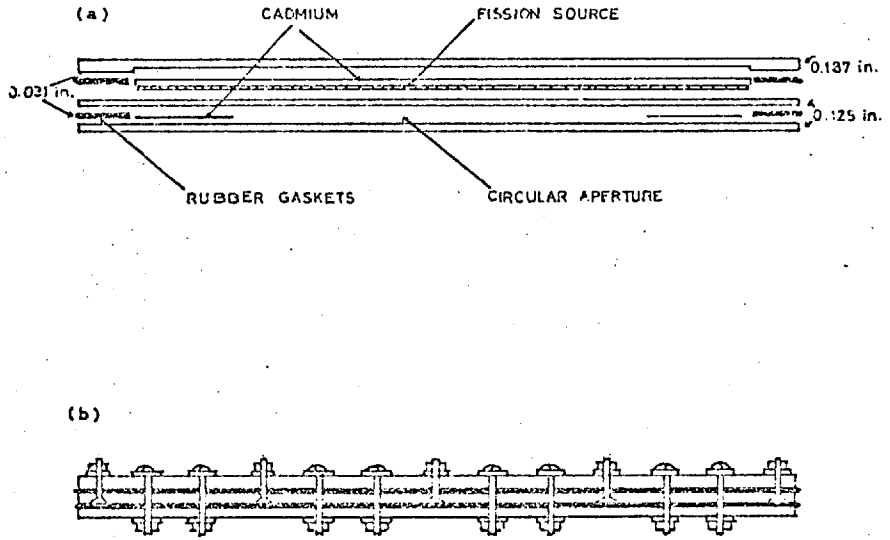

FIG (F-5-2) THE FISSION SOURCE

(a) A BLOWN UP SECTION OF FISSION SOURCE AND ITS CAN

(b) A SECTION OF THE CAN SHOWING THE ARRANGEMENT OF SCREWS

5.3. THE CADMIUM SHUTTER AND THE TANK HOUSING FRAMEWORK.

To correct for the effect of the fast neutrons entering the tank and being slowed down to the detector energies, a cadmium shutter is used in order to repeat the measurements when the fission source is not triggered by being screened off from the thermal neutrons.

The cadmium shutter was constructed in the form of a tray with its sides curving upwards at an angle of 45°, just scraping the bottom of the tank. This is intended to prevent the fission source being triggered by any scattered stray neutrons which could enter obliquely if there was a gap, when cadmium shutter is in the source 'covered' position.

The cadmium shutter is 13" x 13" in dimensions and consists of 0.020" thick cadmium sheet sandwitched between 1/16" thick aluminium sheets. This shutter is framed on three sides in 'TUFNOL' cut in a shape of a 'rectangular' figure of 'U'. The Tufnol frame carrying the shutter can slide quite frictionlessly in guide-rails made from 1/4" aluminium channel. The movement of the cadmium shutter is affected from outside the biological shield of the reactor, by remote control. Two 'BOWDEN' cables have been used. One end of each is connected to

the opposite ends of the shutter frame and the other two ends of these cables to the control wheel via two drums. These cables are wound on the drums carrying the control wheel, in opposite directions so that as the control wheel is turned, the drum winds the 'inner' cable and unwinds the other by an equal amount. The exact positioning of the cadmium shutter for the 'source bare' and 'source covered' positions is achieved by locating two micro-switches on the frame work at the pre-set end positions, of the shutter traverse and indicating on the instrument control pannel by lighting the appropriate lamps.

The tank housing frame-work which supports the experimental tank and also incorporates the cadmium shutter housing and its attachments, is made from 1" square cross-section aluminium tubing ('Speedframe', Dexion Ltd.). This frame, the outside dimensions of which are 54" x 46", rests on a 4" layer of canned slab of wax, (ducted), surrounded by antimony-free lead blocks, (purity 99 %), on the base plate. Fig (F.5.1) includes the tank housing frame-work and fitted cadmium shutter arrangement.

5.4. THE TRAVERSING MECHANISM

A light scintillation assembly is capable of

traversing in a vertical direction on an axis passing through the centre and perpendicular to the plane of the fission source. The traversing mechanism for the counter consists mainly of two stainless steel lead-screws 1" in diameter and having a square thread of pitch 5 mm. PTFE bearings (Glaciar 'DUG') were used with lead screws to minimise friction. Each of the two stainless steel screws had a phosphorus-bronze nut. A bridge construction was made from stainless steel and 'dural' bars of 0.5" x 1" cross-section, to go over the nuts of the lead screws. The stainless steel bits in the bridge were included to avoid a direct contact of 'dural' and phosphorus-bronze in water, which results in corrosion of aluminium and dural structures even in dimineralised water, (effect being more pronounced in ordinary water). The idea of having vertical ends of the bridge raised from the nuts and then clamping down the counter from the central bar is to avoid having the structural materials in vicinity of the detector. The movements of the traversing mechanism is affected by driving the two lead-screws simultaneously via a single drive shaft and two pairs of gears situated at the top of the tank. A single phase, permanent capacitor type, forward and reverse electric motor type SD15 (M.R. Supplies Ltd.) was used for this purpose. This was a slow speed (10 rpm) and high torque (75 lb-in) motor which ensured a precise control in stopping at the required places (section 5.5). The counter moves upwards

FIG(F-53) THE TRAVERSING MECHANISM

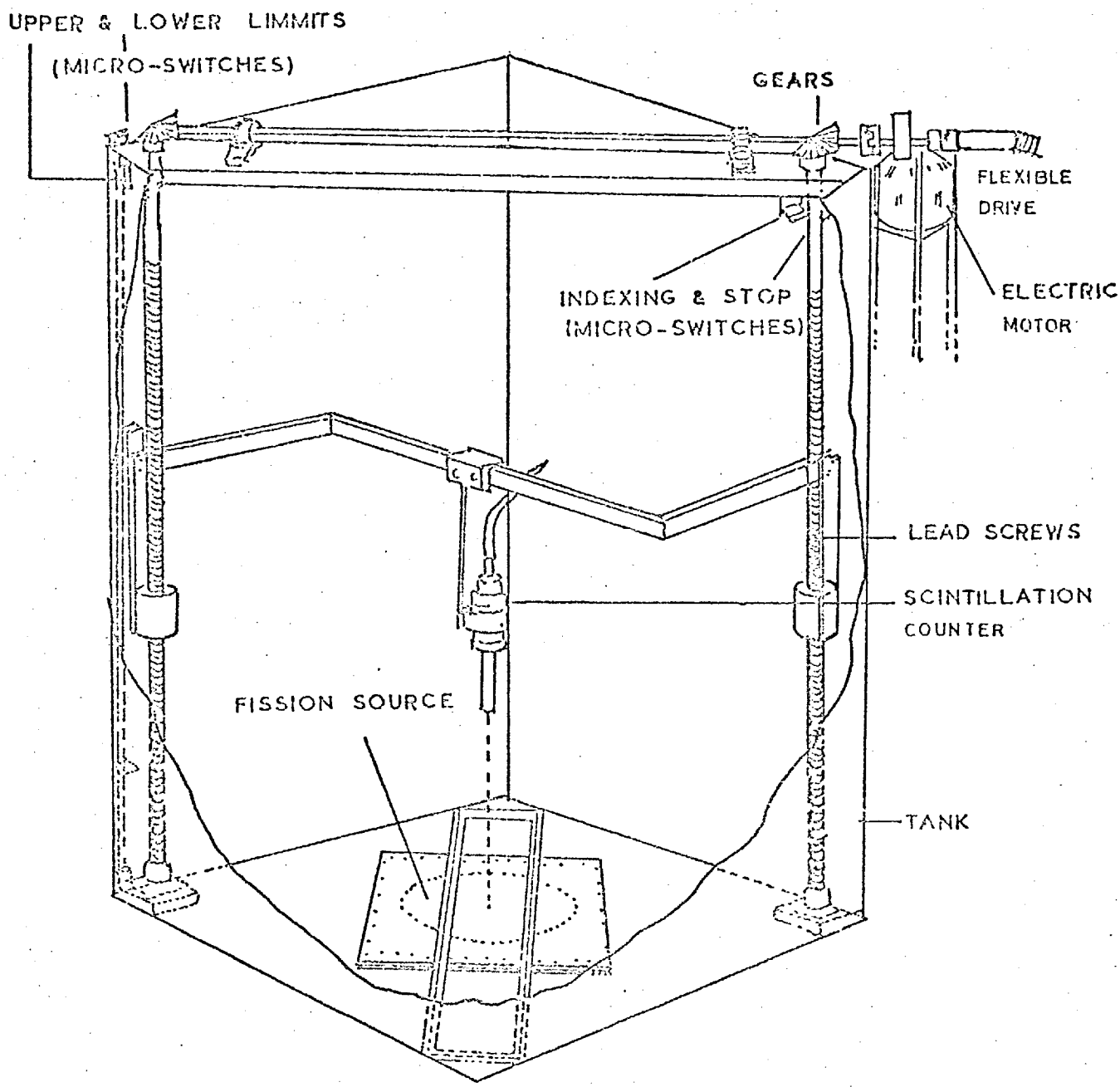

or downwards vertically as the screws are being rotated in one way or the other. Figure (F.5.3) shows the traversing arrangement in the tank.

5.5. THE CONTROL OF THE INSTRUMENTATION

Figure (F.5.4) shows the circuit diagram of the instrument control system. The electric motor driving the traversing mechanism is made capable of stopping at the end of one complete revolution when set at 'Auto-stop' and can go from one end position to the other extremity of its traverse when set at 'Non-stop'. This, however, could be stopped at the end of any required revolution by switching over from 'Non-stop' to 'Auto-stop'. This auto-stopping being achieved by tripping the motor by a roller type micro-switch which is actuated mechanically at each revolution by a cam attached to one of the lead-screws, whereas when set at 'Non-stop' overrides this tripping action. A similar micro-switch is used to index the number of revolutions and hence the vertical distance of traverse. An E.N.M. electric impulse digital counter, forward and reverse type was used, the change of polarity, to add or to subtract the counts, being affected through a relay, when motor direction is reversed. Micro-switches are used to trip the motor when pre-set extremities of the counter traverse are reached. The tripping of the upper limit is quite straightforward but for lower limit

FIG(F.5.4)CIRCUIT DIAGRAM OF THE CONTROL SYSTEM

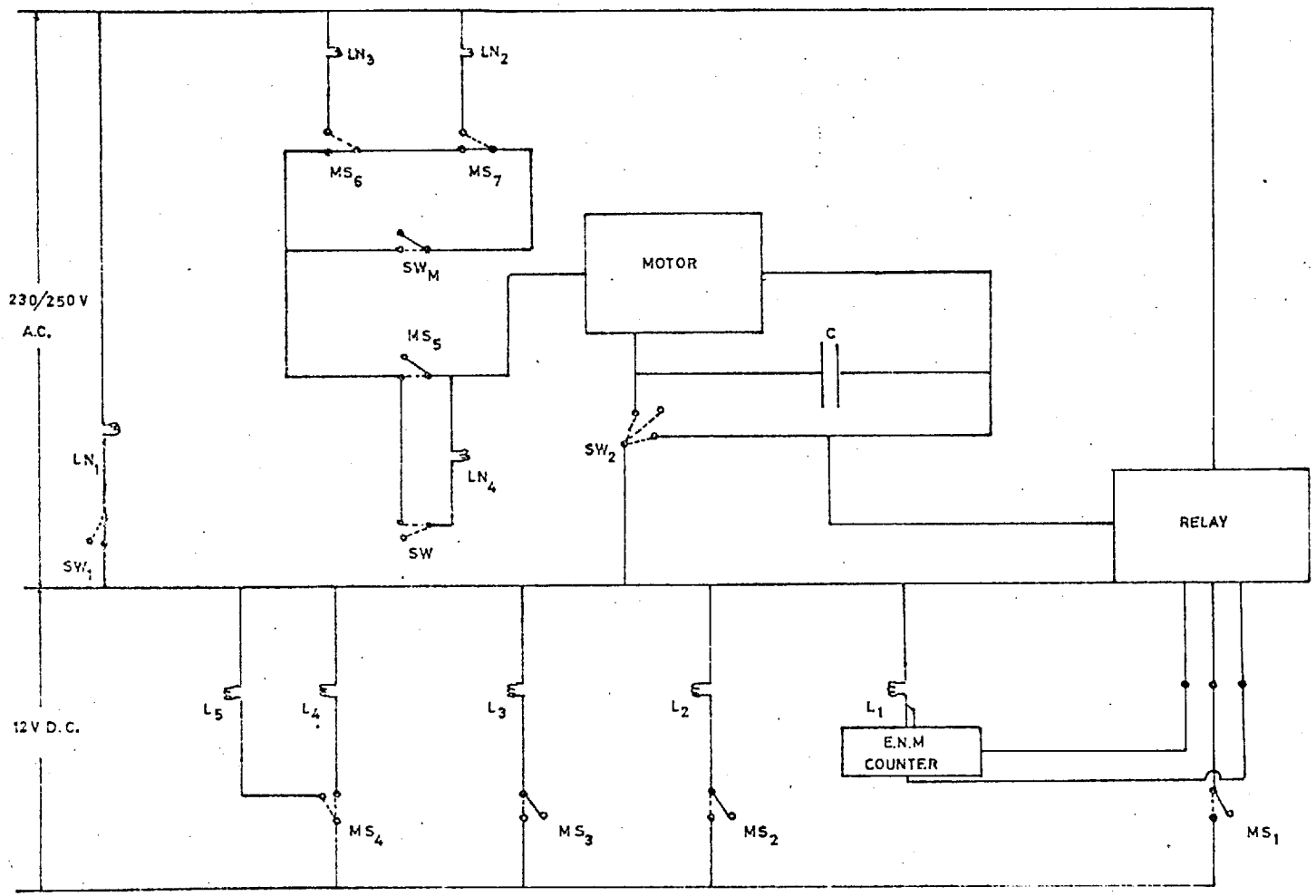

LAMPS

12 VOLT D.C.

L1 REVOLUTION FLASHER.
L2 SOURCE BARE.
L3 SOURCE COVERED.
L4 WATER LEVEL CORRECT.

MAINS(neon lamps)

LN1 MAINS.
LN2 LOWER LIMIT.
LN3 UPPER LIMIT.
LN4 AUTOSTOP/NONSTOP

MICROSWITCHES

MS1 REVOLUTION INDEXING.
MS2 SOURCE BARE.
MS3 SOURCE COVERED.
MS4 WATER LEVEL.
MS5 AUTOSTOP PER REV.
MS6 UPPER LEVEL.
MS7 LOWER LEVEL.

SWITCHES

SW1 MAINS.
SW2 MOTOR (forword/reverse)
SW3 AUTOSTOP/NONSTOP.
SWM MASTER SWITCH.

tripping is realised by the nut on the lead-screw, when moving down, pressing on the perspex spindle positioned appropriately for the lower limit on a spring-loaded aluminium tube positioned vertically, with the top part connected to a lever micro-switch fixed at the top of the experimental tank. The positions of the limit switches as well as indexing switch are displayed in fig (F.5.3).

To keep a check on the water level in experimental tank a combination of a float ball system and a lever-microswitch was used. This was duely indicated on the instrument control pannel.

5.6. THE DISTANCE MEASUREMENT, CALIBRATION AND ACCURACY

The vertical distance moved by the counter is known directly from the number of revolutions knowing the pitch of the lead-screws. The uniformity of the pitch was checked by a series of measurements made using a catheto-meter and an avometer by an electrical contact method each time moving through a known number of revolutions. These measurements were made over a range of about 70 cms. from the bottom of the tank. This was the region over which screws were likely to be used during the experiments. The pitch of the lead-screws were found quite uniform, well within the statistical accuracy of the measuring instruments.

The lower limit of the traverse, when the counter is just in contact with the fission source was made as near as possible to the starting of the first revolution by adjusting the length of the clamp from the bridge as lower limit micro-switch is actuated. This was checked further successively by moving the mechanism through a revolution and measuring distance by interposing accurately known thicknesses and feeler gauge. It was found that it was not quite possible (within a reasonable number of attempts) to coincide precisely the lower limit and the starting point of the first revolution. The difference however, was very accurately known for the purpose of applying correction to the apparent distance measurements.

To check for the stopping accuracy, the automatic tripping was marked each time on the cam for a large number of revolutions, the pitch of the screw being 0.5 cms. represents an uncertainty in the position of the detector as 0.002 cm. Care was taken to take all observations with the counter moving in the same sense so that the same end of the cam actuates the micro-switch. An overall accuracy of better than 0.003 cm is achieved in distance measurements.

The distance measurement accuracy was checked again for the second bridge arrangement for the second series.

5.7. THE TEMPERATURE CHECK

The vertical access of the thermal column was screened off by asbestos sheet from the horizontal access where an experiment with a heated moderator was in progress. In order to keep a check of any rise in temperature of moderator in the present experiment against the possibility of an accidental leakage of heated vapours from the neighbouring experiment, three 'chromel-alumel' thermo-couples were installed at three different regions of the experimental tank. No temperature rise however was observed.

5.8. THE NEUTRON DETECTOR AND THE SCINTILLATION ASSEMBLY.

The scintillator used in the present series of experiments was similar to the one used for Radium-Berylium and Antimony-Berylium sources etc.(chapter 4), as neutron measurements in a high background of gammas is required. A half an inch diameter boron polyester detector (enrichment 90 % in B^{10}), Nuclear Enterprises type NE 401 and a Twentieth Century photomultiplier tube type BMS 10/14 B were used. A light-guide was constructed from perspex, tailored to a logrithmic spiral (R.5.2), with an input end of 12.75 mm diameter of the same size as the scintillator and the output diameter of 19 mm

matching the photomultiplier tube end. The photo-multiplier tube has ten stages for which a voltage dividing net-work of eleven 330 KΩ resistances was constructed. A water-tight and of course light-tight assembly was constructed from 'dural' to house the scintillator, light-guide, the photomultiplier tube and allied electronics. The details of the assembly are shown in figure (F.5.5).

5.9. THE NEUTRON COUNTING SYSTEMS

The scintillation counter described above was used in the main counting channel. In order to monitor the possible fluctuations in the reactor power a boron tri-floride (BF_3) counter (Twentieth Century Electronics type 5B40/6) was used. This counter was suitably clamped to the tank housing framework over the thermal column. The counter was covered partially with a cadmium sheet having a window, the size of which was adjusted such that the count rate was comparable to the count rate of the main counting channel of about the mean of the maximum and the minimum count rates, under various controlled conditions of flux measurements. The order of this count rate was chosen to be about 6000 cps. This being convenient for the measurements with the main counting channel with the detector at near or at greater distances from the fission source. The counts were taken for a pre-set time, the

value of which increased for both as scintillator count-rate falls as the source-detector distance increases. A cathode follower type NE 5202 A, (Nuclear Enterprises), was used with scintillation counter and a head-amplifier type 1430 A, (Dynatron Electronics Ltd.), with the BF_3 counter, the former being clamped, insulated, outside near the top of the experimental tank and the latter was placed just outside the cave shielding. This was to keep them away as possible from the high radiation area at the same time without any significant loss in the signal values by using unduly long cables between the detectors to the pre-amplification stages. A block diagram of the overall counting systems is included in the figure (F.5.7) and the details of the electronics used for the counting channels are given in Appendix (A.5.1). The electrical supply for all the units in both channels came from the two identical sets of constant voltage transformers and low pass filters, the latter being designed to filter out the mains borne interference.

5.10. THE SHIELDING ARRANGEMENT

In accordance with the requirements for the present experiment, the shielding arrangement of the whole thermal column was modified in conjunction with the requirements of the experiment at the horizontal access. Fig (F.5.6), show the arrangement used for the vertical access of the

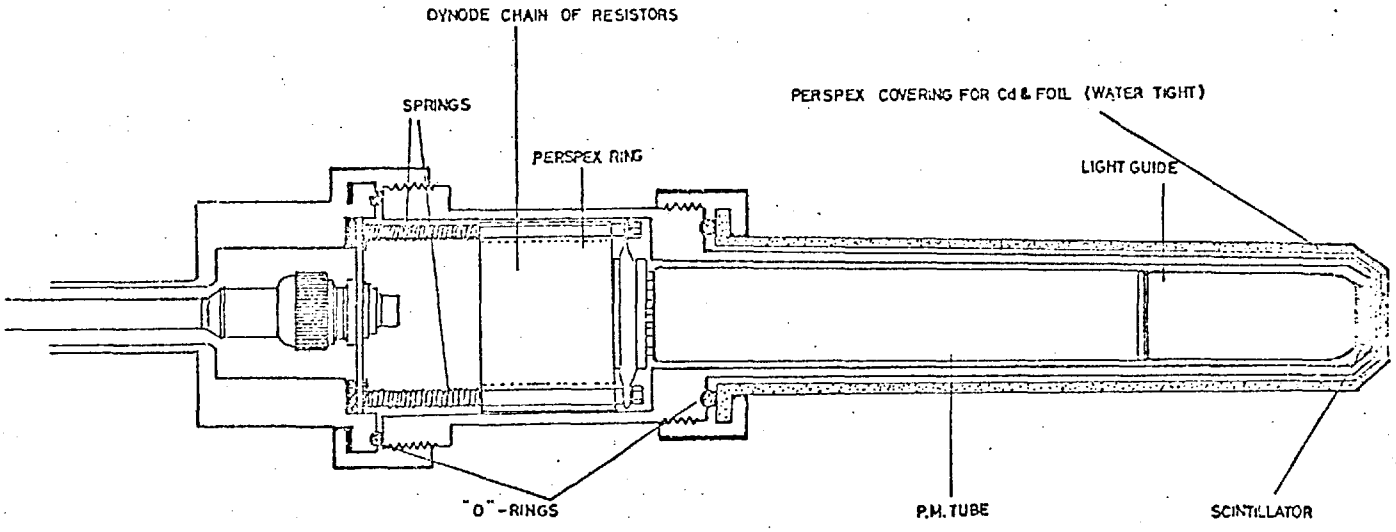

FIG(F.5.5) SCINTILLATION ASSEMBLY

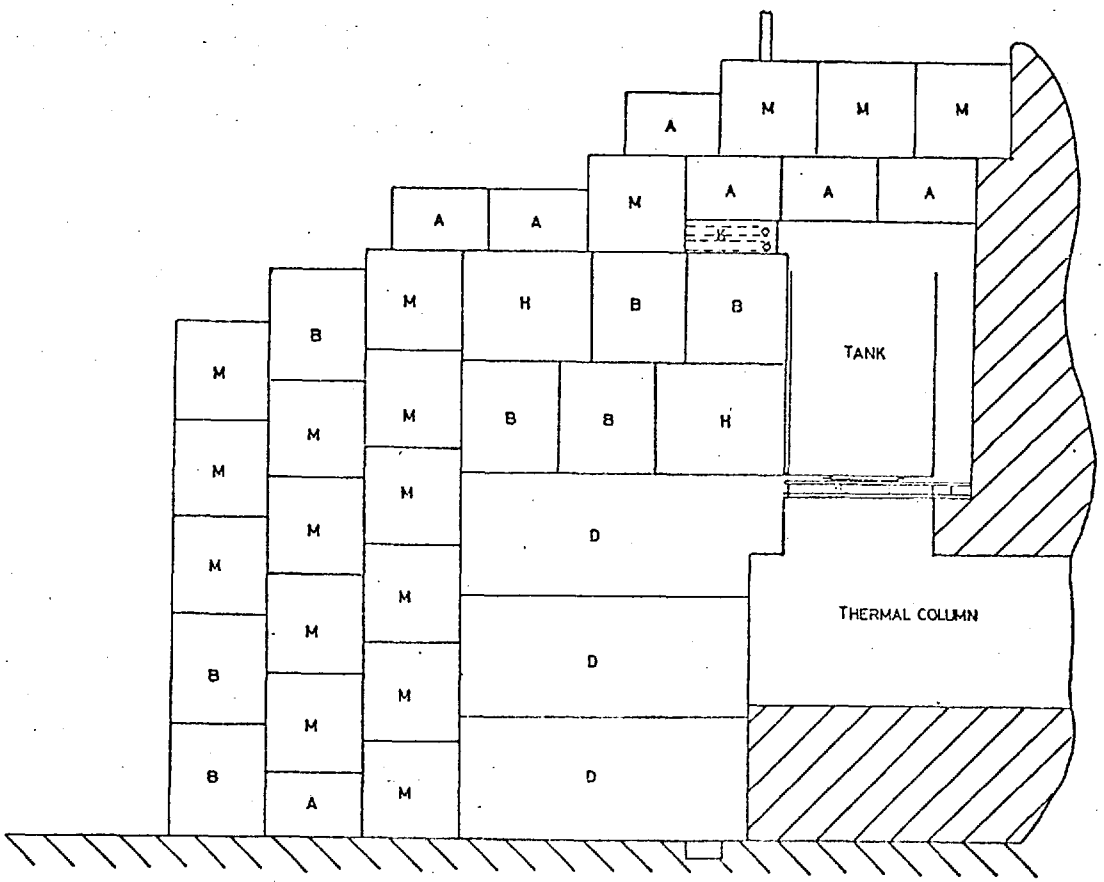

FIG(F.5.6) THE SHIELDING ARRANGEMENT

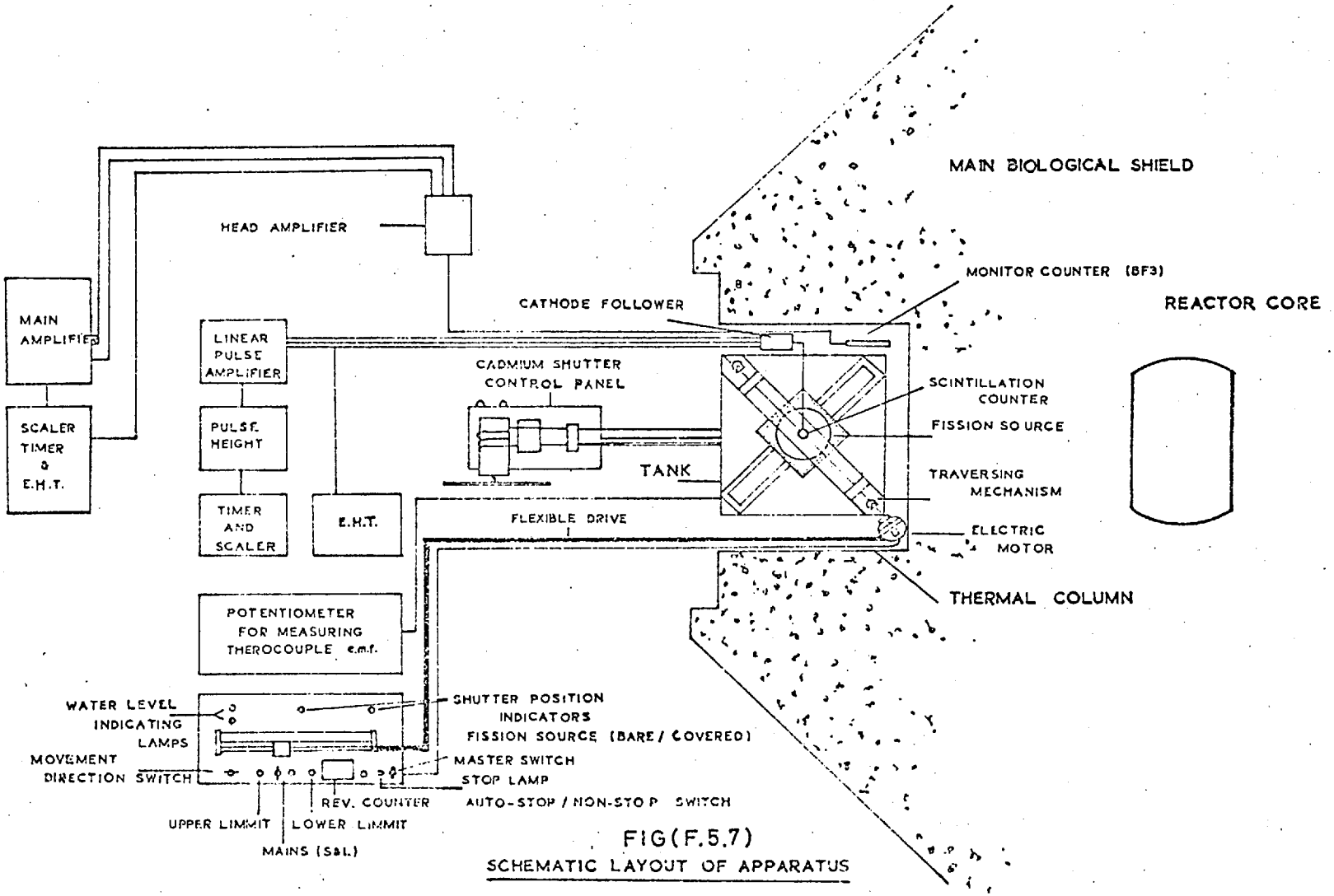

FIG (F.5.7)

SCHEMATIC LAYOUT OF APPARATUS

thermal column. The block 'K' was also introduced in the system which has four, two inch diameter curved conduits, from where the cables the flexible drive and the 'Bowden' cables reached the counting racks and the instrument desk in the reactor hall.

5.11. THE PRELIMINARY EXPERIMENTS

It is necessary that the thermal flux striking the fission source be symmetric about the centre of the disc source. A preliminary check was made for the shape of the flux emerging from the vertical access of the thermal column. This was done by irradiating gold foils and then determining their activities with the Geiger-Muller counter. The foils were 0.002" thick and of diameter of 0.25". These were taped on to a sheet of polythene, arranged at intervals in the form of a cross. The irradiation was done with the polythene sheet stretched at the bottom of the tank. This was done with 'shutter open' position and of course without water in the tank and in the absence of the fission source. The resulting activities showed a cosine type of distribution symmetric with the centre of the experimental tank. This ensured that any further alignment of fission source was not necessary as the frame work ensured symmetric positioning with respect to tank.

The ideal conditions for a slowing down experiment

is to have the source of fission neutrons situated at the centre of the moderating medium. But this results in weakening of the source because of the reduction of the triggering thermal neutrons. A check was however made by positioning the fission source 4 inches above the water boundary by propping up the source carrying framework on two aluminium blocks. The intensity of the fission source in this position was reduced to about 8 % of the value with the same source at the bottom of the tank. Intensity being vital in the age experiments all the subsequent work was performed with the fission source positioned at the bottom of the experimental tank.

Since in the present method of resonance flux determinations, a difference of measurements is required, a careful attention was given towards the stability of the scintillation counter. The response curves were checked, before, after and at times during each experiment. A typical set of response curves for the three controlled conditions of the neutron flux together with the response curves due to a Cobalt^{60} gammas and the electronic noise are shown in fig (F.5.8). The choice of the optimum conditions for the response curves was found from a few trials obtained by varying the amplification gain, the criterion being the maximum possible neutron-to-gamma response. The ratio which can be increased at higher bias settings with relatively little loss in the neutron

FIG (F-5-8) RESPONSE CURVES

NE 401 10 cms. AWAY FROM THE FISSION SOURCE

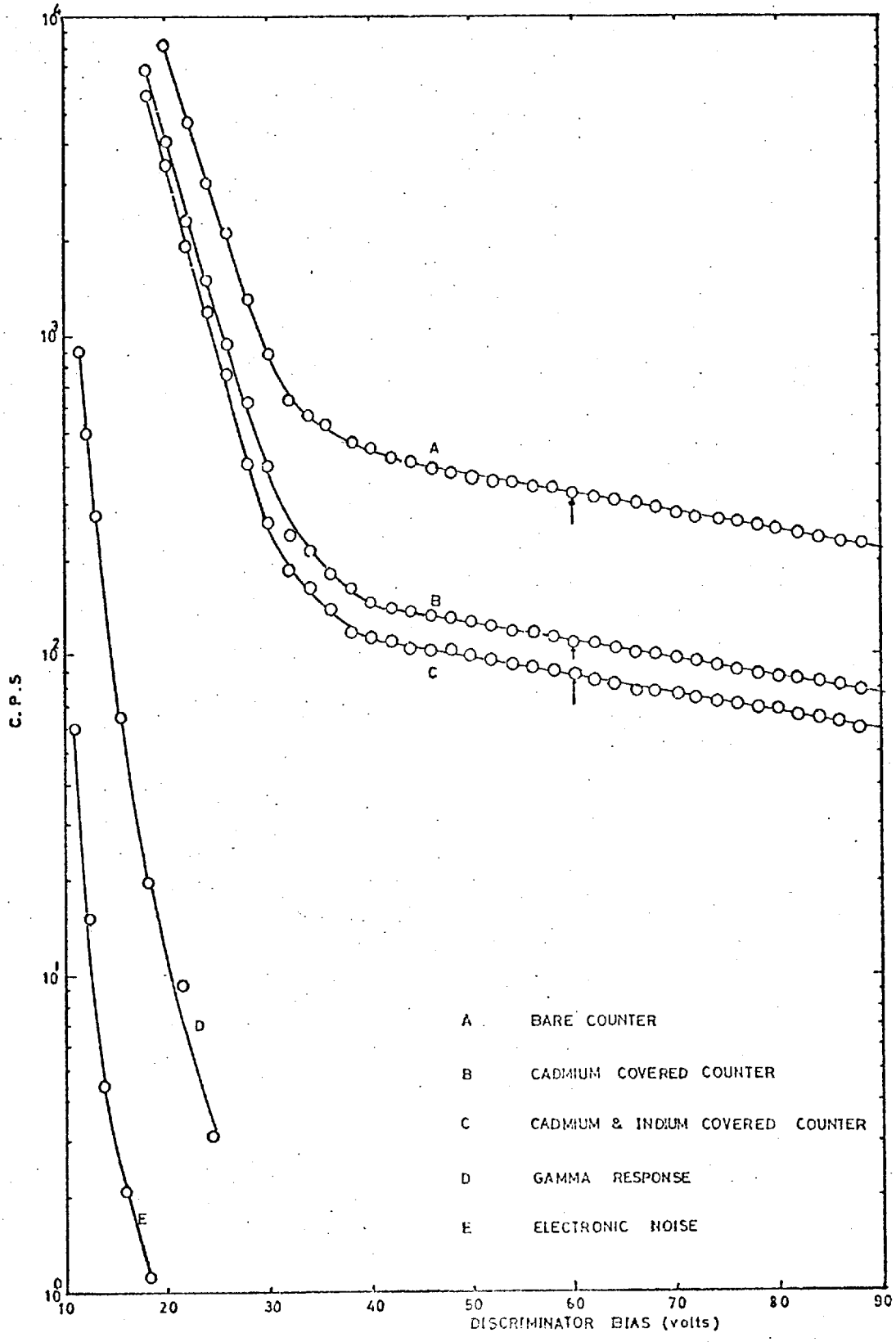

efficiency. The mid-point of BF_3 plateau was chosen for the E.H.T. setting for the counter. As mentioned above in section (5.9) the size of the window of the cadmium cover over BF_3 was adjusted untill the desired count rate was achieved. The plateau of this counter was also frequently checked for stability.

A series of 'Dead-time' measurements were carried out over a wide range of count rates by a step wise variations of the reactor powers. A total of sixteen sets of observations with varying number of data points (reactor powers) at various distances from the fission source were taken. The range covered in these measurements was of high and medium count rates because it is this region where the correction is most significant. For the 'Dead-time' measurements of the monitor, a total of twenty-nine sets of observations were taken varying only the number of data points (reactor powers). The results and the analysis of the dead-time calculations are presented in section (6.2) in chapter 6.

5.12. THE BASIC MEASUREMENTS OF FLUXES

To determine the spatial distribution of the resonance neutron flux about the fission source, a set of six observations under various controlled conditions were taken. The sequence of observations listed below gives

a complete record of the events from which resonance flux of the slowed down neutrons from the source can be extracted, corrected for the background. The observations were,

(1) Cadmium shutter off (source bare)

a) Scintillation counter (Cd. + resonance absorber covered).

b) " " (Cd.) covered only.

c) " " bare.

(2) Cadmium shutter on (source covered)

d) Scintillation counter (Cd. + resonance absorber covered).

e) " " (Cd.) covered only.

f) " " bare.

These observations were taken successively with resonance absorbers as Indium, Gold and Rhodium foils, using fission source of 10" diameter. The above mentioned flux measurements with Indium were also taken using the effective fission source diameters of 8" and 6", successively by using appropriate cadmium apertures as described in section (5.2).

The observations with both the channels were taken for pre-set times of 100, 300, and 1000 seconds for the scintillation counter covered and 30, 100, and 300 seconds when it is bare, the times refering to counter positions as near, at the middle distance, and away from the source.

The units in both the channels started manually at the same instant by operating the starter buttons together. This procedure was necessary as it was not possible to cross-connect the two channels for an automatic transfer of start and stop pulses. The individual channels, however stopped automatically after the elapse of the same pre-set times.

The flux traverses were taken from the nominal zero position to over 40 cms. away from the fission source in the vertical direction. This was done in steps of 0.5 cms. for the near and middle distances. The interval was increased to 1 cm and 2.5 cms at greater distances from the fission source.

5.13. EXPERIMENTS TO CHECK THE UNIFORMITY AND SYMMETRY OF THE FISSION SOURCE

After the fission source had 'cooled' down considerably, having been irradiated during the experiments, an attempt was made to investigate the uniformity and the symmetry of the fission source by measuring the residual activity by β-counting with an end-on Geiger-Müller counter. Since the various concentric rings irradiated for different periods during the experiments, with the central 6" diameter circle having the maximum irradiation and the outer ring the minimum, so a symmetric fall in

FIG(F.5.9) FISSION SOURCE :- POSITIONS OF MEASURED AND CALCULATED β-ACTIVITY

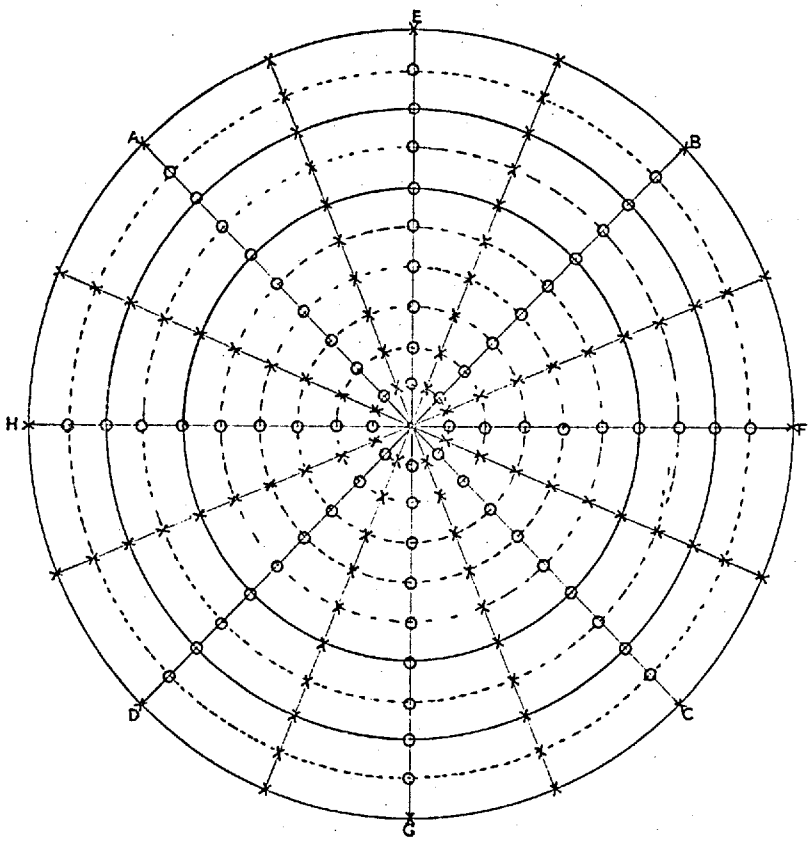

FIG. (F.5.10) FISSION SOURCE :- LINES OF EQUAL ACTIVITY

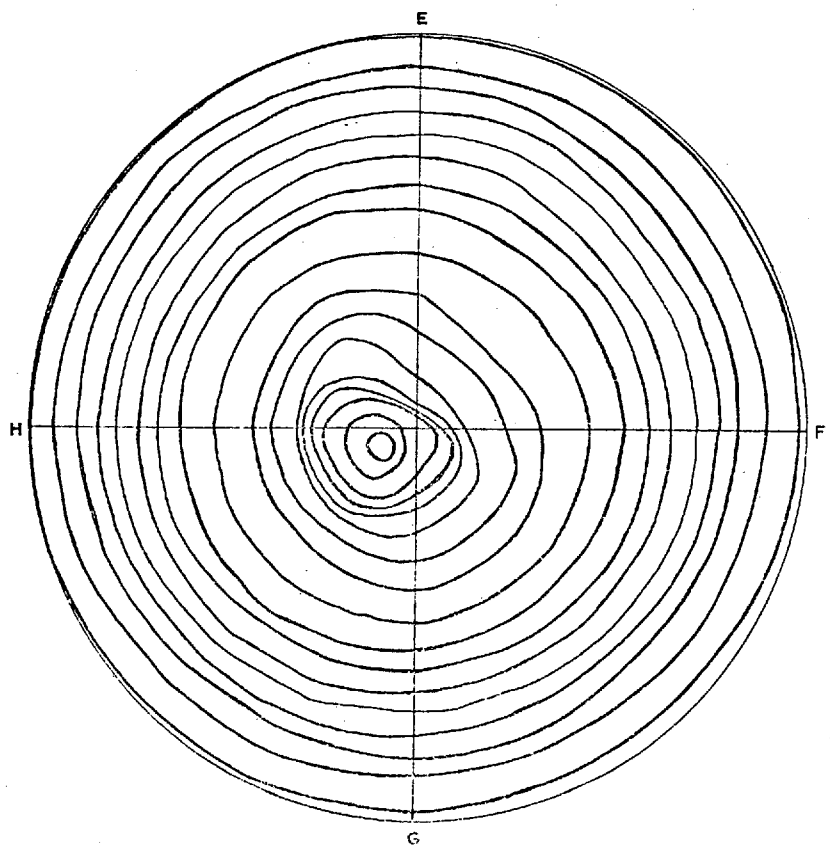

FIG (F·5.11) FISSION SOURCE β-ACTIVITY CURVES

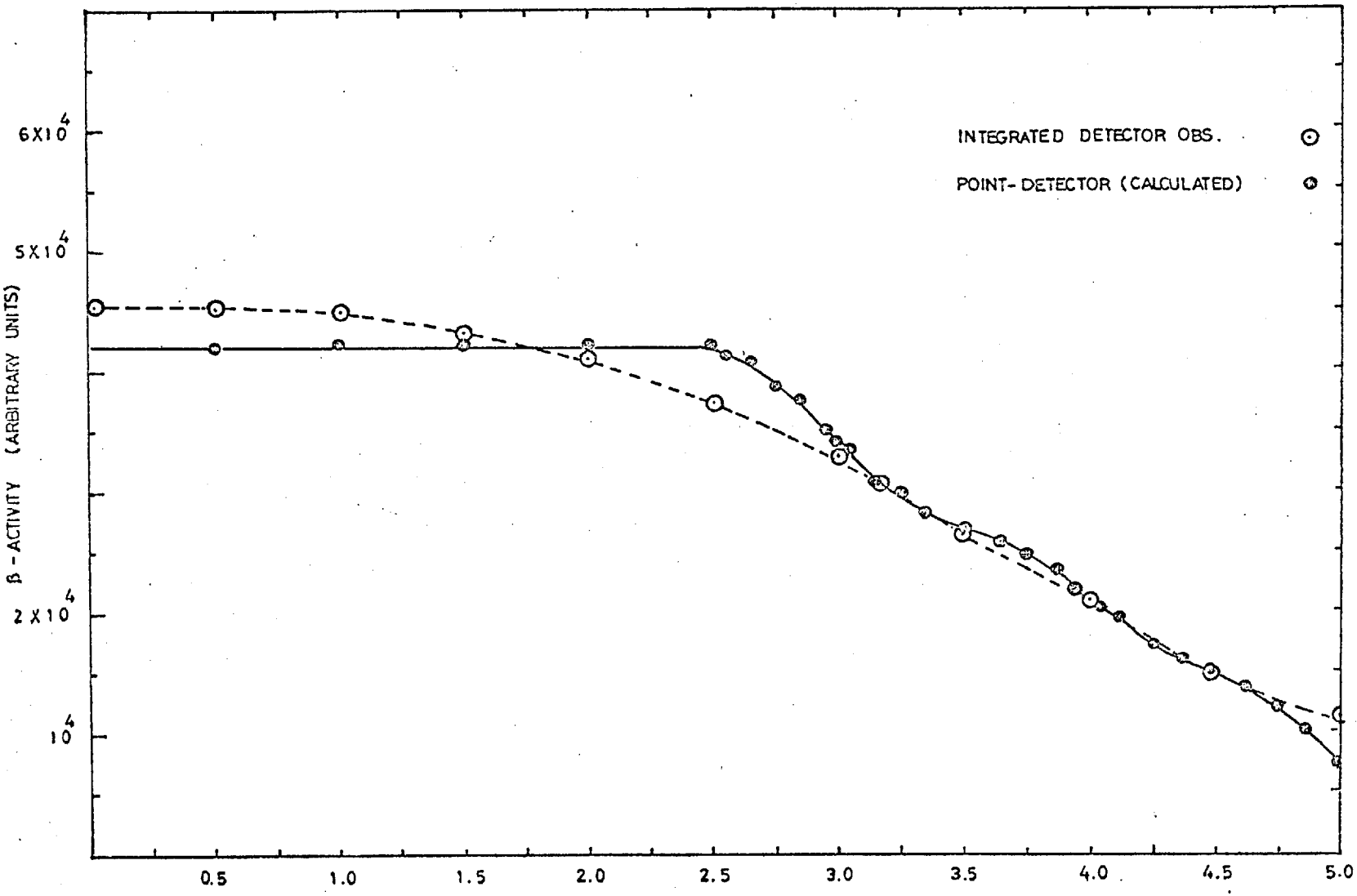

activity was expected. The observations to check for the uniformity and symmetry of the fission source were made at seventy-two different positions along eight directions emanating from the geometric centre of the disc source. These positions are marked in figure (F.5.9) as 'circles'. The other positions, which are marked with the 'crosses' have the activity calculated on the basis of the measured values, on the knowledge of these measured and calculated values, lines of equal activity were drawn, as shown in the figure (F.5.10). This revealed that the centre of the fission source was out by 1.1 cms. from the geometric centre.

Due to the large counter geometry, (1" dia.), the observed count rate is integrated over the area it scans every time. The dotted line in the figure (F.5.11) is the curve passing through the observed readings in a particular direction OG from the centre, see fig (F.5.9). Calculations were then made, making use of the observed 'integrated' data to evaluate arbitrary numbers that are proportional to the activity at each point. This number would represent the proportional activity if it were measured by a point-detector. The continuous curve in the figure (F.5.11) passing through these calculated 'point-detector' activity points show the straightening effect at the rings of uniform activity depending upon their respective irradiation times.

CHAPTER 6.

ANALYSIS OF THE BASIC EXPERIMENTAL DATA.

6.1. THE OVERALL SCHEME OF DATA PROCESSING AND ANALYSIS.

The observed experimental data described in section (5.12) was subjected to a series of systematic operations. An overall scheme of this data processing and analysis is presented in figure (F.6.1). This scheme comprises of a number of programmes written by the present author, using the Imperial College IBM 7090/7094 and the University of London CDC 6600 computers. The succeeding sections will give some idea of these operations. Flow charts of some individual programmes are provided later in this chapter. Because of the limitation of space, the listing of these computer programmes are not included in this thesis.

6.2. EVALUATIONS OF THE DEAD-TIMES AND THEIR ANALYSIS.

The dead-time values for various counting rates for the main and the monitor channels were calculated from the observations described in sec. (5.11) in chapter 5. These observations were analysed by fitting to the expression,

$$P = \alpha \frac{C_{obs}}{1 - C_{obs} \times t_d} \qquad \ldots\ldots(6.2.E1)$$

FIG(F.6.1) A BLOCK DIAGRAM OF THE OVERALL SCHEME OF DATA PROCESSING AND ANALYSIS

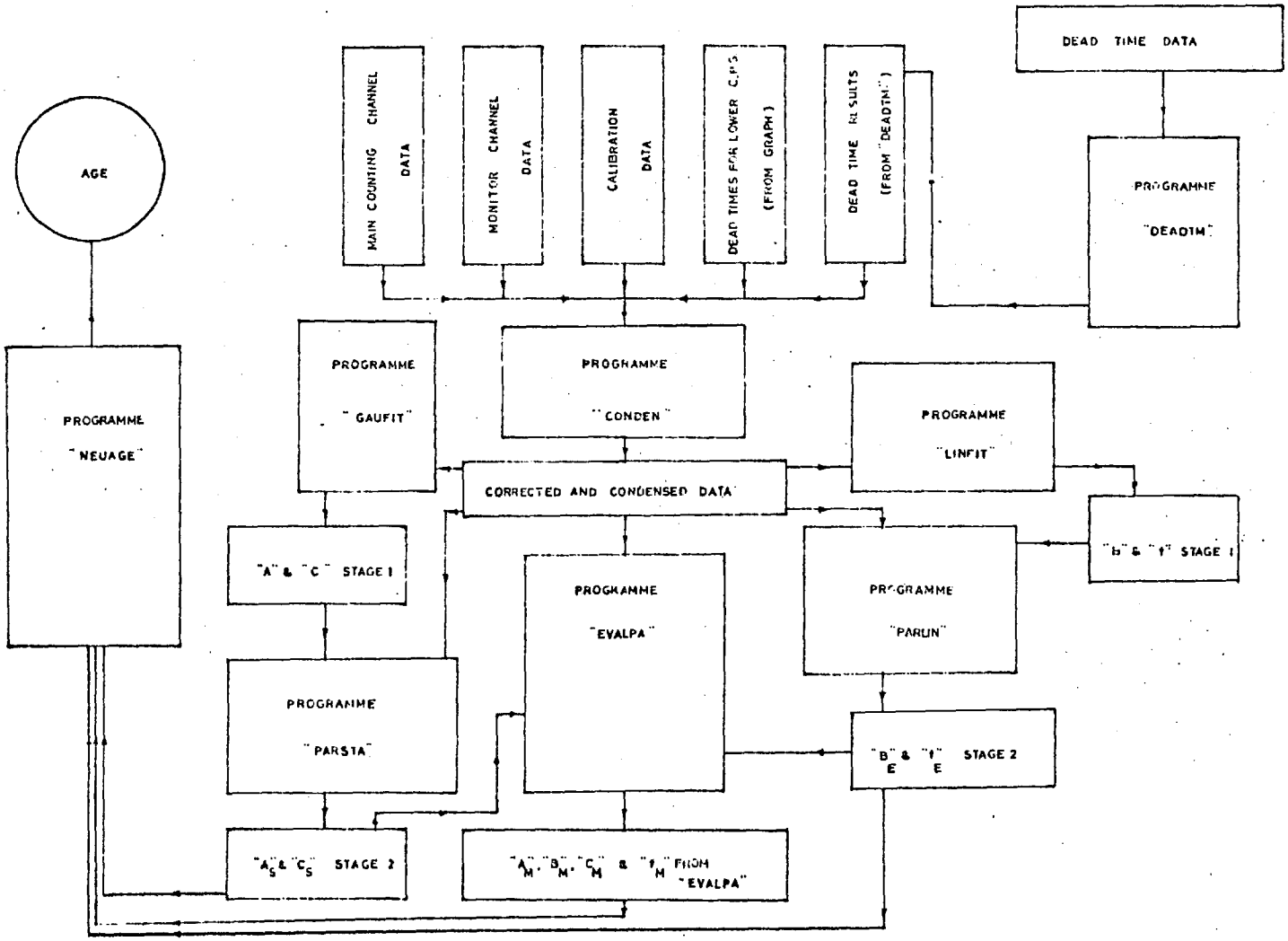

where P ... Reactor power

t_d ... Dead-time

α ... A constant

C_{obs} ... Observed count rates

A programme 'DEADTM' was written for the college IBM 7090/7094 computer to fit the experimental values of the observed count rates against the reactor powers by optimising the values of 'α' and 't_d'.

A block diagram of the programme 'DEADTM' is given in figure (F.6.2). Tables (T.6.1) and (T.6.2) give the results of the dead-time computations respectively for the monitor and the main counting channels. The order of maximum count rate in the dead-time observations, section (5.11), was taken to be ~6000 counts per seconds, which is a typical figure for the monitor reading for the actual experiments in the present series. It is seen that the dead-time for this channel cluster round 8.55 $\pm$0.68 μ-sec. Figure (F.6.3) shows a typical example of the fit to the experimental points. The value of the dead-time leads to the conclusion that the measured counts (at full power), are less by 5.4 % of the true value which in turn can be calculated using the relationship,

$$C_{true} = \frac{C_{obs}}{1 - (C_{obs} \times t_d)} \qquad \ldots\ldots (6.2.E2)$$

FIG (F.6.2) BLOCK DIAGRAM OF PROGRAMME "DEADTM"

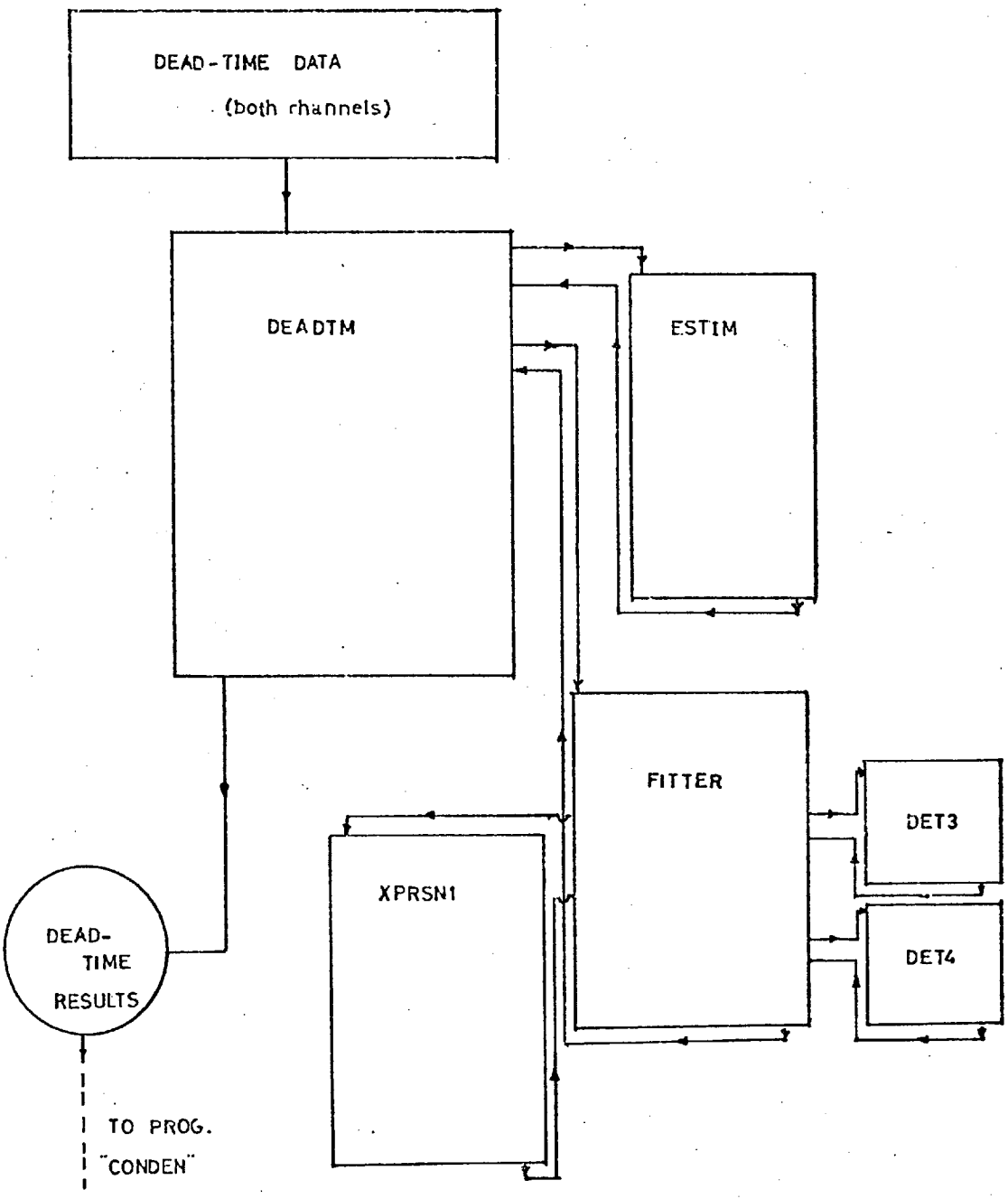

TABLE (T.6.1)

Dead-time results -- The monitor channel.
(The order of count rate taken as ~6000 c.p.s.)

No. of fittings	Dead-time (μ-secs.)	Std. dev. (μ-secs.) (+ / -)
1	9.26	0.80
2	9.32	0.95
3	9.02	0.92
4	9.06	1.02
5	8.14	0.87
6	7.53	0.48
7	8.30	0.48
8	7.58	0.74
9	8.34	0.80
10	8.59	0.69
11	9.27	0.68
12	8.95	0.60
13	8.38	0.41
14	8.22	0.50
15	7.37	0.77
16	7.92	0.75
17	8.85	0.58
18	9.22	0.43
19	8.61	0.63
20	8.87	0.70
21	8.99	0.46
22	8.27	0.85
23	8.12	0.48
24	8.99	0.83
25	8.53	0.79
26	8.75	0.27
27	8.81	0.55
28	8.05	0.64
29	8.77	1.07

Mean Dead-time
$= 8.55 \pm 0.68$ μ-sec.

FIG(F.6.3) A TYPICAL EXAMPLE OF FIT TO THE DEAD-TIME DATA

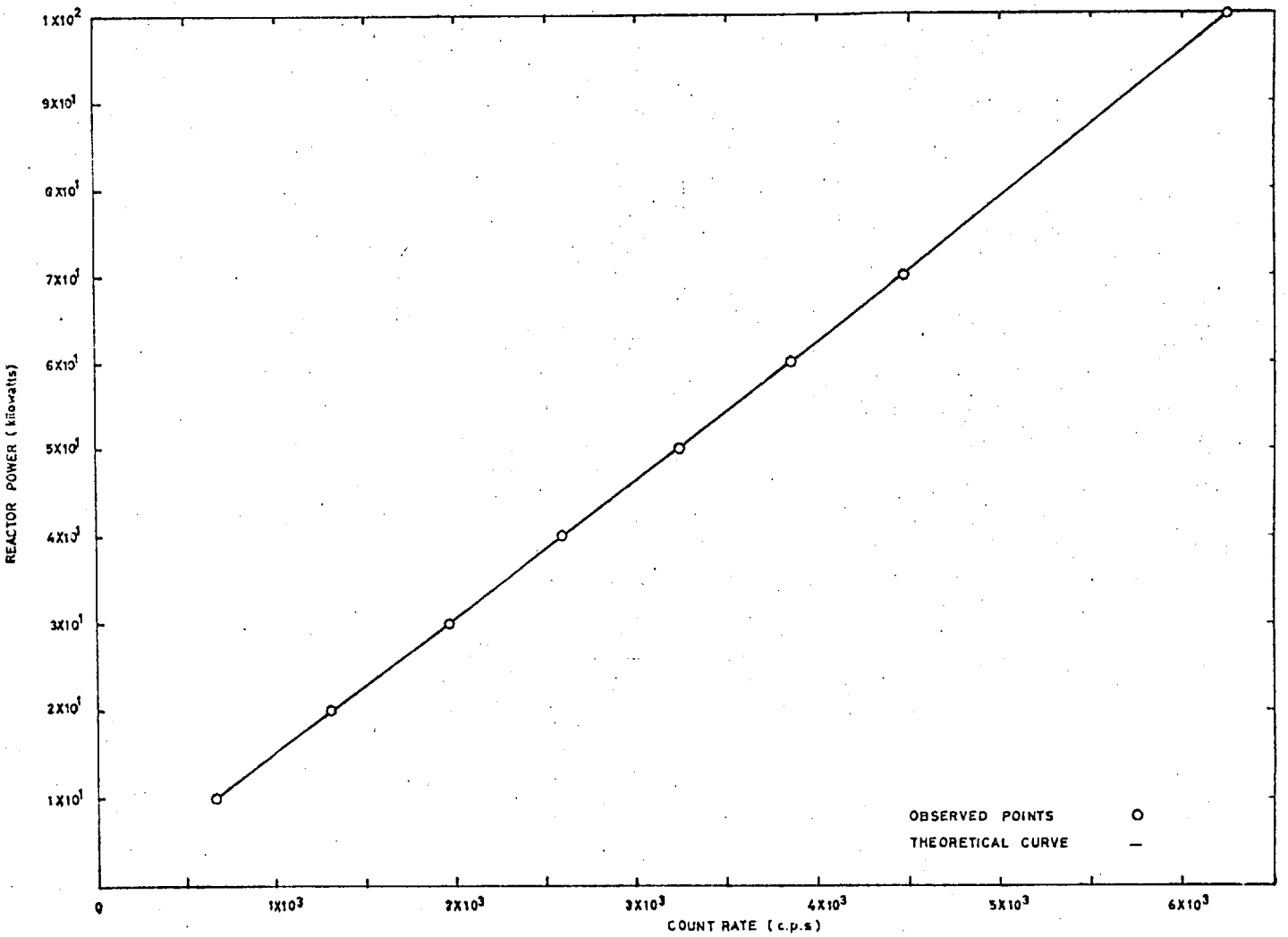

TABLE (T.6.2)

Dead-time results -- The main counting channel.

No of fittings	Distance from the fission source (cms.)	Order of maximum count rate (c.p.s.)	Dead-time (μ-secs.)	Std. dev. (μ-secs.) (+/-)
1	4.0	66500	5.48	0.48
2	5.0	61500	5.36	0.49
3	6.0	55700	5.04	0.62
4	7.0	49100	5.01	0.51
5	8.0	42600	4.70*	0.49
6	9.0	36300	4.38*	0.48
7	10.0	30400	4.07*	0.58
8	10.5	27600	3.79	0.81
9	11.0	25100	3.62	0.57
10	11.5	22700	3.41	1.00
11	12.0	20500	3.17	0.66
12	12.5	18500.	3.08	1.18
13	13.0	16600	2.79	0.71

* Averaged where more than one observations were taken.

Fig (F.6.4) is a plot of the observed monitor readings against the reactor powers. The broken line in this figure represents the true count rate.

The dead-time results of the main counting channel, in the Table (T.6.2) shows that the values vary directly with the order of the maximum count rate. Fig (F.6.5) is a plot of the dead-times against the reactor powers. This

FIG(F.6.4) A PLOT OF MONITOR COUNTRATES AGAINST REACTOR POWERS

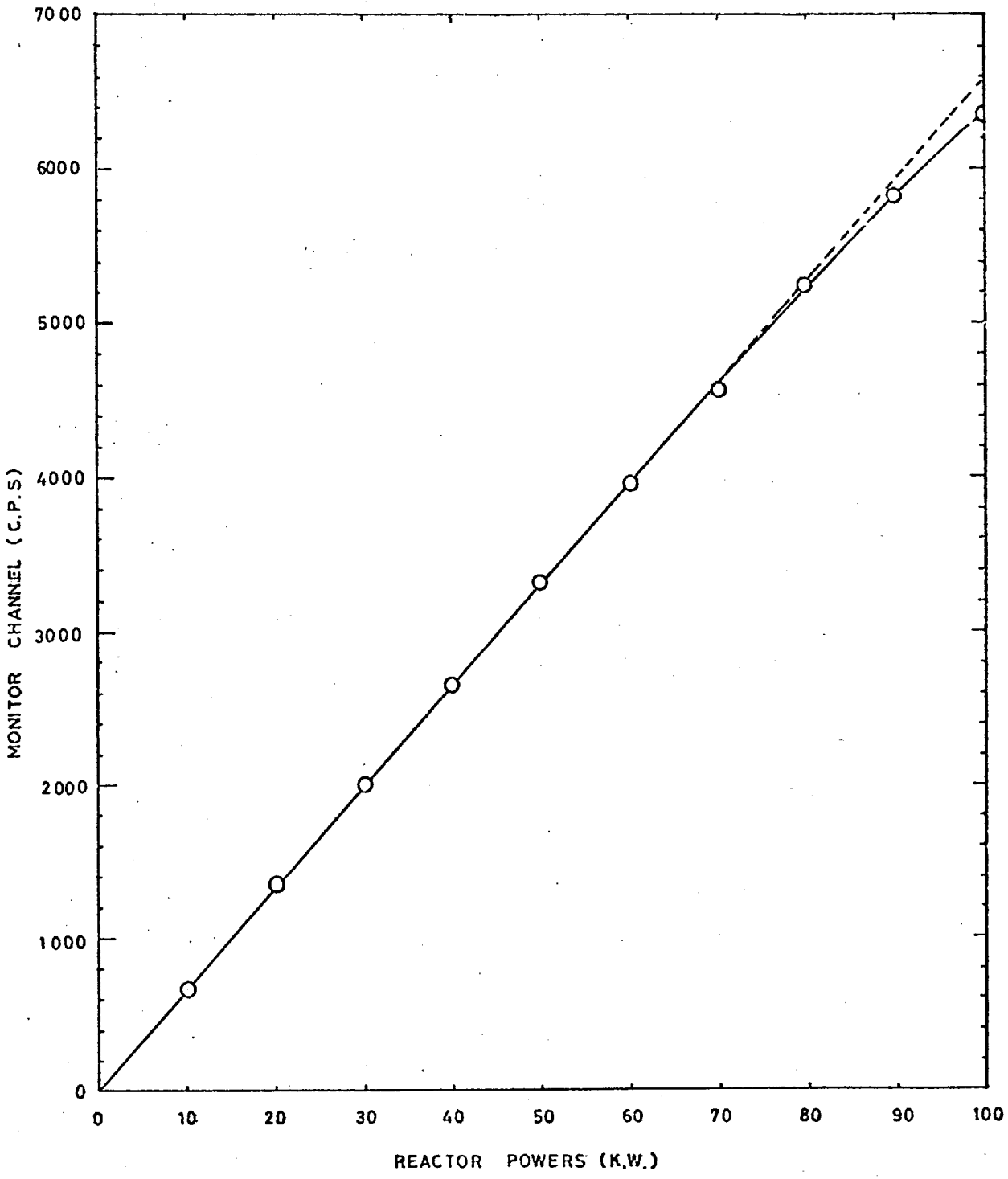

FIG(F.6.5) VARIATION OF DEAD-TIME WITH COUNTRATE

(A PLOT OF THE ORDER OF MAXIMUM COUNTRATES AGAINST DEAD- TIMES. (MAIN COUNTING CHANNEL))

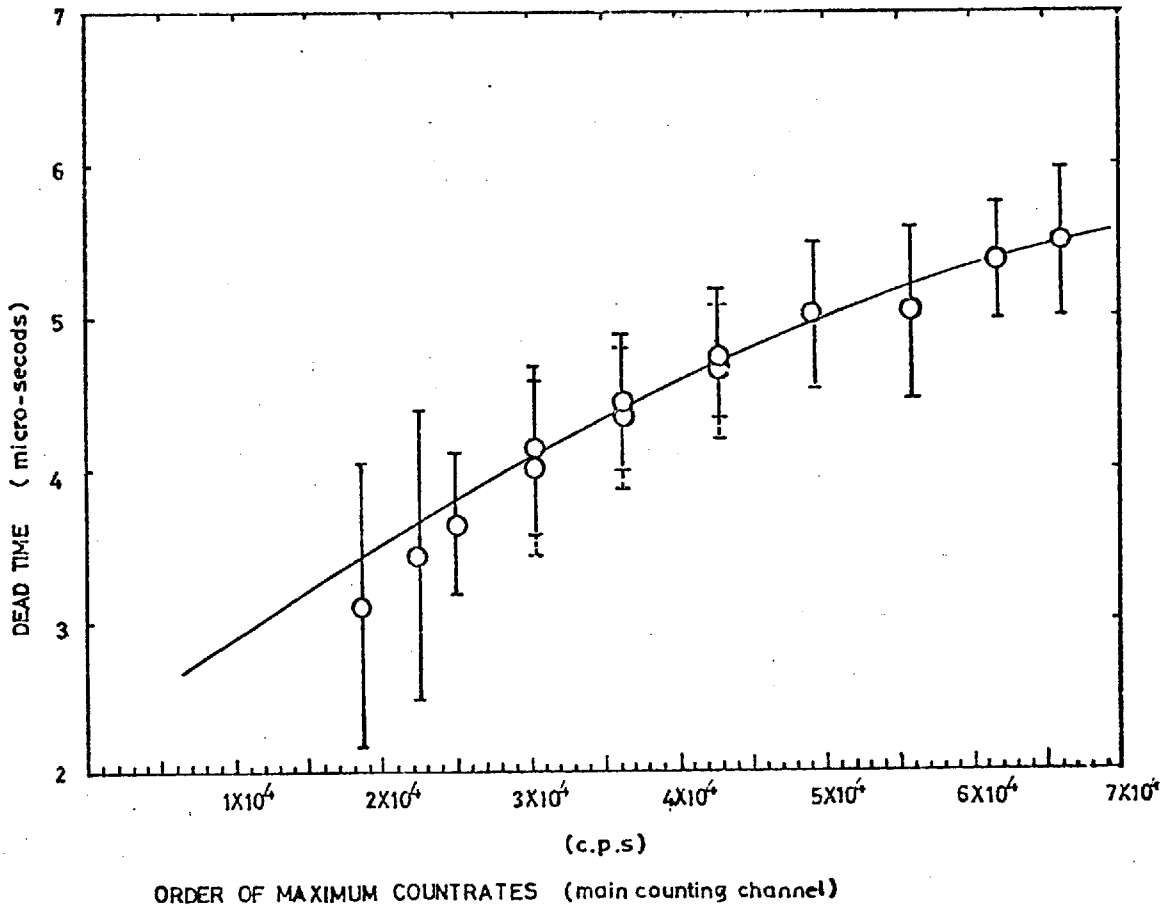

curve is extrapolated to evaluate the dead-times of the lower ranges of count rates. Table (T.6.3) gives some such values obtained from the graph along with some calculated true counts and percentage corrections. Fig (F.6.6) shows the manner and the extent (percentage) that the dead-time corrections are applicable. Corrections to the raw observed data, including those for dead-time are performed in the programme 'CONDEN' to be described in the following sections.

TABLE (T.6.3)

Some dead-time values obtained by graphic extrapolation.

No	Order of count rate (max.)	Applied dead-time (μ-secs.)	Calculated true count rate.(cps)	Percentage correction on the obs. count rate.
1	10000	2.70	10277	2.77
2	7500	2.70	7654	2.05
3	6600	2.70	6719	1.80
4	5700	2.60	5782	1.43
5	5000	2.60	5064	1.20
6	4400	2.60	4450	1.10
7	3800	2.60	3837	0.97
8	3400	2.50	3429	0.85
9	3000	2.50	3022	0.73
10	2600	2.50	2617	0.65
11	2300	2.50	2313	0.56
12	2000	2.50	2010	0.50
13	1700	2.50	1707	0.41

FIG(F6.6) A PLOT OF COUNTRATE AGAINST DEAD TIME CORRECTION

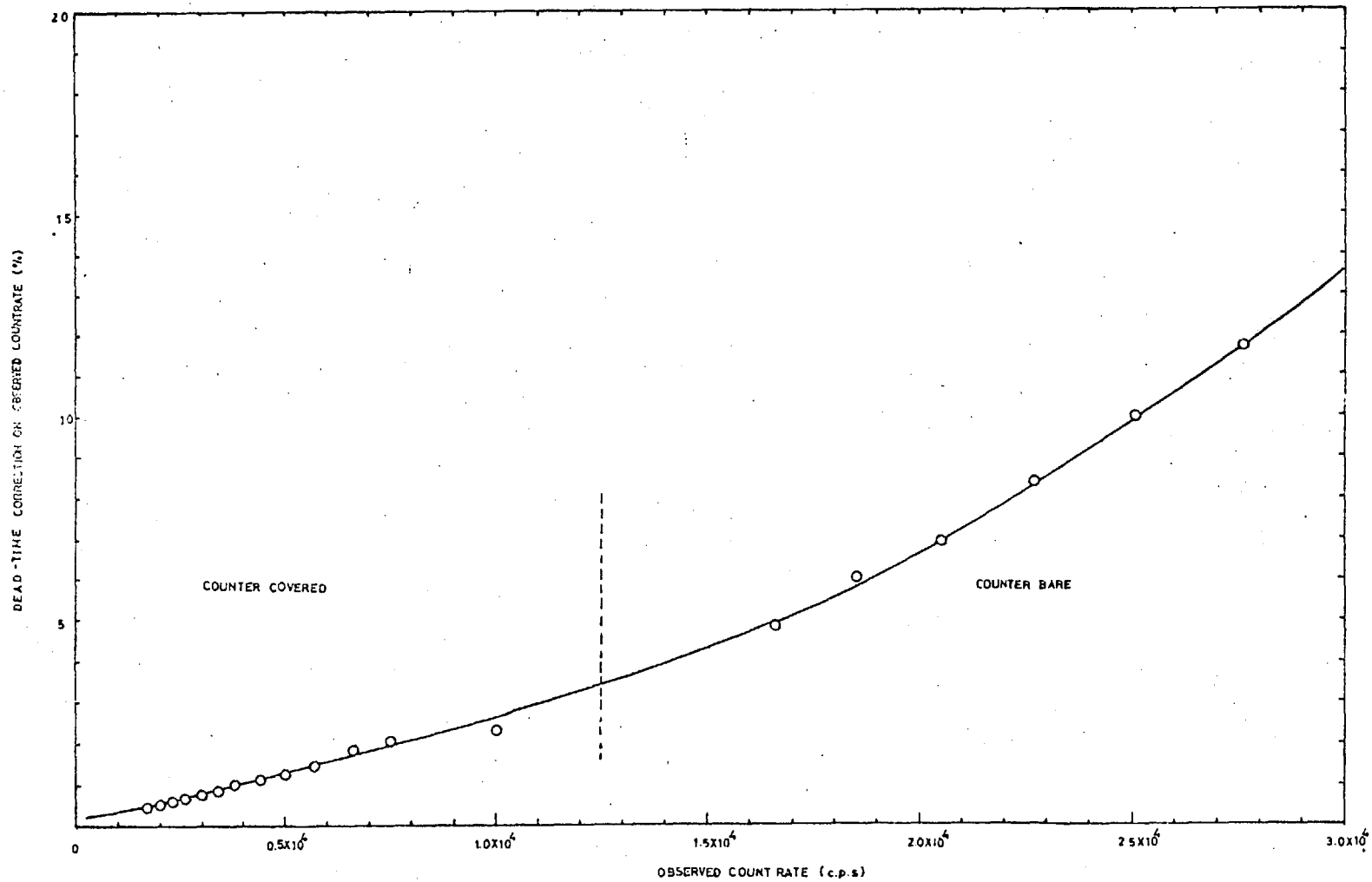

Equation (6.2.E1) is an approximation of the exact expression,

$$C_{obs} = \alpha P e^{-\alpha P t_d} \quad \ldots\ldots \text{(6.2.E3)}$$

This equation was also used for the analysis of the dead-time data but there was no significant difference in the results from using equation (6.2.E3) over those by using equation (6.2.E1).

6.3. TREATMENT OF THE RAW EXPERIMENTAL DATA

A small computer programme 'CONDEN' is written to apply some corrections on the observed data. This programme corrects the raw data, condenses it and then punches for the subsequent analysis. Some of the corrections applied are briefly described in the sections (6.3.1) and (6.3.2).

6.3.1. BASIC CORRECTIONS AND CONDENSING OF DATA.

The dead-time results obtained from the programme 'DEADTM', for the channels and also in the case of the main counting channel, the values obtained by the extrapolation of the computed values, for the lower ranges of count rates by graphic method, are used for correcting sets of observations of the basic flux measurements. The dead-time corrections applied on the monitor data is on the basis of t_d = 8.55 μ-sec., which is the computed

value from observed dead-time data, for the order of the monitor count rate used in the experiments.

In the case of the main counting channel, the dead-time correction is applied appropriate for each range of count rate on the knowledge of the values computed from programme 'DEADTM' as well as from the graphic extrapolation of the computed results given in table (T.6.3). Equation (6.2.E2) is used to calculate the true countrate corrected for the dead-times, in the case of the either channel.

The main counting channel readings were corrected for the possible fluctuations in the reactor power on the knowledge of the monitor readings for each set of the main counting channel. This was achieved by obtaining the monitor averages for each set and normalising the main channel readings against the respective monitor readings. These operations give the fluxes for various controlled conditions corrected for the dead-time as well as for the possible fluctuations in the reactor power during the course of observations. These fluxes are,

(a) With cadmium covered counter and fission source triggered.

(b) With cadmium + resonance absorber covered counter and fission source triggered.

(c) With cadmium covered counter and fission source not triggered.

(d) With cadmium + resonance absorber covered counter and fission source not triggered.

The resultant flux due to the resonance absorber corrected for the background could thus be obtained as,

((a-c)-(b-d)) ..... (6.3.E1)

6.3.2. SOURCE-DETECTOR DISTANCE CORRECTION

A correction was applied to the observed source-detector distance on the knowledge of the calibration data obtained by a series of detailed observations as outlined in sec. (5.6). This correction in the case of the first arrangement of the bridge carrying the detector assembly, as used in this series of experiments was -0.08 cm. In the other series for the case of water moderator containing cylindrical cavities, to be described later in chapter 8, the bridge arrangement was modified to suit the requirements. The correction there on the measured distance was -0.67 cm.

6.4. METHOD OF AGE EVALUATION

6.4.1. THE BASIC DERIVATION

The method of neutron age evaluation involves the determination of mean squared slowing down distance '$\overline{r^2}$' from the source at which the neutron possess the energy 'E' corresponding to the age 'τ' at the field point r. Thus,

$$\overline{r^2} = \frac{\int_0^\infty r^2\, \Phi(r,E)\, 4\pi r^2\, dr}{\int_0^\infty \Phi(r,E)\, 4\pi r^2\, dr}$$

$$= \frac{\int_0^\infty r^4\, \Phi(r,E)\, dr}{\int_0^\infty r^2\, \Phi(r,E)\, dr} \qquad \text{.....(6.4.E1)}$$

The neutron age 'τ' is then given by,

$$\tau = \frac{1}{6}\,\overline{r^2} = \frac{1}{6}\,\frac{\int_0^\infty r^4\, \Phi(r,E)\, dr}{\int_0^\infty r^2\, \Phi(r,E)\, dr} \qquad (6.4.E2)$$

where flux, $\Phi(r,E)$, is taken to be of the type,

$$\Phi(r,E) = A\, e^{-cr^2} + \frac{1}{r^2}\, B\, e^{-fr} \qquad \text{....} \quad (6.4.E3)$$

The flux in the vicinity of the fission source is given dominently by the first part of the right hand side of equation (6.4.E3), and neutron distribution at a considerable distance from the source can be represented by the second part of that expression. The contribution due to the two parts is assumed more evenly balanced in the middle region.

Using expression (6.4.E3) for $\Phi(r,E)$, the equation

(6.4.E2) thus takes the form,

$$\tau = \frac{1}{6} \frac{\int_0^\infty (r^4 Ae^{-cr^2} + r^2 Be^{-fr}) dr}{\int_0^\infty (r^2 Ae^{-cr^2} + Be^{-fr}) dr} \quad ..(6.4.E4)$$

where 'A', 'B', 'c' and 'f' are point source flux parameters.

6.4.2. CORRECTIONS FOR FISSION SOURCE GEOMETRY.

The equation (6.4.E4), of neutron age, was derived assuming a point fission source. However, the fission source used in the present series of age determinations, is of finite plane geometry in the shape of a disc, primarily for the reason of obtaining a sufficient neutron intensity for good counting statistics. The effect on the detector is computed by carrying out integration over the entire source geometry. The flux expression (6.4.E3), thus takes the form, (Derivation in Appendix (A.6.1)).

$$\Phi(r,E) = \frac{2}{X^2} Ae^{-cr_o^2} \left\{ \left(-\frac{1}{2c} \right) (e^{-cX^2} - 1) + B \int_0^X \frac{x\,dx}{(x^2 + r_o^2)} e^{-f\sqrt{x^2 + r_o^2}} \right\}$$

.....(6.4.E5)

where 'X' represents the radius of the fission source and 'r_o' the observed distance from the geometric centre of the fission source. The flux expression (6.4.E5) instead of (6.4.E3), is used for the evaluation of the parameters 'A', 'B', 'c' and 'f' from the observed plane source data.

6.5. DATA ANALYSIS

A complete scheme of data processing and analysis is already shown in figure (F.6.1). The observed data after having been corrected and condensed in programme 'CONDEN' results in the corrected true values of fluxes for the various controlled conditions as mentioned in section (6.3.1). The resultant resonance fluxes for various source-detector distances can be obtained using the expression (6.3.E1).

A block diagram of programme 'EVALPA' is shown in the figure (F.6.7). This programme is written to evaluate the parameters 'A', 'B', 'c', and 'f' in equation (6.4.E5) by fitting to the resonance flux data obtained. A method of least squares is used for fitting. Parameters are optimised to give the closest fit to the experimental points. The fitting subroutine, 'FITTER' is a modified version of 'PARFIT'. The fitting procedure being based on the expansion of the theoretical expression in a

FIG.(F.6.7) BLOCK DIAGRAM OF PROGRAMME "EVALPA"

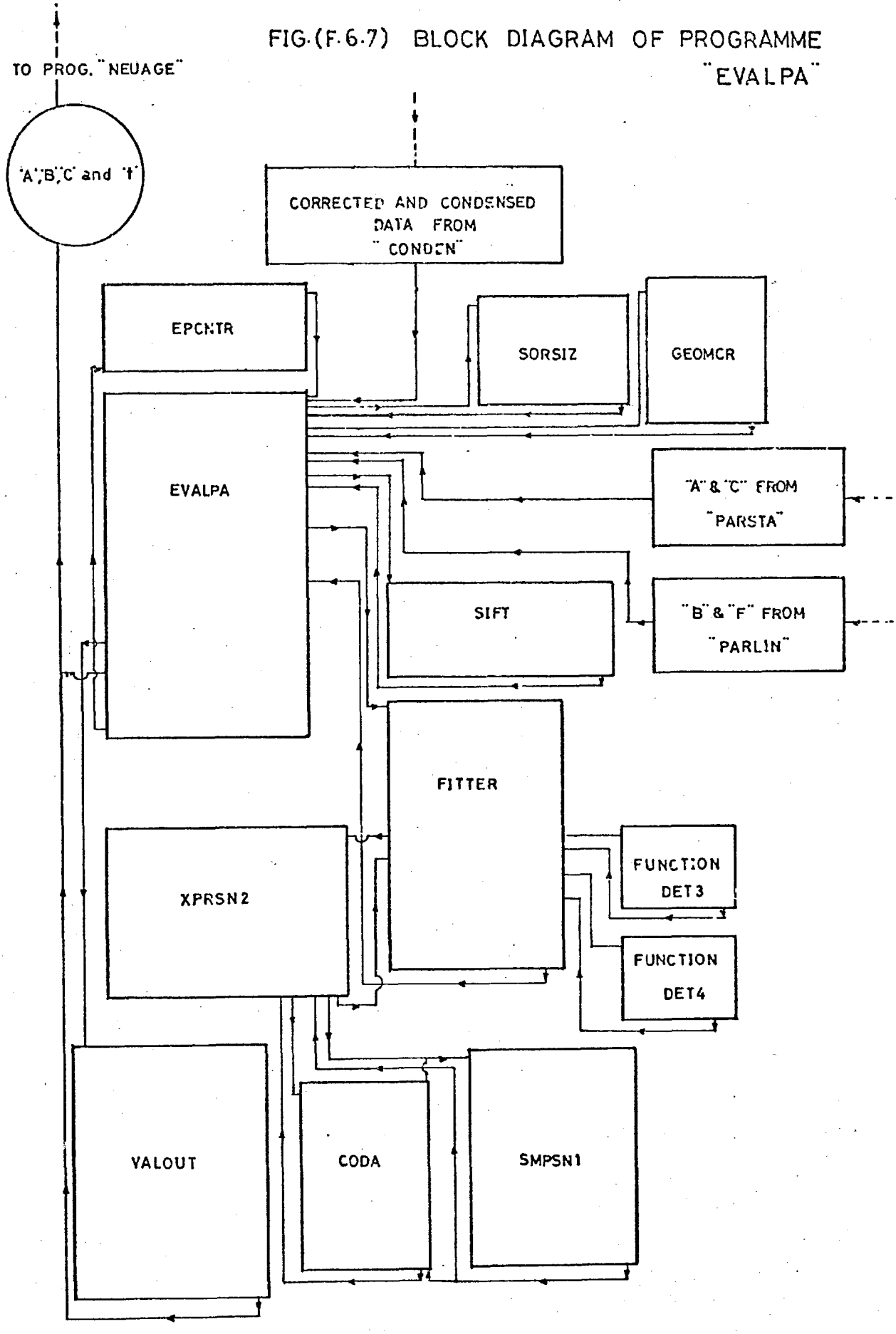

Taylor's series in the parameters about its initial guess values. The condition that the sum of deviations be minimum with respect to the changes in each parameter, yields a set of linear equations in parameter increments. The solution of this set enables the initial guess values of the parameters to be modified by these increments. The process is repeated until the increments are smaller than the convergence criteria.

In the first version of the programme 'EVALPA', the initial guess values were calculated in subroutine 'INGESS', (not shown in the final version, Fig (F.6.7)). This subroutine was designed to supply 'good enough' initial guess values, calculated from the observed flux, using a simple point source expression (6.4.E3). These values are averaged over appropriate regions by a number of repeated operations. These were however, found not very adequate, as was revealed by the first few runs of the programme 'EVALPA'. In view of the complexity of the fitting expression (6.4.E5), and the fact that the fitting subroutine being used to its limits, it was thought necessary that a more accurate initial guess values are needed to obtain convergence of the results within a reasonable number of iterations. To achieve this, the subroutine 'INGESS' was then replaced by two stages of fittings which improve these values at each stage. The preliminary two stage fittings are applied

as follows. The flux data was roughly divided into two regions. Point source flux expression (6.4.E3) is applied by parts to the two regions. Data points near the fission source are described by,

$$\Phi_1 = Ae^{-cr^2} \qquad \ldots\ldots (6.5.E1)$$

and for the region at quite a distance away from the source the expression,

$$\Phi_2 = \frac{B}{r^2} e^{-fr} \qquad \ldots\ldots (6.5.E2)$$

holds.

A simple computer programme 'GAUFIT' is written using expression (6.5.E1) to obtain a least squared fitted first stage evaluation of the parameter 'A' and 'c'. Another programme 'LINFIT' evaluate parameters 'B' and 'f' by fitting linearised equation from expression (6.5.E2), to the experimental points away from the fission source. The block diagrams of 'GAUFIT' and 'LINFIT' are provided in figures (F.6.8) and (F.6.9) respectively.

The values of the parameters 'A', 'c' and 'B', 'f', obtained in the first stage of fittings described above are then fed as guess values of these parameters for the second stage fittings, which again is done for two separate

FIG (F.6.8) BLOCK DIAGRAM OF PROGRAMME "GAUFIT"

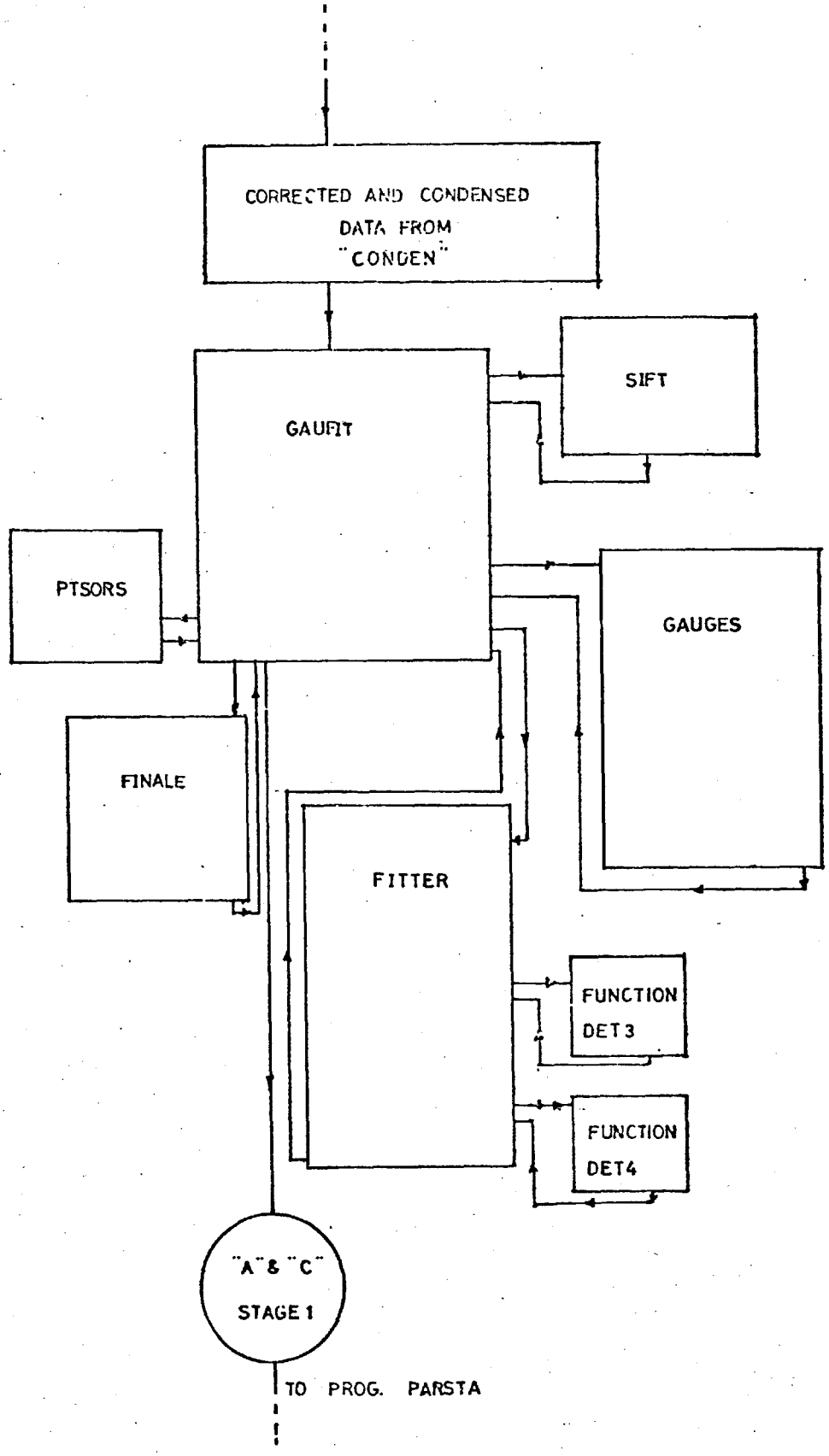

FIG(F.6.9) BLOCK DIAGRAM OF PROGRAMME "LINFIT"

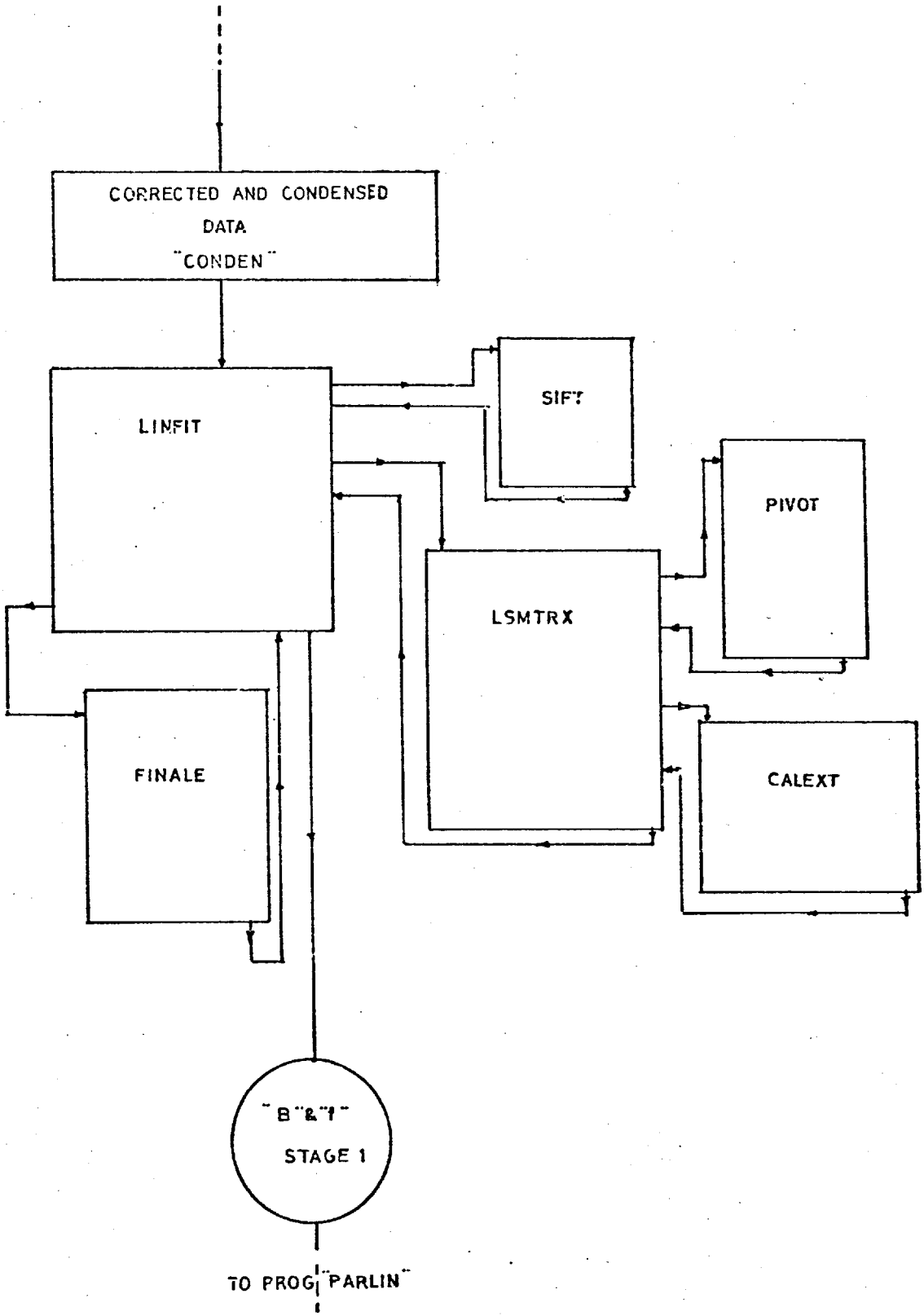

regions but this time using expressions which incorporate the corrections due to the geometry of the disc fission source. Thus using the expressions,

$$\Phi_1 = \frac{2}{X^2}\left\{Ae^{-cr_o^2}\left(-\frac{1}{2c}\right)\left(e^{-cX^2}-1\right)\right\}..(6.5.E3)$$

$$\Phi_2 = \frac{2B}{X^2}\left\{\int_o^X \frac{xdx\ e^{-f\sqrt{x^2+r_o^2}}}{\left(x^2+r_o^2\right)}\right\}..(6.5.E4)$$

respectively for the near and the distant regions from the fission source. Two programmes 'PARSTA' and 'PARLIN' which are the special cases of programme 'EVALPA', using equations (6.5.E3) and (6.5.E4), yield more refined values of 'A', 'c' and 'B', 'f' in separate second stage fits.

To obtain numerical values of the integrals occurring in the fitting expression (6.4.E5) as well as in two out of four of its partial derivatives (w.r.t. the parameters) in subroutine 'XPRSHN', subroutine 'SMPSN1' is written to carry out integration using Simpson's rule, with intervals halving until the difference between the successive values is less than accuracy limit set.

In all stages of fits, subroutine 'SIFT' is included,

which functions as a means of dropping off points at the start or at the end. It helps to obtain a number of fits for the same data by varying the extremities of regions, thus enabling to achieve best fits.

In the final evaluation of the parameters 'A', 'B', 'c', and 'f' with programme 'EVALPA', using the complete expression (6.4.E5) and the entire data points, the initial guess values are taken from the results of the programmes 'PARSTA' and 'PARLIN'.

6.6. EVALUATION OF NEUTRON AGE.

The values of the point source parameters 'A', 'B', 'c', 'f', which are obtained by fitting the modified expression (6.4.E5) to the observed fluxes from the disc fission source are then used in the equation (6.4.E4) for the evaluation of neutron age.

It was found that although a very good fit was obtained to nearly all the experimental points using only expression (6.4.E5), but at very very near distances and far distances, expressions (6.5.E3) and (6.5.E4) respectively provide excellent fits at the two end regions. This stands to reason as in the immediate vicinity of the source, first term of the equation (6.4.E5) is dominent so expression (6.5.E3) holds, and at considerable distances

from the fission source, beyond which the distribution is asymptotic and one can safely use the expression (6.5.E4) as the contribution due to the first term in (6.4.E5) dwindles to nothing at such distances. The fits to the observed points are made, with the major central portion being fitted by the expression (6.4.E5) and expressions (6.5.E3), (6.5.E4) fitted the first few and the last few points. The continuation of fits was ensured by getting a number of sets of fits by varying the number of points. The process employed is as follows. First individual best fits to the observed points were made region by region. Then the boundries of these fits are varied slightly by taking-in or excluding points of the adjecent fits until the curves merge into each other forming a perfectly smooth and continuous curve as well as fitting all points well.

Each integral in the equation (6.4.E4) could be divided up at points R_1 and R_2, where R_1 is very near to the fission source, upto which 'PARSTA' fit is applicable and R_2 being the point beyond which 'PARLIN' fitting is used. In the major middle region 'EVALPA' fit holds between R_1 and R_2.

A programme 'NEUAGE',(block diagram, fig(F.6.10)) is written to evaluate the neutron age. The integration from zero to R_1 is done using Simpson's rule taking only

FIG (F.6.10) BLOCK DIAGRAM OF PROGRAMME "NEUAGE"

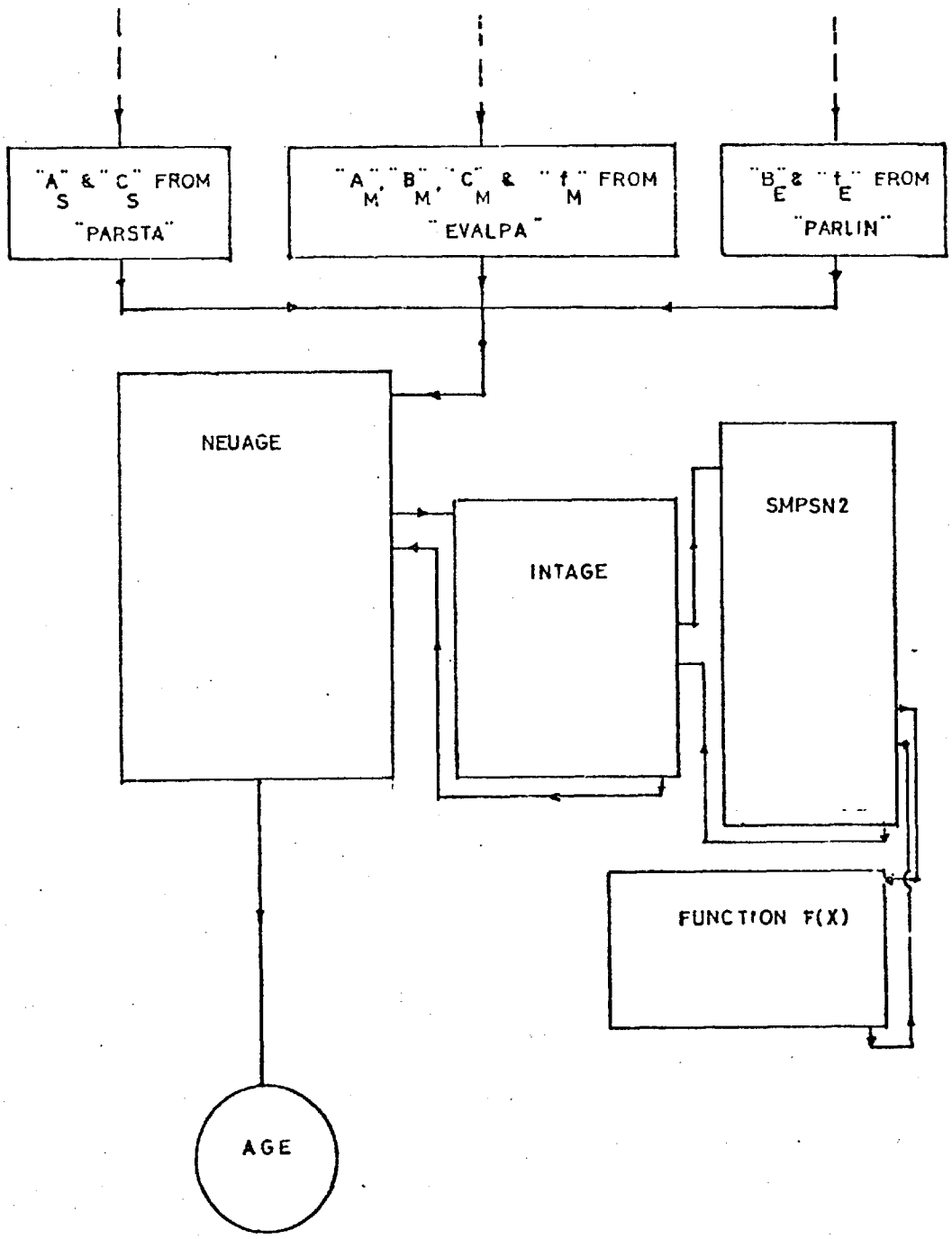

the first term of equation (6.4.E4). The integration of the middle region between R_1 and R_2 is again done with Simpson's rule but taking both terms into account. The integration between R_2 and ∞ is done analytically. The equation (6.4.E4) thus assumes the following modified form.

$$\tau = \frac{1}{6} \frac{\text{(Integral 1)} + \text{(Integrals (2+3))} + \text{(Integral 4)}}{\text{(Integral 5)} + \text{(Integrals (6+7))} + \text{(Integral 8)}} \quad \text{.....(6.6.E1)}$$

Where these integrals with their appropriate limits are given below.

$$\text{(Integral 1)} = \int_0^{R_1} (r^4 A_s \exp(-c_s r^2))dr. \quad \text{.....(6.6.E2)}$$

$$\text{(Integrals (2+3))} = \int_{R_1}^{R_2} (r^4 A_m \exp(-c_m r^2) + r^2 B_m \exp(-f_m r))\, dr. \quad \text{..(6.6.E3)}$$

$$\text{(Integral 4)} = \int_{R_2}^{\infty} (r^2 B_E \exp(-f_E r))dr. \quad \text{.....(6.6.E4)}$$

$$\text{(Integral 5)} = \int_0^{R_1} (r^2 A_s \exp(-c_s r^2))dr. \quad \text{.....(6.6.E5)}$$

$$\text{(Integrals (6+7))} = \int_{R_1}^{R_2} (r^2 A_m \exp(-c_m r^2) + B_m \exp(f_m r))\, dr. \quad \text{.....(6.6.E6)}$$

$$(\text{Integral 8}) = \int_{R_2}^{\infty} (B_E \exp(-f_E r))dr. \qquad .....(6.6.E7)$$

In the above set of equations,

('A_s' and 'c_s')..... are values of parameters obtained from 'PARSTA' fit

('A_m','B_m','c_m' & 'f_m').. are values of parameters obtained from 'EVALPA' fit

and ('B_E' and 'f_E')..... are values of parameters obtained from 'PARLIN' fit.

The analytical solutions of the integrals '4' and '8' mentioned in this section are given respectively by,

$$\frac{B_E}{f_E} \exp(-f_E R_2)\left(R_2^2 + \frac{2R_2}{f_E} + \frac{2}{f_E^2} \right) \quad ..(6.6.E8)$$

and $$\frac{B_E}{f_E} \exp(-f_E R_2) \qquad ..... (6.6.E9)$$

The results of the age calculations using the equation (6.6.E1) are given in the following chapters.

CHAPTER 7.

RESULTS OF NEUTRON AGE MEASUREMENTS IN WATER.

In this chapter the basic results are obtained of the ages of the neutrons from a fission source to the detector energies in the cases of indium, rhodium and gold resonances in water. The values of the parameters 'A_s', 'C_s', 'A_m','C_m', 'B_m', 'f_m', and 'B_E', 'f_E', from the regional final stage fits by the programmes 'PARSTA', 'EVALPA' and 'PARLIN' are used in programme 'NEUAGE' for the evaluation of the neutron ages. This programme is based on the equation (6.6.E1), the derivation of which and the details of the fittings of the appropriate parts and as a whole are already given in the previous chapter. The value of the age obtained in the case of indium will be compared with the existing experimental and calculated values. The present age determinations of the fission neutrons to the resonance energies of rhodium and gold are however, the first of their kind as there exists no published values in this category. The finally corrected values of all the present age determinations to be described in this chapter as well as those in the case of water containing cylindrical cavities, (chapter 8), are obtained in chapter 9, where they are also compared where possible with the published values.

7.1. A BRIEF REVIEW OF THE EXPERIMENTAL DETERMINATIONS OF NEUTRON AGE.

Prior to the present investigation there has been a number of measurements, (R.7.1 to R.7.12), of the age of the fission neutrons to the indium resonance energy. The experimental set-ups used show a considerable variation as far as the geometries of the moderating medium, the composition of the fission source, the dimensions of the source, the detecting foils and their coverings etc., are concerned. Some of the salient features of these equipments used are displayed in Table (T.7.1). In all these previous determinations the basic technique has been the irradiation of the cadmium-covered indium foils at various distances from the fission source. The activities of the foils determined after irradiation represents a quantity proportional to the flux of 1.46 e.v. neutrons at various source-detector separations. The present measurements are the first of the fission neutron age determination involving a different technique. The details of this technique and its advantages over the more commonly used foil activation method, have already been mentioned earlier in this thesis. The results of the present determinations compare well with the best of the experimental values and the theoretical estimates. This comparison is presented in Table (T.9.3) in chapter 9.

TABLE (T.7.1)

Equipmental details of some age measurements.

Experiment, date and reference		Anderson Fermi and Nagle 1944 (R.7.1)	Hill Roberts and Fitch 1948 (R.7.2)	Hoover and Arnette 1950 (R.7.3)	Wade 1956 (R.7.5)
Source Reactor		Met. Lab. CP-2	ORNL-X-10	ORNL-X-10	SR-U^{235}-C Test
Fission source (T-thickness) (D-diameter) (C-composition)	T	(0.7, 0.5, 1.0 cms)	(0.20 cm)	(0.20 cm)	(0.30 cm)
	D	(4.7, 15.2 cms)	(5.08, 1.0, 2.0, 11.3*; 34.2* cms)	(5.08 cm)	(7.0 cm)
	C	(32.4g U_3O_8 5.7% Enr.U) (1690g Nat U) (3433g Nat U)	18 w % U-Al 96 % Enr U	18 w % U-Al 95 % Enr U	~90 % Enr U
Detecting foils (T-thickness) (A-area)	T	100 mg/cm^2	100 mg/cm^2	75 mg/cm^2	100 mg /cm^2
	A	26.0 cm^2	1.6, 1.0, 25.4 cm^2	22 cm^2	1.5 cm^2
Foil covers (material and thickness)		Cd 0.150 cms.	Cd 0.354 Cd 0.318 Al 0.051 cms.	Cd 0.103 Al 0.050 cms.	Cd 0.076 cms.
Water tank (H-height) (A- area)	H	67 cms.	183 cms.	183 cms.	214 cms.
	A	1.67 $cm^2 \times 10^3$	23.2 $cm^2 \times 10^3$	23.2 $cm^2 \times 10^3$	18.2 $cm^2 \times 10^3$

TABLE (T.7.1) ----- CONTINUED -----

-- Equipmental details of some age measurements --

Barkov and Mukhin 1956 (R.7.4)	Blosser and Trubey 1959 (R.7.6)	Lombard and Blanchard 1960 (R.7.7)	Pettus 1960 (R.7.8)	Doerner et al. 1961 (R.7.9)
MIP(USSR) RPT	ORNL-X-10 LTSF	P.S.U. Pool	B and W LPR	Argonne National Laboratory ZPR-IV'
(0.25)cms (0.50)cms	0.01,0.004, 0.010,0.028 cms	0.10 (X1,2 and 3) cms	0.64 cms	(a) 1248 (b) 33 (c) 288 mg/cm^2
(0.8,2.2) cms	(1.11,1.95, 5.0,1.91, 4.07) cms	8.0* cms	5.08 cms	60.96, 45.72, 76.20 cms
U^{235} Oxide	93.15 % Enr U	U-Zr, 1.4 x 10^{21} U atoms $/cm^3$	U^{235}-Al alloy 16.7 g U-235	(a) fully enriched (b), (c) Al-U^{235} alloy
100 mg/cm^2	93 mg/cm^2	100 mg/cm^2	96 mg / cms^2	0.09,20,40, 60,80,120, 240 mg/cm^2
0.9 - 7.5 cm^2	0.95,7.94 cm^2	1.0 cms^2	0.64, 1.28 cm^2	1 cm^2
Cd 0.061 cms	Cd 0.076 cms	Cd 0.103 cms	Cd 0.051 cms	Cd and Al
168 cms	183 cms.	>215 cms	158 cms	182.88 cms
15.2 $cm^2 x\ 10^3$	23.2 $cm^2 x\ 10^3$	>93 $cm^2 x\ 10^3$	14.9 $cm^2 x\ 10^3$	18.5 $cm^2 x\ 10^3$

TABLE (T.7.1) ----- CONTINUED -----

-- Equipmental details of some age measurements --

Jaworowski 1962 (R.7.10)	Paschall 1964 (R.7.11)	Spencer and Williamson 1967 (R.7.12)	Experiment, date and reference	
Stanford Pool Reactor	Atomics International AE-6	Univ. of Virginia Pool Reactor	Source Reactor	
97.4 mg/cm^2	192.9 179.7$_2$ mg/cm^2	Effective 20.6 mg/cm^2	T	Fission Source
7.62 cms	73.025 cms	59.6 cms	D	(T-thickness) (D-diameter)
Highly enriched in U235	Enriched Uranium	U-Al alloy	C	(C-composition)
90 mg/cm^2	37.0 mg/cm^2	37.0 mg/cm^2	T	Detecting foils (T-thickness)
5.06 cms^2	2.84 cms^2	3.143 cms^2	A	(A-area)
Cd	Cd 0.020"	Cd 440 mg/cm^2	Foil covers (material and thickness	
91.44 cms	182.88 cms	122 cms	H	Water tank (H- height
3.7 cm^{2}x 10^3	18.2 cm^{2}x 10^3	14.8 cm^{2}x 10^3	A	(A- area)

The earlier measurements reported indicate a wide disagreement from an overwhelmingly consistant results of the theoretical calculations, (see chapter 2.), of fission neutron age to indium resonance energy in water.

The first of the experimental determinations was by Anderson, Fermi and Nagle, (R.7.1). In this experiment the sources used, though small, were large for a 'point' source and the geometric corrections rather uncertain. The thickness of these sources introduced some perturbing effects. The water tank too was on the smaller side giving rise to a greater flux depression. Hill et al., (R.7.2), at Oak Ridge National Laboratory repeated this experiment systematically with a very much improved apparatus and also increasing the range of measurements considerably. Hoover and Arnette (R.7.3), and much later Wade, (R.7.5), measured age of fission neutrons in water as a part of their determination for the mixtures. Barkov and Mukhin, (R.7.4), in Russia, using basically a similar technique arrived at slightly better value of age than the previous ones. In all these earlier measurements which gave rather high value can to some extent be attributed to an insufficient accounting for effects of the source size on the flux distribution.

In the later determinations however, attention was

given to the study of the various perturbing effects. Blosser and Trubey (R.7.6) concentrated the attention upon the flux distribution in the region close to the fission source and to study the various effects which contribute towards the variation of flux in different independent experiments. These included the effects of water-graphite boundary on the flux in the experimental tank, the effects of the detector on the detected flux and on the flux impinging on the source and source size itself. Lombard and Blanchard, (R.7.7), also took into account the perturbing effects of the source, the detector and the structural materials in the region of flux measurements. It can be seen that with the reference to the conditions peculiar to their experiment a major contribution of error originated from the thickness of the source. Pettus, (R.7.8), in his experiment measured age of pure water as a reference point for his work in the metal-water lattices. Doerner et al., (R.7.9), in a detailed experimental work used three rectangular finite plane fission sources of different size and thicknesses and six sets of indium foils of varying densities, the later being done to obtain the unperturbed flux by extrapolating to zero foil mass. The last three experiments of the age determination in water, by Jaworowski, (R.7.10), by Paschall (R.7.11), and by Spencer and Williamson (R.7.12), all made use of the technique of the flux measurements in the planes parallel to the plane of the

fission source. This consists in irradiating cadmium covered indium foils at different radii from the axis of the fission source, in planes that are parallel to it. The activities at large radii could then be extrapolated to ∞ to get the area integral of an infinite plane detector. This being equivalent, (R.7.13), to data taken by a point detector along the axis perpendicular to an infinite fission source. The neutron age in this case is obtained as one-half of the second moment of the neutron flux. Of the three experiments mentioned above, Jaworowski's, whose equipment was less sophisticated and the analysis less detailed came up with a very low value of the measured age.

7.2. SOME DESIGN CONSIDERATIONS

In water moderator, a very rapid attenuation of both the fast and the slow neutrons necessitates an extreme refinement of measurements of flux distribution in the neighbourhood of the fission source. This puts very stringent conditions on the equipments of the age experiments. To be able to measure fluxes to a sufficient distance away from the fission source, well into the asymptotic region, sources of considerable strength are necessary. A fission source of essentially infinite plane geometry is very difficult to achieve in view of prohibitive cost and other considerations. Finite plane

or nearly 'point' fission sources are more often used. The point fission sources usually tend to be thicker as effort is made to accommodate a lot of fissile material in small lateral dimensions. Finite plane sources offer useful and the best practical alternative. Corrections of some sort for the geometry are necessary to reduce the experimental data either to apply 'infinite plane' or 'point' kernels. Whatever may be the size, the fission source has to be thin as a thicker source acts as a sink for the neutrons of a few electron volts energy and thus depressing and distorting the shape of the flux distribution being measured. The ideal boundary conditions for a neutron slowing down experiment would be to have a neutron source located at the centre of a large volume of the medium concerned. But in that case the thermal neutrons to trigger the source have to diffuse through the medium and their number is greatly reduced thus weakening the fission source. The relaxation length of the thermal neutrons being about 1 inch in water, the fission source placed as little as 4" from the boundary gives less than 8 % of the number of fissions with the same source placed at the bottom of the water tank, (sec. 5.11), at the water boundary. The source, (section 5.2), was of Uranium-Aluminium alloy of thickness 0.020 inch and the effective diameters of 6, 8, and 10 inches. The source had an estimated efficiency of 96 % . The structural materials of the fission source can, the detector housing

and the traversing mechanism, all were designed so as to cause negligible perturbation in the entire system. Extreme care was however taken particularly in vicinity of the detector to avoid any structural material which may cause neutron streaming or perturbation of flux inherent in foil activation set-up. The size of the scintillator, (sec. 5.8), is taken very near to a point. The presence of a light-guide behind the scintillator, apart from its main function of transmitting the luminations efficiently, also approximates for a minimum of foreign material in area surrounding the detector in the sense that the nuclear properties of perspex are nearly the same as those of water. The thickness of cadmium foil covering the top of the fission source and around the detector was 0.020 inch which is quite adequate for removing almost all, (R.7.6), the thermal neutrons. One thing which does not pose any practical problems in the design of a slowing down experiment in water is the size of the moderating medium. The volume of water taken was well above the least size suggested, (section 4.2), for the avoidance of any measurable flux distortion.

The various measurements and the techniques of data treatment have already been mentioned in the review in the section above. In the present case the experimental data is taken essentially with a point detector along the axis perpendicular to the circular lamina of fission

source of finite dimensions. The expression of neutron flux in the case of point source-point detector is then modified by considering the disc fission source to be made up of a large number of point sources and thus integrating the expression over the entire source size. The parameters of the flux expression are evaluated by fitting the modified expression to the observed flux. Fitting procedure is carried out region by region and the parameter values are then used in the determination of neutron age.

7.3. AGE OF FISSION NEUTRONS TO INDIUM RESONANCE ENERGY IN WATER.

The technique and the theory of the data analysis for the present series of experiments are detailed out in the previous chapter. The resultant fit in the case of indium is displayed in the Table (T.7.2), which is the combined fit to the observed data by the programmes 'PARSTA', 'EVALPA' and 'PARLIN'. Tables (T.7.3), (T.7.4) and (T.7.5) give the values of the parameters as obtained by the above mentioned fitting programmes. Figure (F.7.1) is a plot of '$r^2\Phi$' against 'r', where r is the observed distance of the detector from the fission source. The figure shows the integrated curve and includes all three regions. The continuity of the curve with the best fits to the observed data points was ascertained by the method already described in chapter 6.

TABLE (T.7.2)

Tabulated flux distribution of the slowed down neutrons of indium resonance energy from fission source in water.

r	Observed Φ(r sqd)	Calculated Φ(r sqd)	r	Observed Φ(r sqd)	Calculated Φ(r sqd)
3.9166	5584.591	5629.723	19.9166	3485.214	3601.222
4.4166	6953.482	7053.272	20.4166	3531.143	3381.817
4.9166	8280.849	8152.682	20.9166	3337.762	3166.499
5.4166	9137.227	9160.941	21.4166	3061.732	2956.874
5.9166	10097.431	10043.991	21.9166	2681.584	2748.513
6.4166	10755.740	10774.738	22.4166	2718.787	2570.971
6.9166	11431.473	11333.826	22.9166	2180.370	2403.792
7.4166	11624.044	11709.947	23.4166	2203.322	2246.516
7.9166	11854.295	11899.704	23.9166	2392.268	2098.680
8.4166	11655.341	11712.862	24.4166	2037.960	1979.827
8.9166	11878.718	11688.955	24.9166	1789.581	1842.566
9.4166	11728.830	11568.284	25.4166	1915.374	1727.275
9.9166	12230.512	11360.295	25.9166	1573.274	1594.704
10.4166	11017.466	11075.606	26.4166	1437.704	1495.377
10.9166	10593.015	10725.590	26.9166	1577.548	1384.889
11.4166	10205.867	10321.978	27.4166	1351.562	1290.854
11.9166	9984.128	9876.478	27.9166	1258.316	1202.900
12.4166	9402.972	9400.427	28.4166	1316.165	1130.670
12.9166	8373.031	8904.507	28.9166	1021.390	1058.824
13.4166	7514.270	8398.502	29.4166	1053.088	998.039
13.9166	7748.706	7891.130	29.9166	889.391	930.487
14.4166	6549.963	7390.175	30.4166	780.332	872.431
14.9166	6984.942	6901.426	31.4166	636.508	752.556
15.4166	6514.269	6430.222	32.4166	759.970	654.400
15.9166	6106.093	5980.441	33.4166	560.474	576.112
16.4166	5374.757	5554.848	34.4166	414.888	502.084
16.9166	5129.074	5192.207	35.4166	376.129	442.886
17.4166	4624.126	4890.475	36.4166	462.729	389.256
17.9166	5036.189	4592.296	37.4166	289.898	340.085
18.4166	3997.447	4317.412	38.4166	191.926	304.333
18.9166	4047.477	4055.738	39.4166	263.921	269.249
19.4166	3817.855	3807.095	40.4166	235.926	236.551

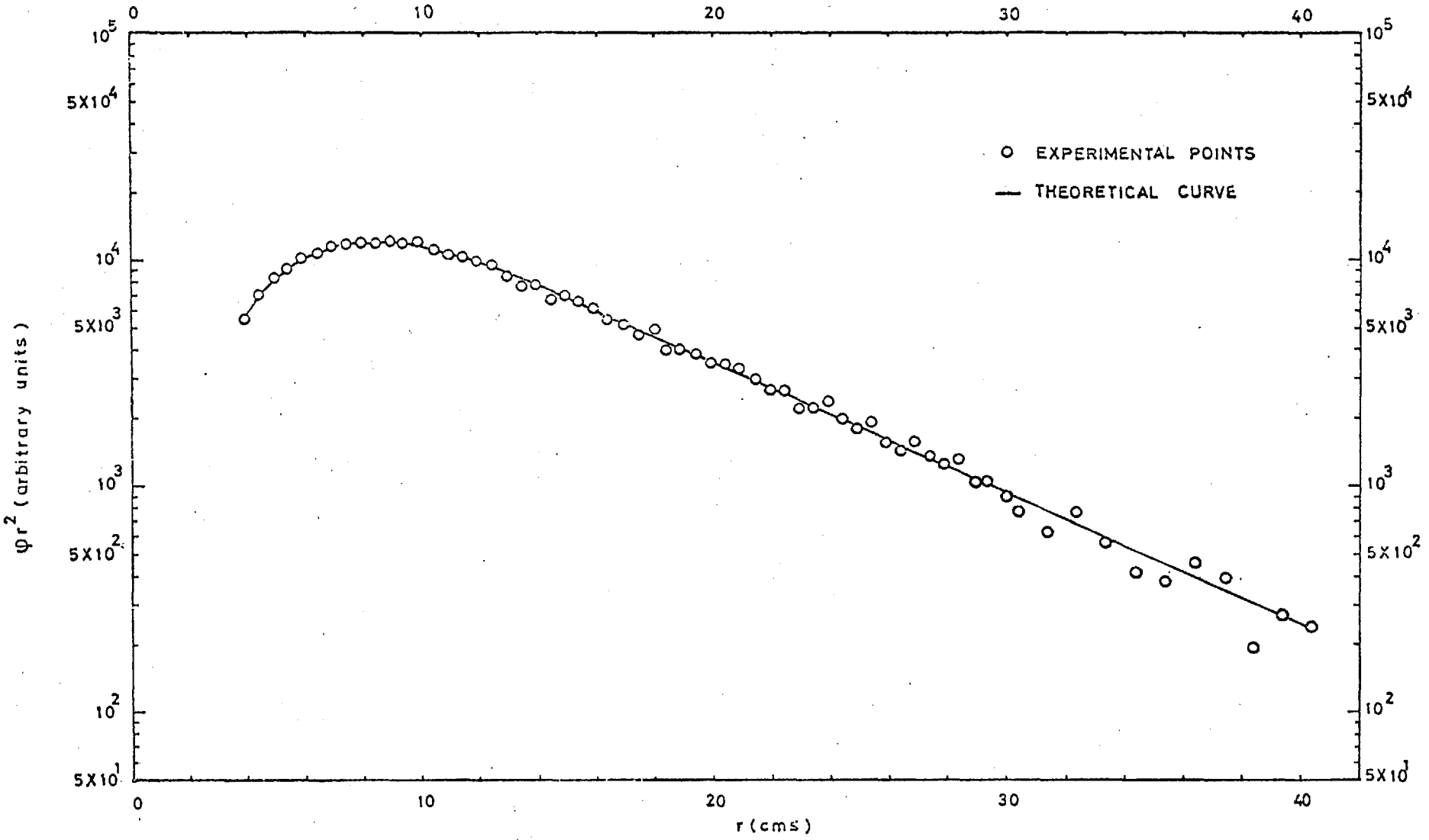

FIGURE (F.7.1) SPATIAL DISTRIBUTION OF INDIUM RESONANCE NEUTRONS FROM FISSION SOURCE IN WATER.

TABLE (T.7.3)
Parameter values for indium from programme 'PARSTA'.

Parameters		
Name	Value	Std. Dev.
'A_s'	.1287357E+04	.3231297E+02
'C_s'	.1492280E-01	.2828367E-03

TABLE (T.7.4)
Parameter values for indium from programme 'EVALPA'.

'A_m'	.4448970E+03	.6392466E+02
'B_m'	.4959915E+05	.4698200E+04
'C_m'	.1284892E-01	.4726514E-03
'f_m'	.1236747E+00	.5701254E-02

TABLE (T.7.5)
Parameter values for indium from programme 'PARLIN'.

'B_E'	.1194464E+06	.1379185E+05
'f_E'	.1538085E+00	.4641467E-02

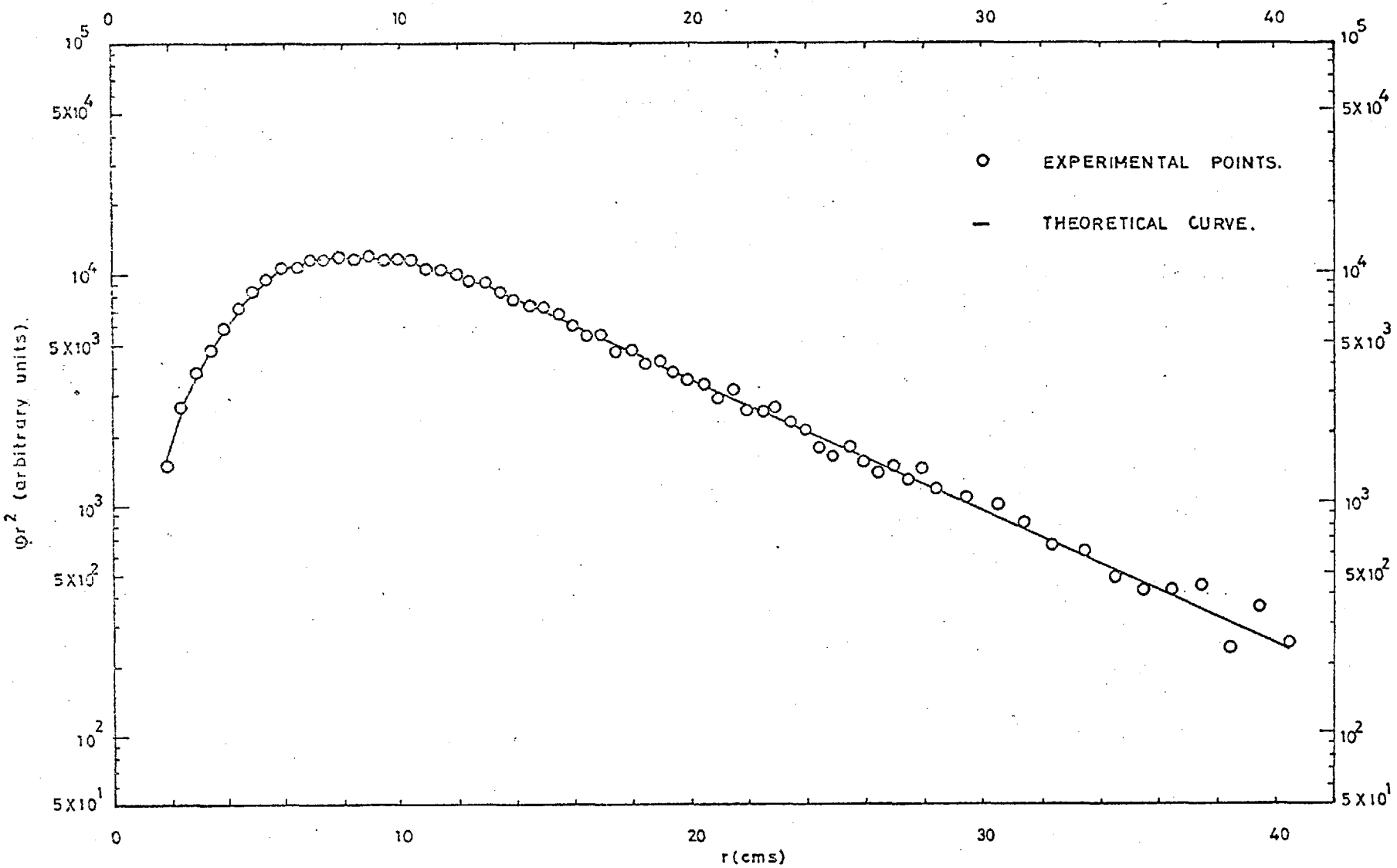

FIGURE (F.7.2) SPATIAL DISTRIBUTION OF INDIUM RESONANCE NEUTRONS FROM FISSION SOURCE IN WATER. - Set 2.-

The limit of the first region, R_1, beyond which the 'EVALPA' fit is applicable, is taken to be 5.4 cms from the position of the fission source. The other limit, R_2, which marks the begining of the asymptotic region, is 25.0 cms. These limits were arrived at by taking the middle points of the ranges of overlap of the adjecent fits. Since these fits merge into each other smoothly, any slight variation of the limits within the overlapped regions does not affect the value of neutron age. Using the values of the parameters from the Tables (T.7.3), (T.7.4) and (T.7.5) within the prescribed limits, the equation (6.4.E5), yields a preliminary value of the age of fission neutrons to indium resonance energy in water as 27.36 cms^2, using a 10 inch diameter source.

In view to extrapolate the age value to a point source and to check the consistancy of the measurements, observations were made using 8" and 6" diameter sources. With the 8" source, a remarkably good set of points were obtained. The 6" source yielded good near distance points but at greater distances, due to poorer intensity of the source the scatter of the points was great. Only the near distance points were optimised and used with the 8" data. This formed set 2. The regional fittings were carried out in the usual way and the tabulated fitted data along with the parameter values are given in the tables from (A.T.7.1) to (A.T.7.4) in Appendix (A.7.1). The flux plot of 'Φr^2' against 'r' is given in figure (F.7.2). The neutron age obtained in this case was 27.24 cms^2.

TABLE (T.7.6)

Tabulated flux distribution of the slowed down neutrons of gold resonance energy from fission source in water.

r	Observed Φ(r sqd)	Calculated Φ(r sqd)	r	Observed Φ(r sqd)	Calculated Φ(r sqd)
2.4166	639.397	621.042	18.9166	857.786	826.271
2.9166	1035.699	895.365	19.4166	835.650	775.240
3.4166	1104.570	1213.760	19.9166	873.239	730.623
3.9166	1708.759	1572.619	20.4166	662.896	698.011
4.4166	1964.381	1967.909	20.9166	631.423	652.052
4.9166	2351.026	2350.217	21.4166	799.453	616.418
5.4166	2484.040	2521.347	21.9166	431.890	586.947
5.9166	2582.114	2661.550	22.4166	613.644	549.341
6.4166	2750.640	2764.076	22.9166	465.584	519.457
6.9166	2881.762	2828.932	23.4166	481.039	490.151
7.4166	3145.263	2857.389	23.9166	552.372	462.303
7.9166	2735.549	2851.824	24.4166	385.886	433.813
8.4166	2909.827	2815.513	24.9166	416.438	409.593
8.9166	2483.654	2752.398	25.4166	376.223	386.571
9.4166	2866.151	2666.848	25.9166	456.228	367.682
9.9166	2494.033	2563.418	26.4166	264.633	342.866
10.4166	2669.598	2446.632	26.9166	411.213	322.071
10.9166	2473.730	2320.792	27.4166	283.901	304.248
11.4166	2391.292	2189.835	27.9166	307.009	285.350
11.9166	1956.687	2057.217	28.4166	271.491	269.238
12.4166	2183.747	1925.851	28.9166	169.207	256.162
12.9166	1613.234	1798.082	29.4166	225.015	241.790
13.4166	1777.981	1675.693	30.4166	281.557	214.301
13.9166	1537.354	1559.939	31.4166	175.425	188.583
14.4166	1248.771	1451.666	32.4166	231.993	168.598
14.9166	1172.651	1351.128	33.4166	172.791	151.262
15.4166	1598.549	1268.445	34.4166	99.915	134.173
15.9166	1266.340	1193.411	35.4166	49.546	119.084
16.4166	1209.841	1115.641	36.4166	131.127	106.389
16.9166	873.444	1054.621	37.4166	102.748	94.388
17.4166	1089.881	989.774	38.4166	63.815	83.696
17.9166	830.502	935.493	39.4166	122.199	74.590
18.4166	1068.192	876.181	40.4166	79.959	66.576

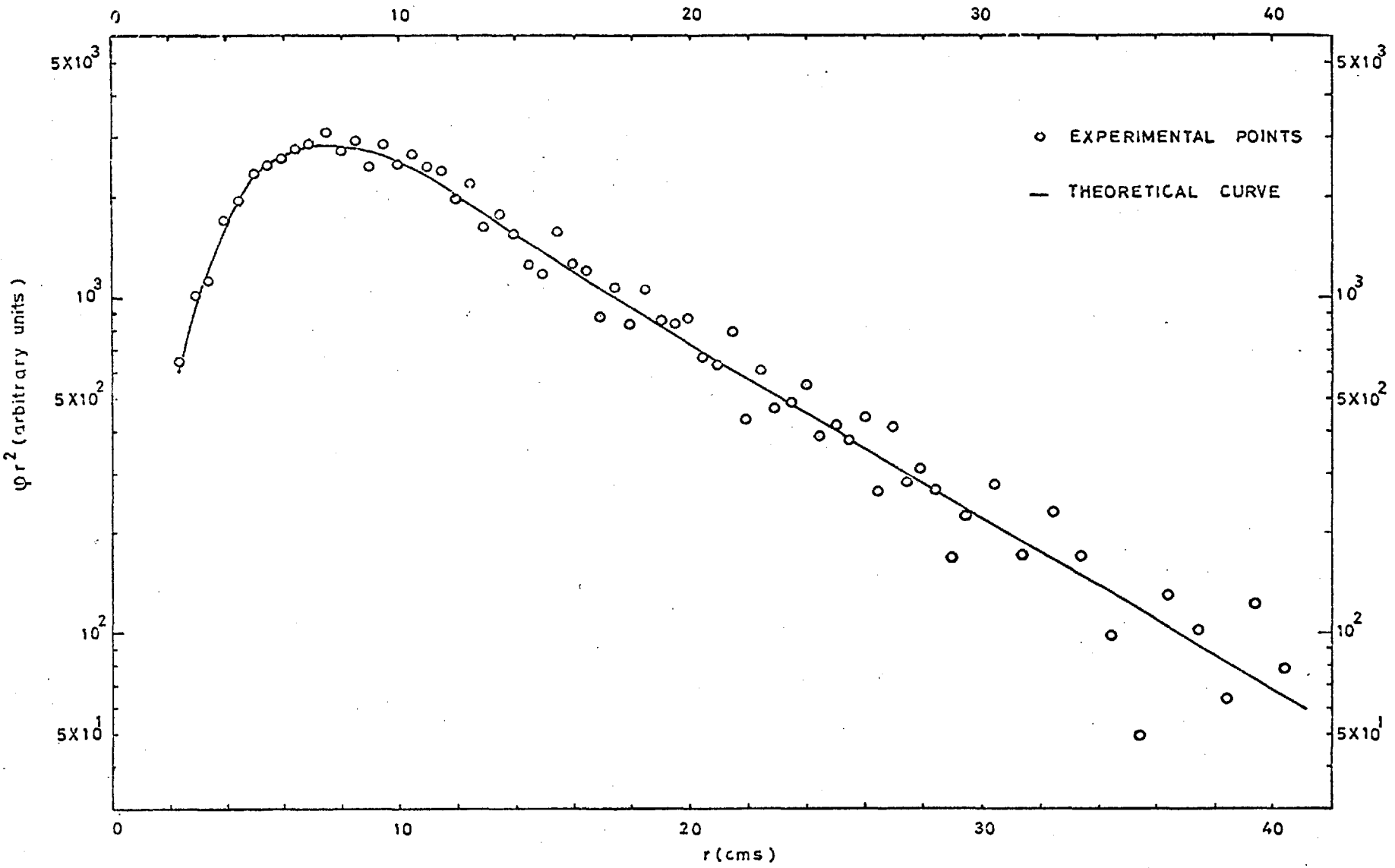

FIGURE (F.7.3) SPATIAL DISTRIBUTION OF GOLD RESONANCE NEUTRONS FROM FISSION SOURCE IN WATER.

7.4. AGE OF FISSION NEUTRONS TO GOLD RESONANCE ENERGY IN WATER.

Due to a considerable scatter of points in the case of gold data, a greater effort was needed in obtaining the best regional fits that are at the same time continuous with the adjecent fits. Consequently a greater number of cases were considered by shifting the bounds of the regions slightly one way or the other by including or by dropping off points in the fitting procedure. The final fitting is given in Table (T.7.6). Figure (F.7.3) shows the plotted out observed and calculated fluxes. Tables (T.7.7), (T.7.8) and (T.7.9) show the parameter values in the present case as obtained by the three fitting programmes. The limits R_1 and R_2 are 4.4 and 25.0 cms respectively. Programme 'NEUAGE' using the equation (6.4.E5) evaluates the preliminary value of the age of fission neutrons to gold resonance energy as 23.41 cms^2.

TABLE (T.7.7)
Parameter values for gold from programme 'PARSTA'.

Parameters		
Name	Value	Std. Dev.
'A_s'	.1463863E+03	.2061868E+02
'C_s'	.3855398E-02	.4912392E-03

TABLE (T.7.8).
Parameter values for gold from programme 'EVALPA'.

'A_m'	.1958116E+03	.5449088E+02
'B_m'	.1253987E+05	.6245223E+04
'C_m'	.1810929E-01	.2583187E-02
'f_m'	.1258441E+00	.2001691E-01

TABLE (T.7.9).
Parameter values for gold from programme 'PARLIN'.

'B_E'	.4698946E+05	.9438108E+04
'f_E'	.1764119E+00	.1804576E-01

7.5. AGE OF FISSION NEUTRONS TO RHODIUM RESONANCE ENERGY IN WATER.

The final stage fittings in the case of rhodium data is listed in the Table (T.7.10) and the parameter values along with the calculated standard deviations on each are given in Tables (T.7.11), (T.7.12) and (T.7.13). Figure (F.7.4) shows the flux plot with 'Φr^2' against 'r' where the experimental points and the fitting curves include all

TABLE (T.7.10)
Tabulated flux distribution of the slowed down neutrons of rhodium resonance energy from fission source in water.

r	Observed Φ(r sqd)	Calculated Φ(r sqd)	r	Observed Φ(r sqd)	Calculated Φ(r sqd)
3.9166	2813.742	2767.196	18.4166	1911.151	1845.939
4.4166	3396.915	3411.708	18.9166	1580.244	1722.941
4.9166	4079.087	4091.523	19.4166	1469.757	1606.925
5.4166	4770.340	4601.874	19.9166	1637.237	1497.669
5.9166	4948.846	5050.691	20.4166	1532.990	1394.927
6.4166	5582.063	5424.264	20.9166	1180.573	1298.441
6.9166	5749.662	5750.338	21.4166	1222.218	1207.938
7.4166	5798.386	5857.636	21.9166	1008.525	1123.143
7.9166	5866.422	5885.020	22.4166	1045.927	1035.928
8.4166	5631.955	5858.420	22.9166	928.380	969.566
8.9166	5748.358	5776.748	23.4166	974.196	900.234
9.4166	5673.854	5651.695	23.9166	769.827	835.515
9.9166	6187.042	5487.494	24.4166	859.322	780.146
10.4166	5832.486	5290.689	24.9166	628.678	728.876
10.9166	4742.865	5067.906	25.4166	754.483	676.460
11.4166	5348.147	4825.637	25.9166	549.916	627.666
11.9166	4236.734	4570.056	26.4166	626.064	582.267
12.4166	3824.796	4306.865	26.9166	426.071	539.952
12.9166	3943.577	4041.179	27.4166	512.963	509.472
13.4166	3723.451	3777.440	27.9166	532.935	469.366
13.9166	3358.973	3519.383	28.4166	388.653	440.520
14.4166	3344.514	3270.022	28.9166	535.667	415.104
14.9166	3274.710	3031.794	29.4166	256.926	378.463
15.4166	2539.886	2806.106	29.9166	397.775	353.960
15.9166	2771.238	2594.166	30.9166	374.821	309.487
16.4166	2148.561	2421.001	31.9166	360.132	270.136
16.9166	2341.079	2268.569	32.9166	171.007	236.208
17.4166	2321.651	2133.623	33.9166	258.135	206.900
17.9166	2112.970	1976.115	34.9166	159.896	179.409

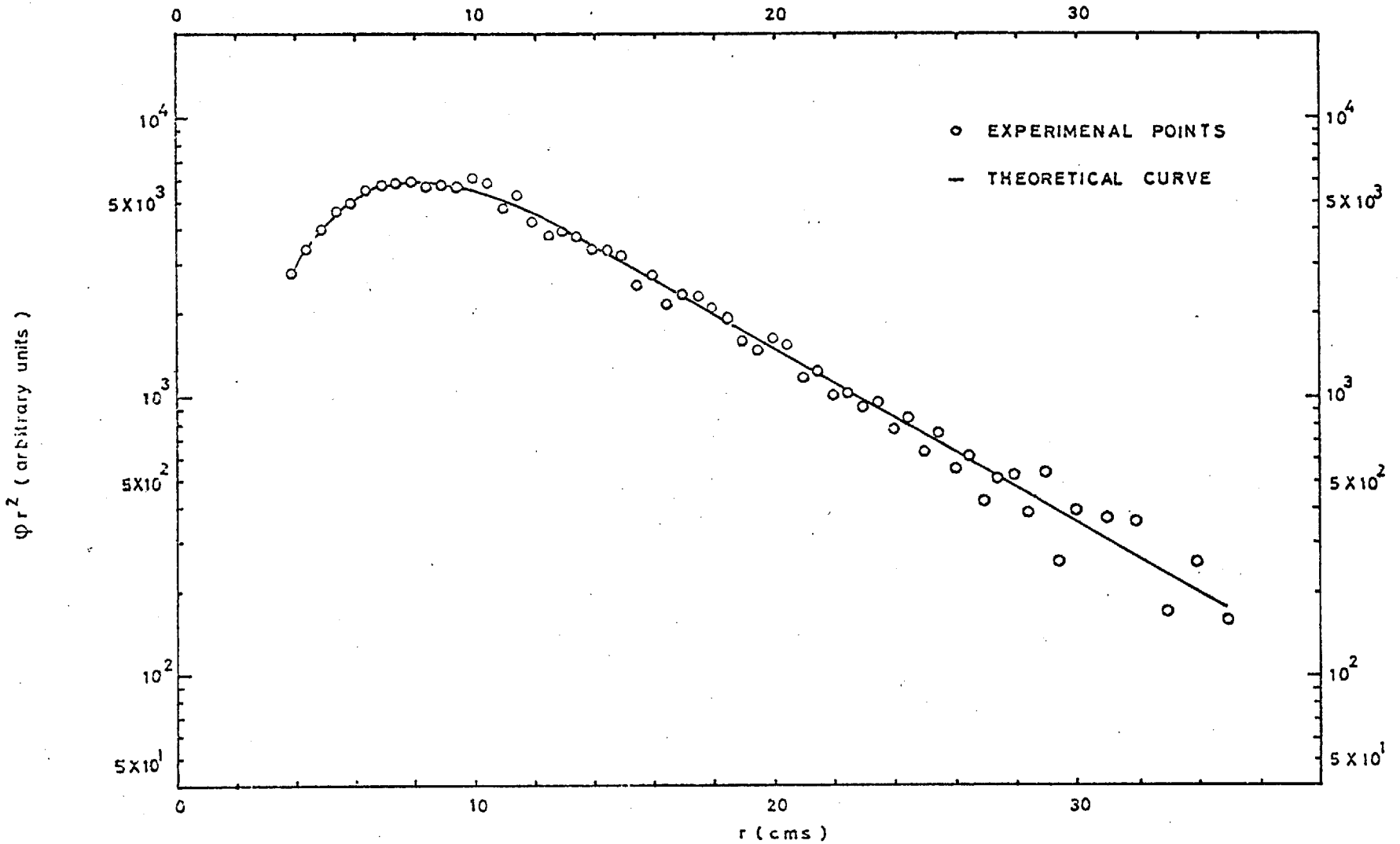

FIGURE (F.7.4) SPATIAL DISTRIBUTION OF RHODIUM RESONANCE NEUTRONS FROM FISSION SOURCE IN WATER.

TABLE (T.7.11)
Parameter values for rhodium from programme 'PARSTA'.

Parameters		
Name	Value	Std. Dev.
'A_s'	.4737123E+03	.2515278E+02
'C_s'	.1262971E-01	.9606722E-03

TABLE (T.7.12)
Parameter values for rhodium from programme 'EVALPA'.

'A_m'	.2368393E+03	.4827090E+02
'B_m'	.3427661E+05	.7462798E+04
'C_m'	.1443062E-01	.1032129E-02
'f_m'	.1440642E+00	.1216014E-01

TABLE (T.7.13)
Parameter values for rhodium from programme 'PARLIN'.

'B_E'	.6727660E+05	.6454270E+04
'f_E'	.1675045E+00	.1086914E-01

the three regional fits. The limits R_1 and R_2 arrived at in the usual way are 8.91 and 28.0 cms respectively from the position of the fission source. The neutron age evaluation using programme 'NEUAGE' results in the preliminary value of age to rhodium resonance energy as 27.63 cms^2, using 10 inch fission source.

7.6. EXTRAPOLATION FOR THE POINT SOURCE GEOMETRY.

The neutron age values obtained in the section 7.3. to indium resonance energy using 10 and 8 inch diameter sources provide data for the extrapolation of the value of age for a point fission source. This extrapolation in figure (F.7.5) results in the value of 26.8 cms^2 in the case of indium. This correction of 2.05 % will also be applied to other results in order to convert them to point source results.

7.7. EVALUATION OF THE EXTENT OF ERROR ON THE DETERMINED NEUTRON AGES.

The values of the parameters of the equation (6.4.E5) along with their standard deviations, as obtained in the data analysis in the three cases have already been given in the sections above. A look at the equation (6.4.E5), suggests that the value of age would be more sensitive to the errors on the exponential values in the expression

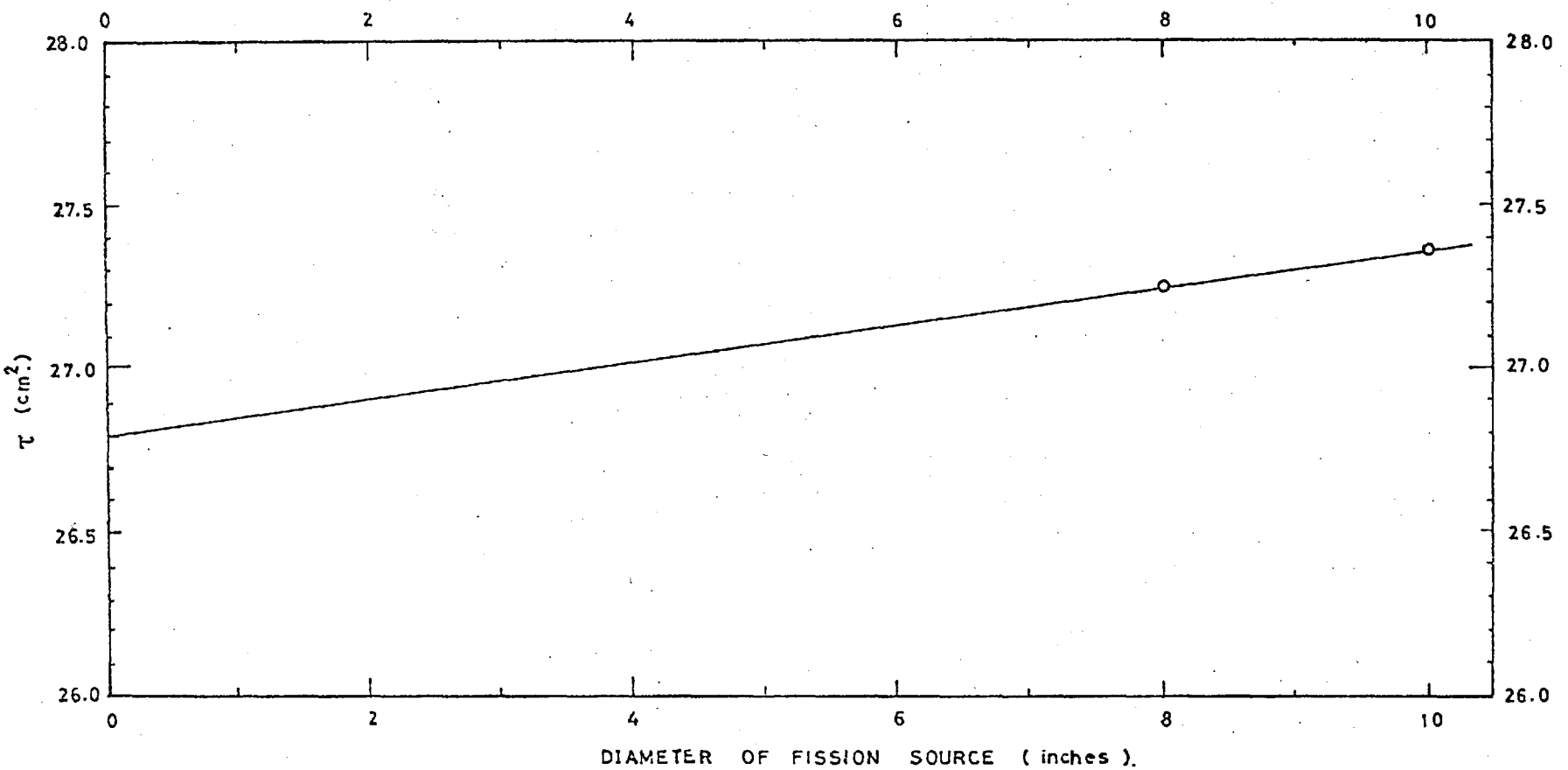

FIGURE (F.7.5). A PLOT OF 'τ' AGAINST THE SOURCE DIAMETER.

and particularly so for the extrapolated contribution to the integral of the measured data.

TABLE (T.7.14).
Preliminary values (point source) of the ages with the bounds of error calculated from the scatter of points.

Data	Age (cm^2)	Bounds of error (cm^2)
In	26.80	$\pm$0.94
Au	22.93	$\pm$1.62
Rh	27.06	$\pm$1.11

An error equal to the standard deviation was put on the parameters of intrest, and the age evaluation was again carried out. The difference of the two values of ages calculated with the correct values of the parameters and the ones with the altered values on the knowledge of their standard deviations, gives an estimate of error on the values of the determined ages. Table (T.7.14), above, gives the ages in the three cases along with their errors so estimated. The limits of error represents the range or the bounds within which the ages determined from the above sets of data can vary on account of the scatter cf the experimental points.

CHAPTER 8.

NEUTRON AGES IN A MEDIUM CONTAINING CYLINDRICAL CAVITIES.

8.1. INTRODUCTION AND THEORY.

To provide for the cooling facility and to extract heat from a nuclear reactor, spaces for coolant circulation are provided. Gases being useful coolants, have been used in many reactors. Since in the case of the more commonly used coolant gases, neutron scattering and absorption are negligible, so for the purpose of evaluation of the reactor parameters in a moderator containing pipes can be regarded as empty spaces in the moderating material. The effect of the empty channels on the reactor parameters is of great importance in the reactor design. In a moderator of a given overall density the number of collisions of the neutrons from the fission energy to a fixed lower energy of detecting instrument, remains unaltered but the presence of the empty channels in the moderator causes a rise in the effective mean free path in the system. The way it happens differs from one case to another depending upon the size of the holes and the spacings between them. Considering the present case of the hole diameter being greater than the mean free path in the solid material and the lattice pitch many folds greater than that, some free paths would be greatly lengthened as compared to the others which travel

entirely in the moderator without encountering any of the cylindrical cavities.

Many authors have attempted to study the effect of holes in moderator and its various aspects. Many kinds of cavities have been subject of studies but undoubtedly the configuration of a regular array of cylindrical cavities has received most attention for its obvious application to cooling channels in a reactor. Behrens (R.8.1 to R.8.4), proposed a statistical method of calculating the mean square free path. His theories suggest that the migration area varies directly as the neutron mean square free path in a particular direction. His formulations for the axial and the radial streaming converted to the present terminology can be put in the following equations.

$$S_{(axial)} = 1 + \beta + \beta \cdot \frac{r_c}{\lambda_m} \cdot \frac{3}{2} Q \qquad ....(8.1.E1)$$

$$S_{(radial)} = 1 + \beta + \beta \cdot \frac{r_c}{\lambda_m} \cdot \frac{3}{4} Q \qquad ....(8.1.E2)$$

In obtaining the above expressions, Behrens exponential term has been omitted, as for most of the cases this term is infinitesimally small except in the case of very small holes. In the present situation it is not relevant. 'β' is the ratio of the volume of the cavity to the total

volume of the cell (moderator + cavity), 'r_c' the radius of cavity, 'λ_m' the mean free path of the neutron in the moderating material. 'Q' is the ratio of the mean square passage length through the hole to the square of the mean passage length. This value calculated by Behrens for cylindrical cavities of circular section is 1.333. In Behrens theory the calculations are not made from the mean square distance until absorption but from the sum of the mean squares of the elementary paths, the assumption that a free path in every direction always crosses the medium with a mean distance, amounts to the use in a lattice of a property true only in a homogeneous medium. As a result the formula given by Behrens for the radial streaming becomes less reliable particularly for the larger diameter channels. Benoist (R.8.5 to R.8.7) gives a detailed treatment of the neutron transport in heterogeneous medium with holes. He developes an iterative solution of the integral transport equation. His formulations for the fast group, is adapted in the present case of empty channels by equating 'a' - the radius of the fuel rod to zero, which eliminates all the fuel terms. The resultant streaming relations are presented below.

$$S_{(axial)} = 1 + \beta + \beta \cdot \frac{r_c}{\lambda_m} \cdot (Q_z + Q_z' - q_z) \qquad \ldots.(8.1.E3)$$

$$S_{(radial)} = 1 + \beta + \beta \cdot \frac{r_c}{\lambda_m} \cdot (Q_r + Q_r' - q_r) \qquad \ldots.(8.1.E4)$$

where the Qs' are the various definite functions evaluated below. In the present case 'a' being zero, also leads $\alpha = a/c_r$ and $\mu = a/\lambda_u$ to zero. $Q_z = 2F(\alpha)$, $Q_r = F(\alpha)$, produce values as 2 and 1 respectively for $\alpha = 0$. ($F(\alpha)$ is the original Behrens function which was recalculated by Benoist with greater precision.). Q_z' and Q_r' which are functions of α and μ, are zero. q_z vanishes but $q_r = 3q_o/2$ where q_o is a function of $\Upsilon = c_r/\lambda_m$ and of α. The value of q_o can be obtained from (R.8.5), fig 4, for corresponding Υ. Benoist later expression (R.8.7) differs from the earlier one only in the Q values.

$$S_{(axial)} = 1 + \beta + \beta \cdot \frac{c_r}{\lambda_m} (Q_z^*) \qquad \ldots.(8.1.E5)$$

where $Q_z^* = Q_z + Q_z'$ which already have been evaluated above;

and

$$S_{(radial)} = 1 + \beta + \beta \cdot \frac{c_r}{\lambda_m} (Q_r^*) \qquad \ldots.(8.1.E6)$$

with

$$Q_r^* = Q_r + Q_r' - \frac{(1-\mu W_r)G}{\Delta - \mu J} \qquad \ldots.(8.1.E7)$$

with $\mu = 0$, the last part of the equation reduces to G/Δ, and $G = (1+\alpha)(1-\mu W_r) = 1$, for $\alpha=0$ and $\mu=0$, so that

above expression (8.1.E7) becomes,

$$Q_r^* = 1 - \frac{1}{\Delta} \qquad \ldots.(8.1.E8)$$

where,

$$\Delta = \gamma \cdot \frac{\gamma + 1 + \frac{1}{2} \cdot \beta'}{\gamma^2 - \frac{3\gamma+1}{2} \cdot \beta'} \qquad \ldots.(8.1.E9)$$

which can be evaluated. Other authors like Grant (R.8.8) and later Carter (R.8.9) also arrived at radial streaming correction factor similar to Benoist, all the theories being in agreement on the axial streaming.

A group of Japanese authors (R.8.14) to (R.8.19), have developed systematically, a stochastic method of calculating the second spatial moment of the neutron distribution in hydrogenous media. Later they included in their theories, the effect of cavities of various kinds. However, the theories in their present state of developement elude general practical application.

8.2. THE CYLINDRICAL VOIDS.

Other experimental studies concerning the influence on the neutron transport in a moderator containing holes, have largely been done in graphite. A summary of some

results is given by Zhezherun (R.8.11). Experimental work, (R.8.12, R.8.13), has also been carried out in perspex with empty channels and using pulsed neutron source. The purpose of the present series of experiments is to study the effect of neutron streaming in water with array of cavities and to compare the results with theoretical estimations by Behrens and Benoist.

Experimental studies on the effect of empty channels on the age of fission neutrons in water was made using voids simulated by immersing a number of hollow perspex tubes closed at both ends. A detachable 'cubic' structure was made in four parts, each containing nine tubes fitted to two end-plates. The four parts could be installed in the experimental tank with the tubes in the vertical and the horizontal set ups, without disrupting the critical settings of the traversing mechanism. The perspex tubes have the inner diameter of 2.125" and the wall thickness of 0.25". The array was designed in such a way that when the four parts of the 'cubic' structure are clamped in position, the tubes are at a constant pitch of 5" in the system in either case. Figures (F.8.1) and (F.8.3), not drawn to scale, respectively show the arrangement of the vertical and the horizontal set up of tubes in the tank. With the fission source at the bottom of the experimental tank, the end-plates of the tubes were at a distance of 3" from the source. The thickness of perspex discs at the

of cavities was 1 inch. In calculating the effective void ratio to the limit of measurements, the separation of the fission source and the actual voids, was taken into account. The air-to-water ratio was 10.3 % .

8.3. EQUIPMENTAL MODIFICATIONS, TESTS, AND THE NEUTRON FLUX MEASUREMENTS.

The bridge of the traversing mechanism was modified so that this bridge carrying the scintillation assembly, is able to traverse freely both in the case of the vertical and the horizontal arrangements of the tubes. This is done in such a way that in either case it does not upset the constant pitch and the symmetry of the array. The final version of the bridge is already shown in the fig (F.5.3), in chapter 5. It may be remembered that for experiments without the tubes the central bar of the bridge was straight. The present arrangement of the bridge was however subject to the same sort of calibration and source-detector distance correction test as described in section (6.3.2). The distance correction to be applied in the this case was -0.67 cms.

The four part 'cubic' structure after being lowered into the tank was joined in two blocks with perspex spacers and the blocks then clamped down from the top of the tank by aluminium angle frame work. Before the installation of the perspex tubes, each independently sealed tube fitted

to the end plates, were subjected to a prolonged immersion in water. All tubes were proved to be worthy of desired and perfect voidage for the main experiments of the present series.

The measurements of the fluxes are done precisely as described in section (5.12), and the observed indium resonance flux extracted from the data as in sec. (6.3.1).

8.4. THE RESULTS

8.4.1. THE AGE OF FISSION NEUTRONS TO THE INDIUM RESONANCE ENERGY IN WATER CONTAINING VERTICAL CYLINDRICAL CAVITIES.

The resultant fit to the experimental data taken of the indium resonance neutron flux in water containing vertical cylindrical voids, simulated by the perspex tubes is displayed in the Table (T.8.1). The combined fit is obtained as in the cases of the series of experiments with no cavities and likewise fitting region by region using the equations (6.5.E3), (6.4.E5), and (6.5.E4). The criterion of the selection of the best fits was taken the same as for the series in the previous chapter. Tables (T.8.2), (T.8.3), and (T.8.4) give the parameter values as obtained by the fitting programmes. Figure (F.8.2), represents the plot of '$r^2\Phi$' against 'r', where the symbols have their usual meanings.

FIG (F.8.1) ARRANGEMENT OF VERTICAL CYLINDRICAL CAVITIES

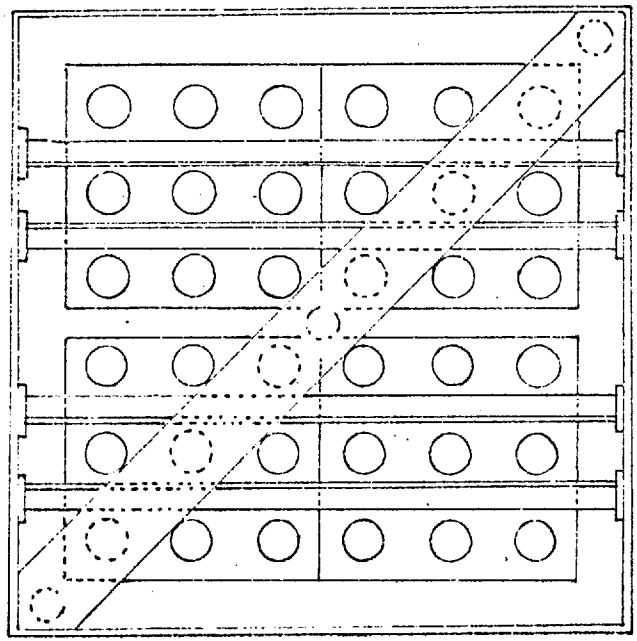

PLAN

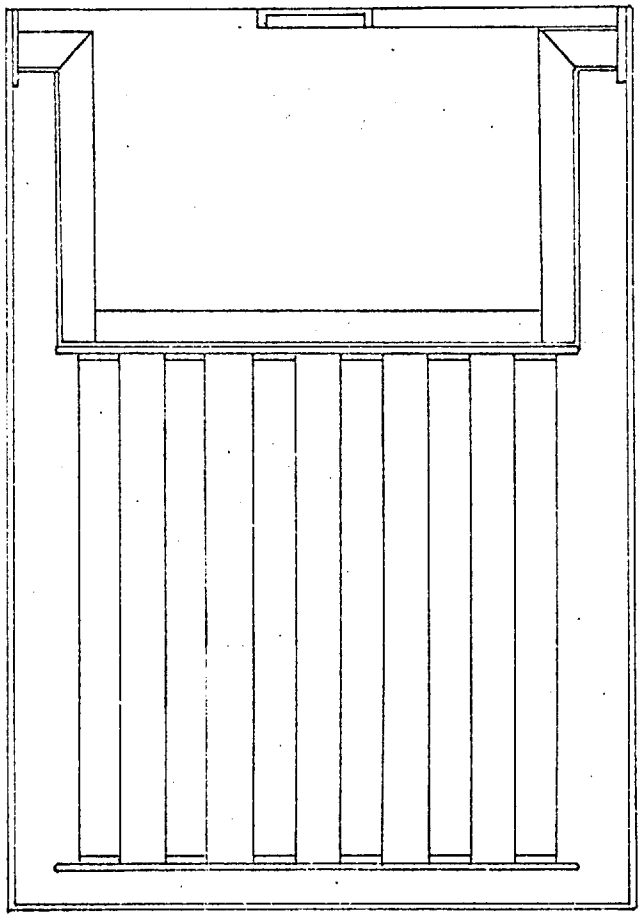

FRONT ELEVATION

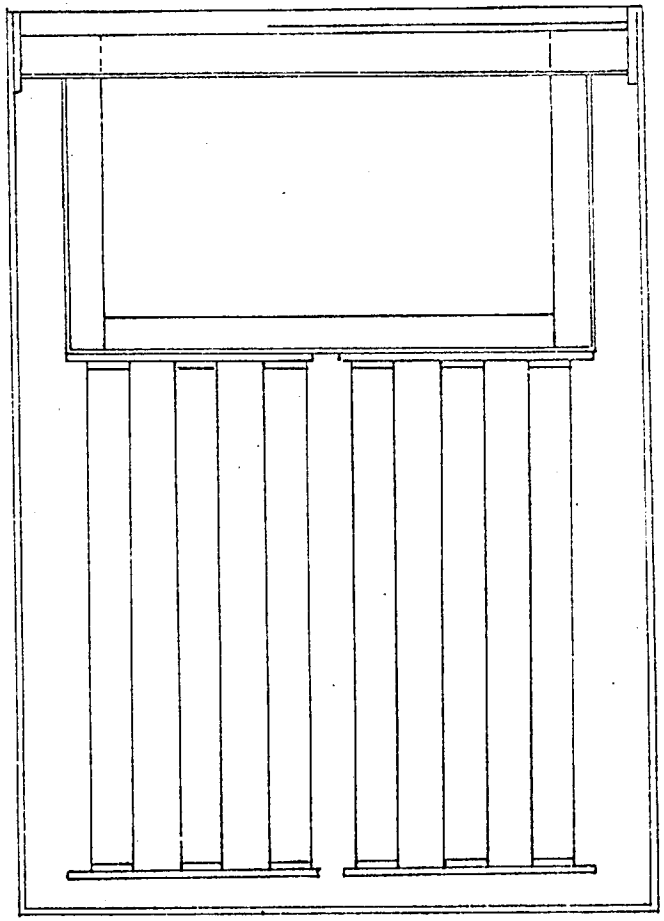

SIDE ELEVATION

TABLE (T.8.1).

Tabulated flux distribution of the slowed down neutrons of the indium resonance energy from fission source in water containing vertical cylindrical cavities.

r	Observed Φ(r sqd)	Calculated Φ(r sqd)	r	Observed Φ(r sqd)	Calculated Φ(r sqd)
2.3291	1104.9367	1135.3140	16.3291	2982.8789	2743.4490
2.8291	1675.2814	1616.0261	17.3291	2279.3857	2621.2176
3.3291	2388.0963	2143.8536	18.3291	2166.0118	2216.3586
3.8291	2416.6976	2698.3763	19.3291	1850.4322	2002.8401
4.3291	3398.6523	3258.7417	20.3291	1482.1231	1772.4365
4.8291	4111.3051	3804.6146	21.3291	1657.6116	1606.5832
5.3291	4158.6791	4317.0546	22.3291	1323.2594	1415.8433
5.8291	5218.3082	4779.2783	23.3291	1125.5243	1281.2716
6.3291	4782.5618	5177.2682	24.3291	1394.4041	1149.4793
6.8291	5430.2583	5500.2080	25.3291	1021.3740	1020.9660
7.3291	5389.0853	5740.2762	26.3291	906.7337	920.1551
7.8291	6191.5202	5894.9559	27.3291	823.9502	827.4282
8.3291	6035.1556	5962.4168	28.3291	647.2827	744.1504
8.8291	5487.5970	5945.7455	29.3291	775.4034	668.6880
9.3291	5797.2860	5850.3003	30.3291	596.0959	600.4233
9.8291	5952.6405	5683.6766	31.3291	551.9787	538.7578
10.3291	5454.4064	5455.1659	32.3291	580.6674	483.1287
10.8291	5495.4765	5227.1985	33.3291	372.6973	433.0020
11.3291	4942.7061	4921.2717	34.3291	417.0312	387.8804
11.8291	5049.1175	4643.7543	35.3291	434.8038	347.3010
12.3291	4473.4859	4451.3670	36.3291	240.2306	310.8366
13.3291	4150.5824	3926.3717	37.3291	215.9423	278.0943
14.3291	3296.1380	3507.6045	38.3291	269.9067	248.7137
15.3291	2975.3309	3154.3611			

TABLE (T.8.2)

Parameter values from programme 'PARSTA', (Vertical cavities)

Parameters		
Name	Value	Std. Dev.
'A_s'	.5699482E+03	.3230269E+02
'C_s'	.1391701E-01	.5720720E-03

TABLE (T.8.3)

Parameter values from programme 'EVALPA', (Vertical cavities)

'A_m'	.3090409E+03	.7321119E+02
'B_m'	.1427121E+05	.4903914E+04
'C_m'	.1396368E-01	.9669947E-03
'f_m'	.9672358E-01	.1266911E-01

TABLE (T.8.4)

Parameter values from programme 'PARLIN', (Vertical cavities)

'B_E'	.2654360E+05	.8516255E+04
'f_E'	.1172264E+00	.4137967E-02

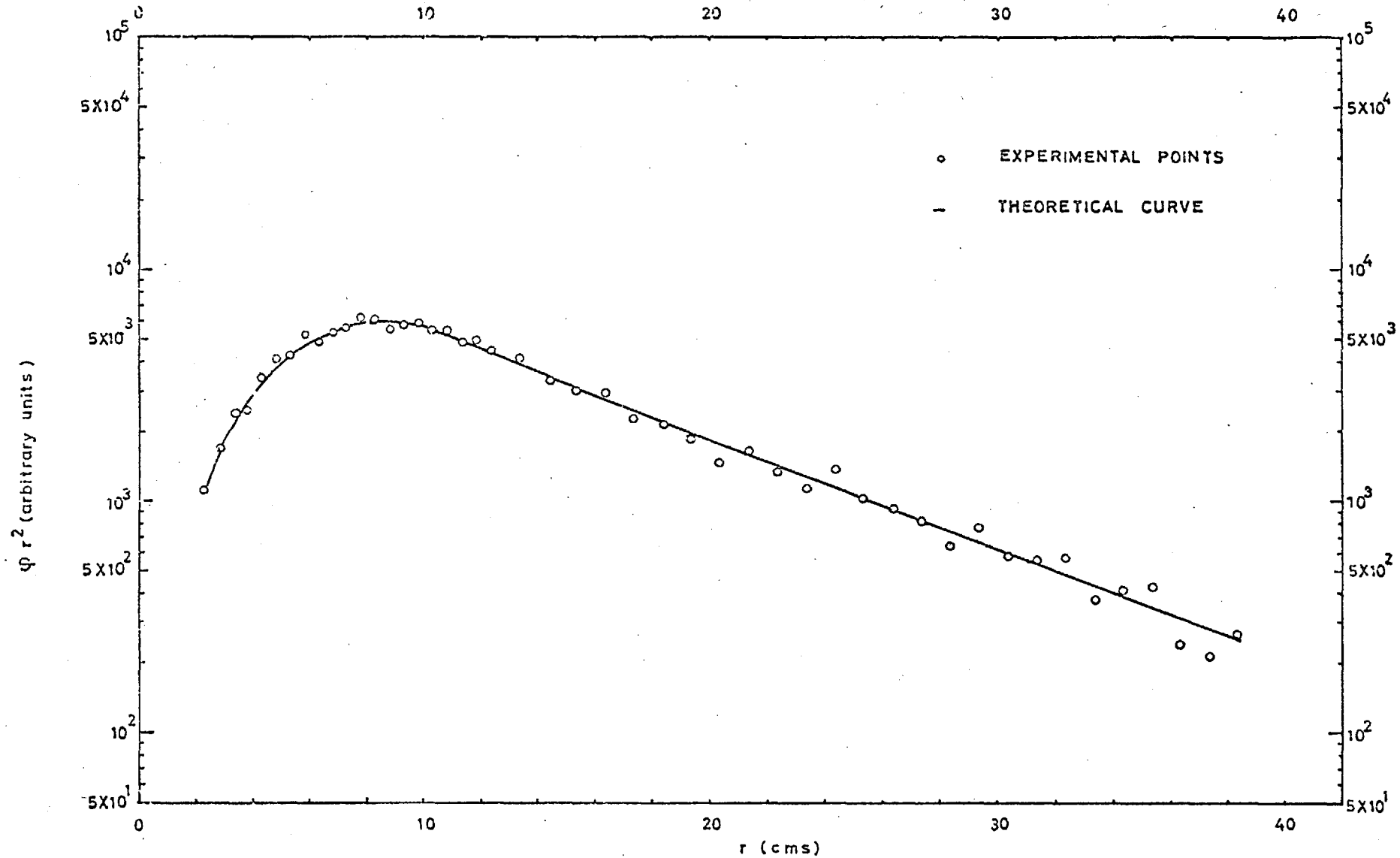

FIGURE (F.8.2) SPATIAL DISTRIBUTION OF INDIUM RESONANCE NEUTRONS FROM FISSION SOURCE IN WATER CONTAINING VERTICAL CYLINDRICAL CAVITIES.

The limit of the first region, R_1, is 8.5 cms., and the second limit R_2 arrived at by the usual procedure is taken to be 29.0 cms. Using the values of the parameters within the prescribed limits the equation (6.6.E1) yields a preliminary value of age of fission neutrons to indium resonance energy in water containing cylindrical voids of size and description mentioned in section (8.2), as 34.35 cms^2.

8.4.2. THE AGE OF FISSION NEUTRONS TO THE INDIUM RESONANCE ENERGY IN WATER CONTAINING HORIZONTAL CYLINDRICAL CAVITIES.

The final stage fittings in the case of the data for the indium resonance flux in water containing cylindrical voids in the horizontal direction is given in the Table (T.8.5). The parameter values along with the calculated standard deviation on each of them, given in the Tables (T.8.6), (T.8.7), and (T.8.8) respectively for the near, the main middle, and the asymptotic region. Fig (F.8.4), gives the plot of the experimental points and the theoretical curve. The near limit, R_1, is 3.5 cms and the other limit R_2 is taken to be 30.0 cms. The resultant preliminary age of the neutrons with the horizontal voids in the water moderator is 31.29 cms^2.

8.5. POINT SOURCE CORRECTION.

The values of the ages in the above cases, measured

FIG(F.8.3) ARRANGEMENT OF HORIZONTAL CYLINDRICAL CAVITIES

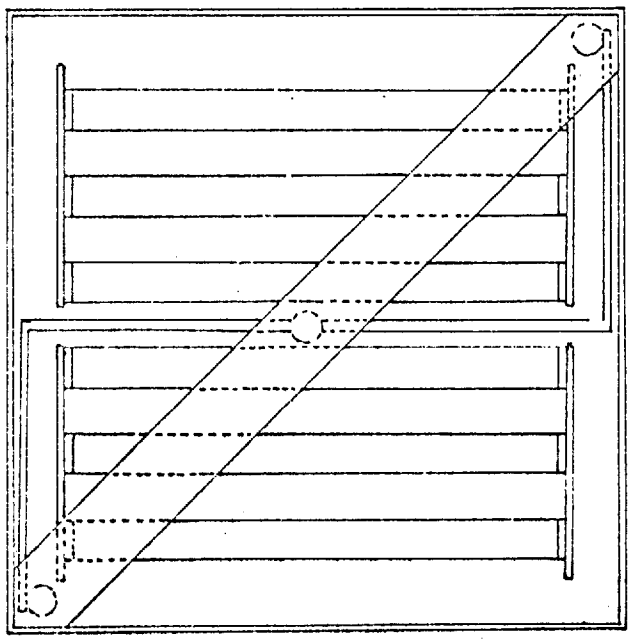

PLAN

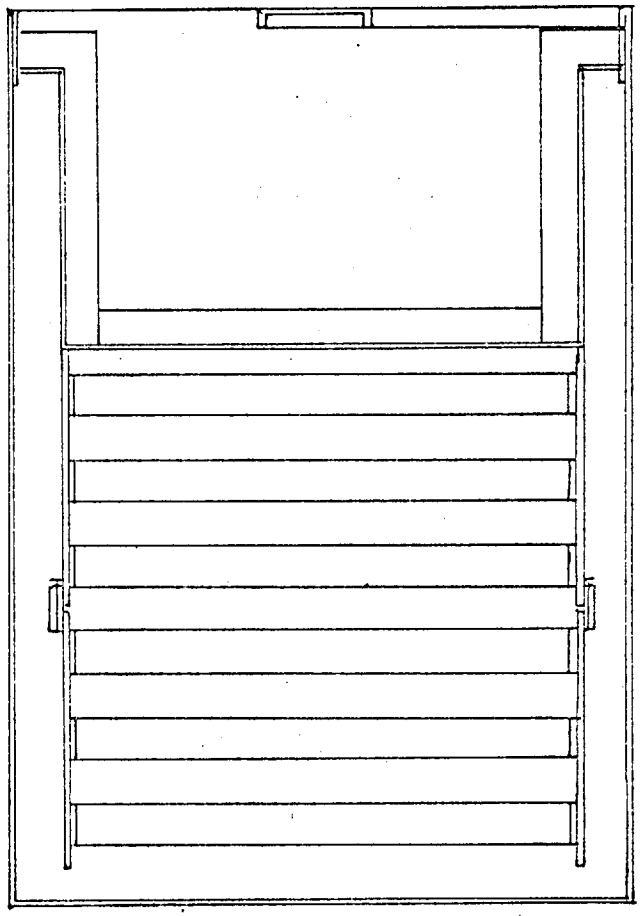

FRONT ELEVATION

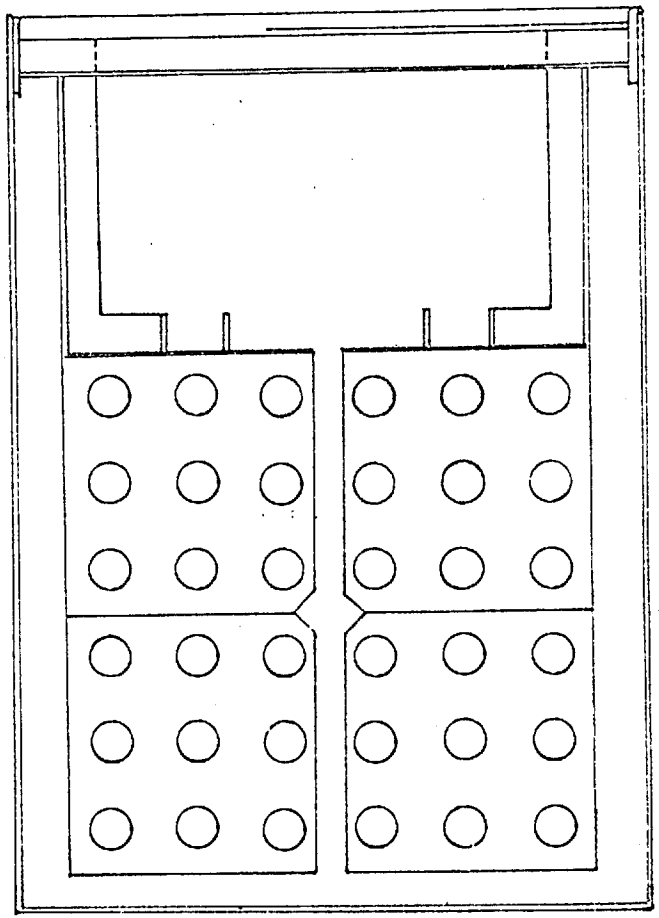

SIDE ELEVATION

TABLE (T.8.5).

Tabulated flux distribution of the slowed down neutrons of the indium resonance energy from fission source in water containing horizontal cylindrical cavities.

r	Observed Φ(r sqd)	Calculated Φ(r sqd)	r	Observed Φ(r sqd)	Calculated Φ(r sqd)
2.3291	5745.7109	5693.1809	15.3291	12528.5406	11614.1105
2.8291	8289.1028	7940.5221	16.3291	11264.7832	10550.5187
3.3291	10300.6855	10251.3500	17.3291	10463.3210	9467.3039
3.8291	12033.4872	11783.8507	18.3291	8373.7412	8521.2683
4.3291	13788.2524	13552.5405	19.3291	7300.0049	7661.9409
4.8291	15498.1180	14747.0386	20.3291	6933.0438	6804.5859
5.3291	15781.6407	15623.6894	21.3291	6190.5305	6091.4737
5.8291	16163.7761	16600.5726	22.3291	5458.7072	5508.4704
6.3291	16570.7385	17262.8920	23.3291	5152.4235	4980.7081
6.8291	16441.9264	17756.7753	24.3291	3774.9495	4496.5832
7.3291	17620.4207	18090.9581	25.3291	4222.1730	4054.0144
7.8291	17798.6603	18275.9908	26.3291	3746.9606	3650.6244
8.3291	18051.0912	18323.8280	27.3291	3663.3329	3283.8754
8.8291	17851.9619	18247.4507	28.3291	3131.1096	2951.1705
9.3291	16312.3860	18060.5071	29.3291	2420.1789	2649.9258
9.8291	18224.7411	17776.9724	30.3291	2330.3405	2377.6225
10.3291	16079.4060	17410.8294	31.3291	2227.4054	2131.8420
10.8291	17277.0413	16975.7745	32.3291	1857.3415	1910.2891
11.3291	16347.1359	16484.9575	33.3291	1724.9173	1710.8056
11.8291	16467.4699	15950.7585	34.3291	1423.6595	1531.3776
12.3291	15359.6669	15384.6098	35.3291	1471.6631	1370.1365
12.8291	15145.7784	14796.8629	36.3291	1530.6157	1225.3580
13.3291	14102.6328	14196.7021	37.3291	855.2371	1095.4573
13.8291	13989.2020	13592.1061	38.3291	968.3997	978.9834
14.3291	12704.4340	12880.4491	39.3291	927.9176	883.3791

TABLE (T.8.6)

Parameter values from programme 'PARSTA', (Horizontal cavities)

Parameters		
Name	Value	Std. Dev.
'A_s'	.4312456E+04	.2791863E+03
'C_s'	.2180816E-01	.1463221E-02

TABLE (T.8.7)

Parameter values from programme 'EVALPA', (Horizontal cavities)

'A_m'	.2759364E+03	.6162711E+02
'B_m'	.1142879E+06	.1639224E+05
'C_m'	.1399631E-01	.2237215E-02
'f_m'	.1193030E+00	.9092240E-02

TABLE (T.8.8)

Parameter values from programme 'PARLIN', (Horizontal cavities)

'B_E'	.1077030E+06	.1468441E+05
'f_E'	.1179995E+00	.2950852E-02

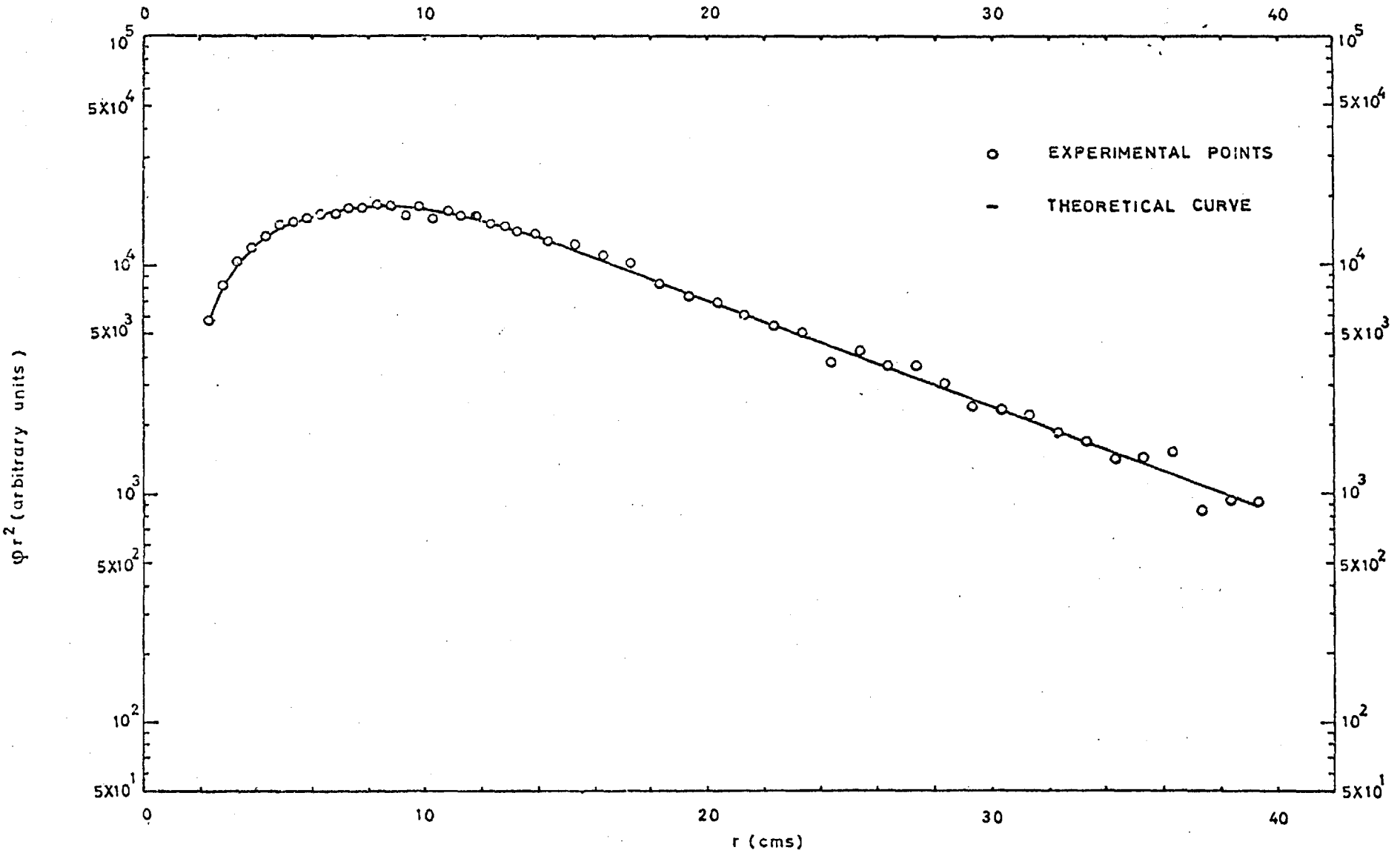

FIGURE (F.8.4) SPATIAL DISTRIBUTION OF INDIUM RESONANCE NEUTRONS FROM FISSION SOURCE IN WATER CONTAINING HORIZONTAL CYLINDRICAL CAVITIES.

with 10 inch diameter fission source, were converted to point source results in a manner outlined in sec. (7.6), and the resultant values are given in the table below with their bounds of error.

8.6. EVALUATION OF THE EXTENT OF ERROR ON THE AGES.

Similar to the method detailed out in section (7.7), an error equal to the standard deviation was put on the parameters of intrest and the age evaluation was again made. The difference between these two evaluations in each case will give an estimate of the bounds of error on the determined values of ages. This is displayed in the Table (T.8.9), below.

TABLE (T.8.9)
Preliminary values (point source) of the ages with the bounds of error calculated from the scatter of the points.

Data	Age (cm^2)	Bounds of error (cm^2)
In(V.C.)	33.65	$\pm$1.17
In(H.C.)	30.55	$\pm$0.96

The correction due to other associated errors will be applied in section (9.1.2) to obtain the final values.

CHAPTER 9.

DISCUSSION OF THE RESULTS AND THE CONCLUSIONS.

9.1. THE CORRECTIONS ON THE MEASURED VALUES AND DISCUSSION.

The preliminary results obtained in the previous two chapters will be corrected and discussed. The corrections are applied for some factors which were not possible to eliminate in the design of the equipment due to some unavoidable practical limitations or could not be accounted for in the experimental intercomparisons. The finally corrected results will be compared with the other measured and the computed results in each category in the following sections.

9.1.1. THE WATER MODERATOR.

The neutron age evaluation in a moderator like water where a rapid loss of energy could occur of a neutron in collision with hydrogen nucleus, the slowing down length is short. This necessitates an extreme refinement of the measuring techniques and the geometries of both the source and the detector, approaching zero dimensions. The concept of the point-source and point-detector, ideal may it be, is far from being a practical one for the actual determinations. Anything approaching these dimensions can only be at the expense of a drastic loss of neutron intensity resulting in a sort of counting statistics poor

enough to defeat the purpose of an accurate measurement. In the present experimental series a reasonable compromise was achieved between the ideal geometry and a sufficient fission neutron intensity to ward off the inaccuracies which beset all such determinations. The fission source is circular lamina made capable of three effective diameters, realised by using the cadmium screens having the apertures of the required sizes. The expression of flux (6.4.E3) is based upon an ideal point-source and a point-detector configuration, and the parameters 'A', 'B', 'c', and 'f' in the expression also refered to that geometry. But for the purpose of improving the neutron intensity, fission sources of larger lateral dimensions were used in the actual measurements. The flux expression modification by carrying out integration over the source size takes care of the corrections applicable. Here the concept of the point fission source was extended to the whole disc of the source. No error could arise as this method sums up the effect due to each point on the disc fission source. The parameters so evaluated are also refered to the point geometries, which in turn could be used in our age equation (6.4.E4), and its other version (6.6.E1) which is modified to take into account the regional fittings. The detecting scintillator was small enough to be nearly approaching the ideal 'point-detector' geometry and the presence of the light-guide of an appropriate size, sec. (5.8), which also helps to simulate for locating the detector isotropically in the neutron flux it is measuring without interfering.

with its other role of transmitting the pulses to the photo-multiplier tube and the counting devices.

The effect of the finite thickness of the source on the neutron age value has been recognised as an important source of error when comparatively thick source is used. The correction applicable primarily on account of the slowing down neutrons that are in vicinity of a thick fission source. Such neutrons have a finite probability of being absorbed in it. This can contribute in two ways. Firstly, the neutrons that are slowed down to the thermal energies, if captured in the source can thereby create more fissions and thus altering the original fission distribution. And secondly, there is some absorption in the source, of the neutrons of the detector energy. The first effect can be effectively eliminated by using the cadmium cover, section (5.2), on top of the fission source. As for the second effect, this could influence the 1.46 e.v. distribution near the source. This absorption reduces the integral in the denominator more than the integral in the numerator of the equation (6.6.E1). It has been shown by Goldstein et al., (R.2.8), also that a thick source has an effect of increasing the neutron age. The expression used by them and by Doerner et al., (R.7.9), is modified for the present case as,

$$\tau_o = \tau_m - 0.00081\ t \qquad \ldots\ldots(9.1.E1)$$

where 'τ_o' is the age for an infinitely thin source, 'τ_m' the measured age and 't' the thickness of the fission

source measured in mg/cms^2. This correction in the case of the present source amounts to 0.94 % , which must be subtracted from the measured age.

On the knowledge of the irradiation times of the different rings of the fission source and with reference to the section (5.13), calculations were made and it was found that the activity of the fission source was uniform. This was reassuring as no correction was necessary on age on this account. However, as mentioned in section (5.13) the centre of source's maximum activity point was off by 1.1 cm. This correction was incorporated in the fitting programmes for repeating the parameter evaluation and the age. It was found that the difference was negligible.

The preliminary experiments concerning the proper location of the fission source in the tank, section (5.11) show that in order to obtain an adequate neutron intensity it is necessary that the fission plate be at the bottom of the tank at the water boundary. In order to avoid the reflection of the degraded fission spectrum from thermal column of the reactors, it has been established by earlier experimenters, that a minimum separation of about 10 cms is necessary to eliminate this effect almost completely. To reduce the fast flux comming from the thermal column of CONSORT II, a ducted and canned block of wax 10 cms thick was positioned in the 20 cms gap between the bottom

of the tank and the thermal column, this block being at over 7 cms from the bottom of the tank. This combination of air gap and ducted block of wax achieved two purposes. Firstly, the presence of the block improved the thermal content of the in-comming neutrons, secondly, it provided an air gap of 20 cms between the fission source and the thermal column. Hence any reflection from it was out of question. The source neutrons if reflected back into the medium where measurements are being carried out have the effect of reducing the age. This effect in the above mentioned set-up is entirely avoided.

The canned fission source, section (5.2), which is positioned very accurately and firmly at the bottom of the tank and the question of any displacement of the reference point, (taken on the surface of the fission source), does not arise.

Neutron age measurements in the past have been often dogged by the ambiguity in the correct knowledge of the source-detector distance because of the difficulty of the positioning of the foils, cadmium covered for irradiation. This can arise from the spaces within the cadmium covers. The foil holders and the props etc., also introduce some structural materials in the neighbourhood of the measuring region, which promotes perturbation and the streaming of neutrons. A very high degree of accuracy is achieved in

the present set up for the distance measurements where an accuracy of upto 0.003 cms is realised. With the distance accuracy of this order and no uncertainty at either end no error is envisaged.

As far as the size of the moderating medium for the measurements of flux, infinite dimensions are not altogether necessary. For all practical purposes a moderating medium of an appropriate size could be used without any undue leakage of the neutrons from the system. This size has already been discussed in detail in section (4.2). The size of the moderator used is taken to be above the suggested safe limits, thus any concievable leakage from the system without any empty channels is negligible. The size of the moderator is also large enough for the case of cylindrical cavities, however, the streaming correction would be applied in those cases in section (9.2).

In view of the fact that when the detector is at a very close proximity of a fission source howsoever thin it may be, results in some flux depression at the order of such separations. This effect, with the present equipment and using only one available thickness of the fission source, was not determinable. It was considered wise to omit the first couple of points in the analysis work. As the separation of the source and the detector increases this interaction falls off very rapidly.

In the measurements of the neutron age by the foil activation method the effect due to the resonance other than the main one, can contribute greatly to the errors. In the case of indium, for example, about 15 % of the activation is due to non-1.46 e.v. neutrons. If the age measurement was to be directed towards only the higher energy resonances, i.e., to 3.8 or to 9.1 e.v., measured value would be less than that to 1.46 e.v. resonance. And if on the other hand the primary age measurement is to be restricted only to the region below the main resonance, the age would be greater than the true 1.46 e.v. age. In actual practice, both in the case of the foil activation method and the present one, when measuring age to 1.46 ev resonance, both the above mentioned effects are present and can influence the measurements. But whereas present method reduces the interfering effect due to the higher resonances for its lesser sensitivities at those regions, is equally vulnerable in the case of the lower regions of energy between the cadmium cut-off energy and 1.46 e.v. Two corrections are applicable in the case of indium, one on either side of the main resonance, the sign and the magnitude of these corrections are given in Table (T.9.2), but the overall correction in the case of indium is 0.18 %. For the case of gold, the small jagged peaks for higher resonances, spanning between 60 e.v. and 300 e.v. have a combined average intensity of 0.05 % of the main one, can in no way have any effect on the measured quantity. The

only possible interfering effect can be due to the region below the main resonance of 4.91 e.v. The correction in the case of gold will be 0.1 % . In the case of rhodium the higher resonances are even less significant. The correction applicable is entirely due to below the main resonance. The correction is 0.21 % .

Error could arise possibly by the perturbation of the resonance flux by the source of input neutrons feeding the fission source. The thermal flux obtained in the case of the present measurements, is from the vertical access of CONSORT II, and contained about 5 % of the epithermal flux. This small amount of fast flux possibly could be a disturbing factor in an orthodox method of age measurements. But in the present case as the difference of measurements is required in determining the resonance flux, any such effect cancells out.

No correction is necessary for water displacement as care has been taken to minimise this factor. Neutron mean free path is not appreciably altered when the other materials are used in very small quantities. A detailed discussion of this aspect has already been done in the earlier chapters.

Error can arise from an incorrect extrapolation of the neutron flux to infinity. In most of the previous

age determinations only a few last measured points were used to evaluate the relaxation length for adding the extrapolated contribution to the integral of the measured data. Two types of errors can result when extrapolating to infinity. Firstly, because of the functional form, if inept, applied for the measured flux beyond the last of the measured points. Secondly, error from the counting statistics of the last few points in the asymptotic region where the relaxation length and the value of the fitted flux at the measured points being determined. In the case of the present determinations as described in chapter 6, a great care was taken for each individual fit as well as for the continuity of each fit with the neighbouring ones. Fit to the asymptotic region with the programme 'PARLIN' was done even more carefully as a correct fitting to this data means a correct extrapolation to infinity. Care also was taken of this region because this part being distant from the fission source and hence the scatter of the experimental points is greater. The error bounds were then calculated on the knowledge of this scatter of the points although very much over-estimates the error on the age, also points to the fact that a bad and an inaccurate fit in this region can contribute to the error far more than an inept functional form. As in a typical case of the age evaluation, the extrapolated contribution determined in the case of indium by graphic method, amounts to less than 1.5 % of the total. Any error on the 1.5 percent of the

contribution cannot have any significant effect on the value of the age. The 'bounds of error' mentioned above and calculated in the previous chapters, in fact refers to the extremities of the scatter of the observed points. For the purpose of quoting the possible error on the value of the age from the measured points on account of the statistical spread, the 'bounds of error' cannot be used as the least-squared fitting owing to its nature cannot just pass through the extremity points leaving out the main bulk of the points. But in order to obtain a very conservative estimate of the error on the measured age can justifiably be had by getting the two-thirds of the 'bounds of error'. These values for the cases of the resonance filters of indium, gold and rhodium are 0.64, 1.16 and 0.78 cms^2 respectively.

The interfering effect due to the possibility of the fission gammas supplying the photo-neutrons in water and other materials is not very easy to estimate to a great degree of accuracy particularly in the case of the gammas comming from the reactor core. The nature and the method of obtaining resonance neutron flux in the present case eliminates the interfering effect automatically when the differences are taken of the fluxes.

The present age experiment was performed with water temperature that averaged around 75.8°F. The temperature

fluctuations were no more than $2^{o}F$. In order to compare the measured value with the theoretical calculations it is necessary to apply correction for the water density as the calculated results are based upon the water density of 1.0 gm/cms^2. Since the value of age varies inversely with the square of the density, it leads to a correction of 0.62 % on the value of the measured age.

TABLE (T.9.1).

The errors associated with the present measurements.

Errors		In	Au	Rh
σ_1	Error based on the statistical spread of the experimental points.	$\pm$ 0.64	$\pm$ 1.16	$\pm$ 0.78
σ_2	Error on the applied correction for absorption of the neutrons other than the main resonance, in the filters used. (40 % of the correction)	$\pm$0.019	$\pm$0.009	$\pm$0.023
σ_3	Error on the extrapolated contribution correction (+/-, 30 % of the correction).	$\pm$0.123	$\pm$0.108	$\pm$0.124
σ_4	Error on correction for the finite source thickness. (+/-, 20 % of the correction)	$\pm$0.051	$\pm$0.044	$\pm$0.052
σ_5	Error on the correction for the water density. (+/-, 2^{o} F, +/-, 0.04 %).	$\pm$0.010	$\pm$0.010	$\pm$0.010
σ =	PROBABLE ERROR $((\sigma_1)^2+ (\sigma_2)^2+ (\sigma_3)^2+ ..)^{0.5}$	$\pm$0.654 (cms^2)	$\pm$1.165 (cms^2)	$\pm$0.791 (cms^2)

Table (T.9.1) given on the previous page outlines various associated errors peculiar to these measurements, and probable error is calculated for each. Table (T.9.2), below lists the corrections that are applicable on the measured ages, and the corrected values are obtained.

TABLE (T.9.2).

Summary of the results.

	In (cms^2)	Au (cms^2)	Rh (cms^2)
Measured age (Reservance energy)	26.80 (1.46 ev)	22.93 (4.9 ev)	27.06 (1.26 ev)
Correction for the density of water to correct to 1.0 gm/cm^3. (0.62 %).	(-)0.170	(-)0.146	(-)0.172
Correction for non-'main' resonance absorption in the filters used.	(+)0.081 (-)0.032	..... (-)0.024	..... (-)0.058
Correction for the finite source thickness. (0.94 %)	(-)0.256	(-)0.220	(-)0.259
Measured age (Corrected), and probable error on it.	26.42 $\pm$0.65	22.54 $\pm$1.16	26.58 $\pm$0.79

Minus (-) sign indicates that the experiments with these errors have a higher measured age than without it. Plus (+) sign, the opposite.

Table (T.9.3) on the next page gives a comparison of the measured values of flux age of the fission neutrons to indium resonance in water.

TABLE (T.9.3)

Comparison of the results.

Author	Reference	Measured age (cms^2)
Anderson, Fermi and Nagle	(R.7.1)	32.3
Hill, Roberts and Fitch	(R.7.2)	30.8
Hoover and Arnette	(R.7.3)	30.03
Barkov and Mukhin	(R.7.4)	29.4 ± 1.5
Wade	(R.7.5)	31.0 ± 1
Blosser and Trubey	(R.7.6)	26.7
Lombard and Blanchard	(R.7.7)	27.3 ± 0.9
Pettus	(R.7.8)	27.0 ± 0.9
Doerner et al.	(R.7.9)	27.86 ± 0.10
Joworowski	(R.7.10)	24.6 ± 1.5
Paschall	(R.7.11)	26.48 ± 0.32
Spencer and Williamson	(R.7.12)	26.24 ± 0.3
Present Measurements ———		26.42 ± 0.65

It can be seen from Table (T.9.3) that the present value of the age of fission neutrons to indium resonance is in good agreement with the best of the experimental determinations and also the results of the theoretical calculations as given in chapter two.

9.1.2. WATER MODERATOR CONTAINING ARRAYS OF CYLINDRICAL CAVITIES.

For the purpose of applying corrections on the measured values of ages in water containing cylindrical cavities in the horizontal and the vertical directions, various factors applicable have already been discussed in the section above in greater detail amongst a comprehensive survey of the various sources of error. As for size of the moderator in the case of the cavities, fresh calculations were made on the lines mentioned in section (4.2). The calculations using the observed ages in the respective cases. It was concluded that the size of the moderator used even with the presence of the cavities is still large enough to study the effects of the neutron streaming from the cavities without introducing error due to insufficient moderator size.

The statistical error on the measured values of ages are calculated from the bounds of error in a manner as mentioned in section (9.1.1). These values are 0.77 cms^2, and 0.64 cms^2, respectively for the vertical (axial) and the horizontal (transverse) voids.

TABLE (T.9.4).

The errors associated with age measurements in moderator with cavities.

	Errors	In(V.C)	In(H.C)
σ_1	Error based on the statistical spread of the experimental points.	$\pm$ 0.77	$\pm$ 0.64
σ_2	Error on the applied correction for absorption of the neutrons other than the main resonance, in the filter used. (40 % of the correction).	$\pm$ 0.019	$\pm$ 0.019
σ_3	Error on the extrapolated contribution correction. (+/-, 30 % of the correction).	$\pm$ 0.151	$\pm$ 0.138
σ_4	Error on the correction for the finite source thickness. (+/-, 20 % of the correction).	$\pm$ 0.063	$\pm$ 0.057
σ_5	Error on the correction for the water density. (+/-, 2 F, +/-, 0.04 %).	$\pm$ 0.010	$\pm$ 0.010
σ	PROBABLE ERROR $=((\sigma_1)^2+ (\sigma_2)^2+ (\sigma_3)^2+ \ldots)^{0.5}$	$\pm$ 0.79 $\approx\pm$ 0.8	$\pm$ 0.66 $\approx\pm$ 0.7

Table (T.9.4) above, gives the errors associated with the present measurements and the probable error on each have been evaluated. Table (T.9.5) lists the corrections that are applicable on the measured ages and the finally corrected values are obtained.

TABLE (T.9.5)

Summary of the results.

	In(V.C) (cm^2)	In(H.C) (cm^2)
Measured ages	33.65	30.55
Correction for the density of water to correct to 1.0 gm/cms^3, (0.62 %).	(-)0.208	(-)0.189
Correction for the non-main resonance absorption in the indium filter used.	(+)0.100 (-)0.041	(+)0.092 (-)0.037
Correction for the finite source thickness. (0.94 %).	(-)0.316	(-)0.287
MEASURED AGES (CORRECTED) with the probable errors.	33.19 $\pm$0.8	30.13 $\pm$0.7

Minus (-) sign indicates that the experiments with these errors have a higher measured age than without it, plus (+) sign, the opposite.

TABLE (T.9.6)

The present streaming ratios and anisptropy factor.

Axial Streaming τ_{VC}/τ_m	Radial Streaming τ_{HC}/τ_m	Anisotropy factor τ_{VC}/τ_{HC}
1.256 $\pm$ 0.043	1.140 $\pm$ 0.038	1.101 $\pm$ 0.036

τ_m - Age in water without cavities.

Table (T.9.6) presents the axial and the radial streaming ratios along with the anisotropy factor. These were obtained from the present experimental determinations of the ages of, fission neutrons in water to the indium resonance energy, and in water containing regular arrays of cylindrical cavities in the axial direction and also water with cavities in the radial direction.

Calculations, based on Behrens and Benoist neutron streaming theories, were made for a particular case of the empty channels in water. Equations (8.1.E1 upto 8.1.E6) were used for these calculations, which also included both of Benoist's expressions for the radial streaming factor. In addition to these, calculations were also made using Grant's theory (R.8.8) and Carter's theory (R.8.9). The values for the radial streaming factor from these gave the same result as with Benoist's earlier expression for the streaming in that direction. In the above calculations, all the theories gave the same result for the axial streaming showing thereby a complete accord, for the case of water containing empty channels. In the calculations above the value of c_r was 2.69 cms. The value of the mean free path of fission neutrons in water, λ_m, evaluated from the fast diffusion coefficient, was taken to be 3.55 cms, this being the averaged value obtained from the three sources quoted below.

(1) (R.9.1), Murray, page 124. ($\overline{D}$=1.143).

(2) (R.9.2) "METHUSELAH" calculations for University of London Research Reactor. ($\overline{D}$=1.2407 cms).

(3) Calculations are made using table (18.3) from (R.9.3), 'The Physics of Intermediate Spectrum Reactors'.

We have, the diffusion coefficient,

$$\overline{D} = \frac{\int \Phi(u)D(u)du}{\int \Phi(u)du} \qquad \ldots.(9.1.E1)$$

Assuming $\Phi(u)$ as constant i.e., 1/E slowing down spectrum, then,

$$\overline{D} = \frac{\int \frac{D(u)du}{\xi\Sigma_s(u)}}{\int \frac{du}{\xi\Sigma_s(u)}} \qquad \ldots.(9.1.E2)$$

or
$$\overline{D} = \frac{\sum_{1}^{n} \frac{D(u)\Delta u}{\xi\Sigma_s(u)}}{\sum_{1}^{n} \frac{1.\Delta u}{\xi\Sigma_s(u)}} \qquad \ldots.(9.1.E3)$$

Where summation from 1 to n would apply to groups 1 to 12 which cover the epicadmium range. Using the values from taole (18.3), reflector, in equation (9.1.E3) yields value of $\overline{D}$=1.162 cms.

Any variation caused due to the choice of λ_m in the

FIGURE (F.9.1) PLOT OF STREAMING FACTORS AGAINST VOID RATIOS

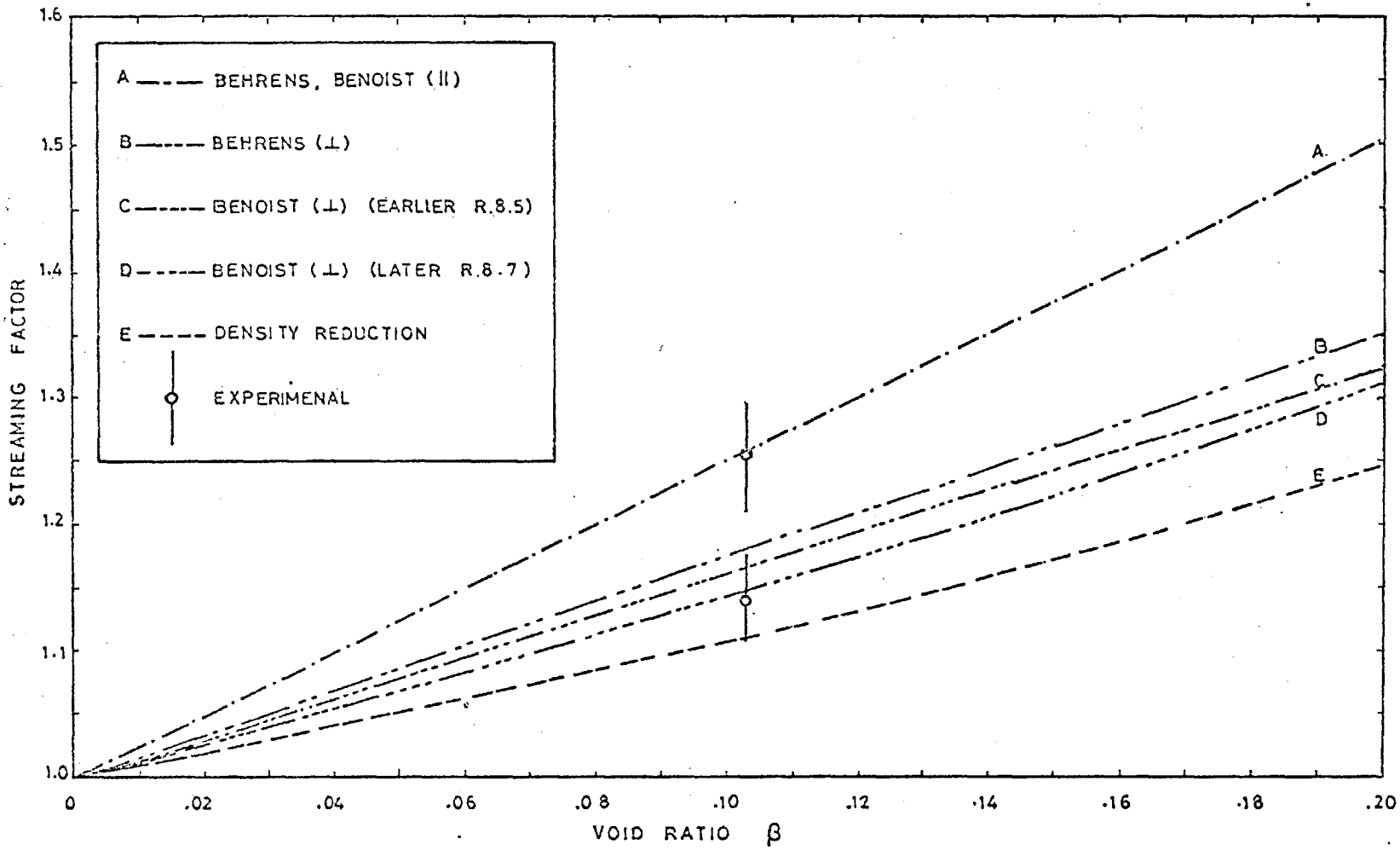

above range does not exceed 3 % . The results of the streaming calculations are shown in Figure (F.9.1). It is clear from the figure that the measured axial streaming ratio is in a good agreement with the theoretical values of Behrens and Benoist. The measured radial streaming factor shows better agreement with Benoist's theories, particularly with his later expression for the radial streaming factor. For the sake of comparison, calculations were also made for a simple density correction by merely reducing the density of water to allow for the voids. These values were plotted on the same graph. It is seen that the streaming factor in the axial direction, as expected, is well above than the one obtained by merely reducing the density of water. As the neutrons emanating from the fission source, with the bulk of these neutrons, in a sort of a cone, travelling almost parallel to the channels have a great deal of chance to cover long distances in the empty channels, hence the obvious discrepancy. It is also very intresting to note that the radial streaming curves and the experimental value, are also significantly above the simple density correction curve. This means that with the tubes in the transverse position, the movement of the majority of neutrons is nearly perpendicular to the channels. They travel short distances alternately in voids and moderator. A simple minded approach would be to consider the neutron transport in such a case as in a diluted medium. This sort of approximation would have been quite valid for the case

FIGURE (F.9.2) PLOT OF ANISOTROPY FACTORS AGAINST VOID RATIOS

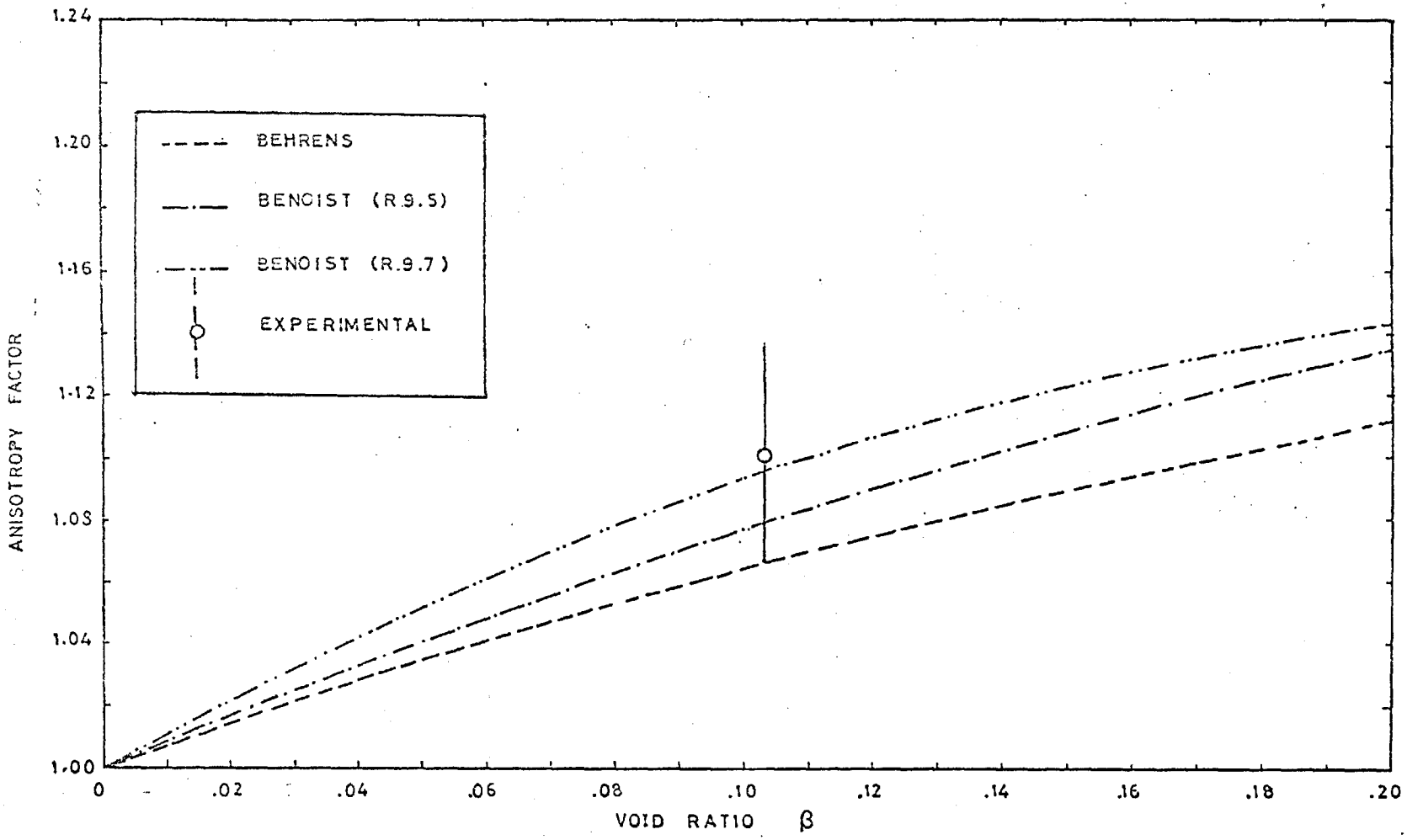

of anisotropic cavities of very small radius or randomly dispersed voids of small dimensions. But the apparent disagreement shows that even in the case of the radial streaming it would be wrong to approximate to the simple density correction, in water, with cavities of the size as in the present case. It also means that for cavities of the dimensions as in the present series of experiments a significant number of neutrons could stream along in the radial direction. Fig (F.9.2) is a plot of anisotropy factor against the void ratios. The anisotropy factor is calculated from Behrens theory and Benoist both sets of expressions. The experimentally obtained value show a better agreement with the anisotropy factor calculated from Benoist's later expression.

9.2. CONCLUSIONS.

The present method of neutron resonance flux measurements of using a scintillation detector in conjunction with an appropriate neutron 'resonance filter' has proved its soundness of technique over a wide range of measurements. It has thus established itself as an alternative technique which is equally reliable, less cumbersome and less time consuming than the foil activation method. By virtue of the fact that this method involves a difference of measurements, certain disturbing effects in the required measurements are automatically eliminated in the

differences. The success of the present technique with three resonance filters as indium, rhodium and gold, paves way for extention of this method for its use with some other resonance absorbers. It is however, important that the choice of an appropriate scintillator be made accordingly, with the sensitivity of the scintillator matching the resonance energy region of the filter in use. Stability of the counter and the allied electronics is stringently demanded for the success of the neutron resonance filter technique.

The present detecting method could effectively be extended for its application for an 'infinite detector' geometry. This can be achieved by employing one or more identical detectors aligned in a plane parallel to the plane of the fission source, in addition to the axial detector. The axial detector, apart from providing the axial flux, could also act as monitor when the additional detector(s) is(are) being used at various other positions in the plane. The observed fluxes from the different radii then be extrapolated to obtain the flux that could be expected from an infinite detector. This could be an asset particularly in the case of the measurements in medium with voids.

The age measurements in graphite, in water and water with cavities based on the present measuring technique

are consistant with the theoretical values of recognised accuracy. This demonstrates the basic reliability of the equipment and the experimental techniques and provides additional verification of theory.

The expression (6.4.E2) has been used for the age evaluation in moderator containing cavities. This expression is, however, for an isotropic system. This has been applied with success in the present case of comparitively low void ratio. At very high void ratios and intensely heterogeneous systems it would not be advisable to use this expression. In fact it would be intresting to establish experimentally the level of anisotropy and the void ratio where this departure occurs. It is recommended that such an experimental venture be accompanied with Monte Carlo calculations to facilitate step by step comparison.

REFERENCES

(R.2.1) HURWITZ, H., and ZWEIFEL, P.F.,
J. Appl. Physics, 26, 923, (1955).

(R.2.2) CERTAINE, J.,
U.S.A.E.C. Report. NDA 15-94 (August 1957).

(R.2.3) GOLDSTEIN, H., and CERTAINE, J.,
U.S.A.E.C. Report. ORNL 2389, section 8.12,
(18th Oct. 1957).

(R.2.4) JOANOU, G.D., GOODJOHN, A.J., and WIKNER, N.F.,
Trans. Amer. Nucl. Soc. Vol. 4, Number 2,
Nov. 1961, p 278.

(R.2.5) COVEYOU, R.R.,
U.S.A.E.C. Report. ORNL 2081, (1956).

(R.2.6) BROWN, H.D.,
Proc. of the 2nd U.N. International Conf. on
the peaceful uses of Atomic Energy Vol 16,(1958)

(R.2.7) COVEYOU, R.R., and SULLIVAN, J.G.,
Proc. of the 2nd U.N. International Conf. on
the peaceful uses of Atomic Energy, Vol 16,(1958).

(R.2.8) GOLDSTEIN, H., SULLIVAN, J.G., COVEYOU, R.R.,
KINNEY, W.E., and BATE, R.R.,
U.S.A.E.C. Report. ORNL-2639, (1961).

(R.2.9) ALTER, H.,
Nucl. Sci. and Eng. 23, 264, (1965).

(R.2.10) CERTAINE, J., and ARONSON, R.,
U.S.A.E.C. Report. NDA 15G-40, (1954).

(R.2.11) REIER, M., OBENSHAIN, F., and HELLENS, R.L.,
U.S.A.E.C. Report. WAPD-T.576, (1957).
(also Nucl. Sci. and Eng. 4,1, (1958)).

(R.2.12) GOLDSTEIN, H.,
U.S.A.E.C. Report. NDA 15C-15, (1953).

(R.2.13) LUSTIG, H., GOLDSTEIN, H., and KALOS, M.H.,
U.S.A.E.C. Report. NDA 086-2, (1958).

(R.2.14) MacGREGOR, M.H., MORAVCSIK, M.J., and
STAPP, H.P.,
Annual Rev. of Nucl. Sci.,Vol. 10. 291, (1960).

(R.2.15) HUGHES, D.J., and SCHWARTZ, D.B.,
"NEUTRON CROSS SECTIONS" BNL-325, 2nd Edition,
Suppliment No: 1.

(R.2.16) OKAZAKI, A.,
Phys. Rev., 99, 55, (1955).

(R.2.17) BOCKELMAN, C.K.,
Phys. Rev., 80, 1011, (1950).

(R.2.18) BOCKELMAN, C.K., MILLER, D.W., ADAIR, R.K.,
and BARSCHALL, H.H.,
Phys. Rev., 84, 69, (1951).

(R.2.19) FOSSAN, D.B., WALTER, R.L., WILSON, W.E.,
and BARSCHALL, H.H.,
Phys. Rev., 123, 209, (1961).

(R.3.1) AMALDI, E.,
Encyclopedia of Physics, Vol. 38/2, (1959).

(R.3.2) WEINBERG, A.M., and WIGNER, E.D.,
The Theory of Neutron Chain Reactors. (Chicago Press)

(R.3.3) PLACZEK, G.,
Manhatten Report, A-25

(R.3.4) MARSHAK, R.E.,
Rev. Mod. Phys., 19, 185, (1947).

(R.4.1) GRANT, P.J.,
Elementary Reactor Physics, p 76, Perganam Press, (1966).

(R.4.2) DAVY, W.G.,
U.K.A.E.A. Report., A.E.R.E. R/M 96 (1956).

(R.4.3) BOGART, D., CUSICK, J.P., and SHOOK, D.E.,
Trans. Amer. Nucl. Soc. 2, 148, (1959).

(R.4.4) STEICHEN, C.U.,
U.S.A.E.C. Report TID-15614 (1960).

(R.4.5) ROBERTS, L.D., HILL, J.E., and MACAMMON, G.,
U.S.A.E.C. Report ORNL 201, (1950).

(R.4.6) HAIDER, N., GRANT, P.J.,
Brit. J. Appl. Phys., Vol. 17, p 531, (1966).

(R.5.1) JAMES, C.G., and MENELEY, D.A.,
J. of the Brit. Nucl. Engy. Soc., p 103, (1962).

(R.7.1) ANDERSON, H.L., FERMI, E., and NAGLE, D.,
U.S.A.E.C. Report. CP-1531 (1944).

(R.7.2) HILL, J.E., ROBERTS, L.D., and FITCH, T.E.,
U.S.A.E.C. Report ORNL-181, (1948),
J. Appl. Phys., 26, 1013, (1955).

(R.7.3) HOOVER, J.I., and ARNETTE, T.I.,
U.S.A.E.C. Report., ORNL-641, (1950).

(R.7.4) BARKOV, L.M., and MUKHIN, K.N.,
J. Nucl. Energy II, Vol. 4, p 91, (1957).
(Translation from 'ATOMMAYA ENERGIYA'1, No:3, 31, (1956)).

(R.7.5) WADE, J.W.,
Nucl. Sci. and Eng. 4, 12, (1958).

(R.7.6) BLOSSER, T.V., and TRUBEY, D.K.,
U.S.A.E.C. Report., ORNL-2842, p 109, (1959).

(R.7.7) LOMBARD, D.B., and BLANCHARD, C.H.,
Nucl. Sci. Eng., 7, 448, (1960).

(R.7.8) PETTUS, W.G.,
Nucl. Sci. Eng., 11, 129, (1961). (also BAW-146 1960)

(R.7.9) DOERNER, R.C., ARMANI, R.J., ZAGOTTA, W.E., and MARTENS, F.H.,
Nucl. Sci. and Eng., 9, 221, (1961)

(R.7.10) JAWOROWSKI, T.R.,
Trans. Amer. Nucl. Soc., Vol. 5, No:2, (1962).

(R.7.11) PASCHALL, R.K.,
Nucl. Sci. and Eng., 20, 436, (1964).

(R.7.12) SPENCER, J.D., and WILLIAMSON, T.G.,
Nucl. Sci. and Eng., 27, 568, (1967).

(R.7.13) De JUREN, J.A., and REIER, M., and STOOKSBERRY, R.W.
Nucl. Sci. and Eng., 11, 179-191, (1961).

(R.8.1) BEHRENS, D.J.,
U.K.A.E.A. Report., A.E.R.E. T/R 103, (1958)
(Aso appeared in Proc. Phys. Soc., 62A,607,(1949)).

(R.8.2) BEHRENS, D.J.,
U.K.A.E.A. Report., A.E.R.E. T/R 221, (1956).

(R.8.3) BEHRENS, D.J.,
U.K.A.E.A. Report., A.E.R.E. T/R 239, (1958).

(R.8.4) BEHRENS, D.J.,
U.K.A.E.A. Report., A.E.R.E. T/R 877, (1956).

(R.8.5) BENOIST, P.,
U.K.A.E.A. Report., A.E.R.E.-TRANS 842, (1959).
(Report S.P.M. 522, of the Service DE Physique Mathématique, Centre d'Etudes Nucleaires de Saclay, December 1958. Translated by I.S. Grant)

(R.8.6) BENOIST, P.,
U.K.A.E.A. Report., A.E.E.W.-TRANS-4, (1962).
(Report S.P.M. 710, of Service DE Physique Mathématique, Centre d'Etudes Nucleaires de Saclay, Jan. 1962. Translated by Richardson).

(R.8.7) BENOIST, P.,
Nucl. Sci. and Eng. 34, 285-307, (1968).

(R.8.8) GRANT, I.S.,
U.K.A.E.A. Report., A.E.R.E. R/R 2568, (1958).

(R.8.9) CARTER, C.,
Reactor Sci. and Technol. (J. of Nucl. Engy, parts A/B), (1961), Vol 15, pp 76-80.
(Also appears in U.K.A.E.A. Report.,A.E.R.E. 3367. (1960)).

(R.8.10) SCHAEFER, G.W., and PARKYN, D.M.,

Proc. of the Second International conf. on the Peaceful Uses of Atomic Energy, Vol 16, (1958).

(R.8.11) ZHEZHERUN, I.F., J. of Nucl. Engy, Parts A/B, Vol 19, 49-61, (1965).

(R.8.12) COPIC, M., KALIN, T., PREGL, G., and ZERDIN, F., Nucl. Sci and Eng., 19, 74-79, (1964).

(R.8.13) COPIC, M., KALIN, T., PREGL, G., and ZERDIN, F., Proc. I.A.E.A. Symposium, 'Exponential and Critical Experiments', 3, 305, (1963).

(R.8.14) SEKIYA, T., SUITA, T., and MURASE, H., J. of Nucl. Sci. and Technol., 1,1,7-10, (1964).

(R.8.15) SEKIYA, T., SUITA, T., and .URASE, H., J. of Nucl. Sci and Technol., 1,7,236-241, (1964).

(R.8.16) MURASE, H., SEKIYA, T., and SUITA.,T, J. of Nucl. Sci. and Technol., 2,3, 99-103, (1965).

(R.8.17) SEKIYA, T., YAMAGISHI, T., and MURASE, H., Technol. report of Osaka Univ., Vol 16, No. 695, 175-179, (1966).

(R.8.18) SEKIYA, T., TAKEDA, T., Technol. Report of Osaka Univ., Vol 18, No.826, 303-307, (1968).

(R.8.19) TAKEDA, T., SEKIYA, T., Technol. Report of Osaka Univ. Vol 22, No. 1028, (1972).

(R.9.1) MURRAY, R.L.,
Nuclear Reactor Physics, Chapter 5, page 124.
Macmillan and Co Ltd. (1959).

(R.9.2) Private communication.

(R.9.3) The Physics of Intermediate Spectrum Reactors,
(Ed. J.R.Stehn), Naval Research Branch,
Division of Reactor Developement, U.S. Atomic
Energy Commission. UC-81, (Sept. 1958).
(Chapter 18, Table 18.3, reflector).

APPENDIX (A.4.1)

NEUTRON SOURCES

Source	Po^{210}-Be	Sb^{124}-Be	Ra^{226}-Be	Am^{241}-Be
Type	(α,n)	(γ,n)	(α,n)	(α,n)
Strength	1 curie	500 mc	1 curie	1 curie
Physical features	Beryllium powder coated with Polonium metal.	Pressed cylinder of metal Antimony and Beryllium.	Palleted mixture of Beryllium and Ra^{226}.	Palleted mixture of Beryllium and Am^{241}.
Half-life	138.4 days	60 days	1620 years	458 years
Neutron emission n/sec.	2.5×10^6	1.3×10^6	6.5×10^6	2.5×10^6
Gamma dose rate (mR/h) per 10^6n/sec. at 1 m	< 0.1	1000	60	1
Overall dimension (dia.x length)	15 x 17 mm mm	23 x 44 mm mm	22 x 31 mm mm	22 x 31 mm mm

APPENDIX (A.5.1).

DETAILS OF THE COUNTING EQUIPMENTS.

(A) MAIN COUNTING CHANNEL

(1) Cathode follower .... Nuclear Enterprises type NE5202A

(2) (Non-overloading (linear pulse (Amplifier .... " " type NE5202

(3) (Single channel (differential (pulse height (selector .... " " type NE5102

(4) (High voltage (supply .... Philips type PW 4025

(5) (Automatic (scalar-timer .... Ekco type N 530 G

(6) (Frequency (standard .... " type N 694 A

(B) MONITOR COUNTING CHANNEL

(7) (Head-amplifier .... Dynatrons type 1430 A

(8) (Amplifier unit .... " type 1430 A

(9) (Automatic (scalar-timer .... Ekco type N 530 G

Also used with both the channels two identical pairs of the following.

(I) Advanced voltstat .... Advance Component Co. type CVN500A

(II) Radio interference suppressor .... Belling & Lee Ltd. type L 1599

APPENDIX (A.6.1).

FLUX AT A POINT 'P' DUE TO A DISC FISSION SOURCE

Considering neutron flux at a point P due to a point fission source, at a distance r from it as,

$$\Phi_{pt.}(r,E) = Ae^{-cr^2} + \frac{B}{r^2} e^{-fr} \qquad \ldots\ldots (A.6.1.E1)$$

The flux due to a disc source is then given by,

$$\Phi_{disc}(r,E) = \frac{1}{\pi X^2} \int_o^X 2\pi x dx \left(Ae^{-cr^2} + \frac{B}{r^2} e^{-fr}\right)$$

$\ldots\ldots$ (A.6.1.E2)

Where 'X' is radius of disc source and

$$r^2 = x^2 + r_o^2$$

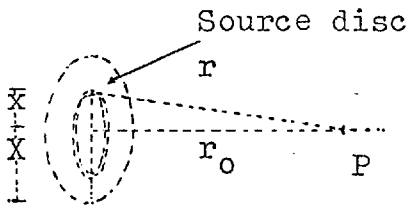

Therefore,

$$\Phi_{disc}(r,E) = \frac{1}{X^2} \left[\int_o^X 2x dx\, Ae^{-c(x^2 + r_o^2)} + \int_o^X \frac{2x dx\, B}{(x^2 + r_o^2)} e^{-f\sqrt{x^2 + r_o^2}} \right]$$

$\ldots\ldots$ (A.6.1.E3)

Evaluating the first integral we get,

$$\Phi_{disc}(r,E) = \frac{2}{X^2}\left[Ae^{-cr_o^2}\left(-\frac{1}{2c}\right)\left(e^{-cX^2}-1\right) + B\int_o^X \frac{xdx}{(x^2 + r_o^2)} e^{-f\sqrt{x^2 + r_o^2}} \right]$$

..... (A.6.1.E4)

TABLE (A.T.7.1)

Tabulated flux distribution of the slowed down neutrons of indium resonance energy from fission source in water. (set 2).

r	Observed Φ(r sqd)	Calculated Φ(r sqd)	r	Observed Φ(r sqd)	Calculated Φ(r sqd)
1.9166	1462.268	1521.283	18.4166	4028.606	4312.446
2.4166	2656.474	2546.976	18.9166	4017.003	3975.089
2.9166	3720.237	3609.522	19.4166	3739.523	3697.852
3.4166	4591.506	4636.829	19.9166	3407.313	3484.699
3.9166	5741.471	5672.977	20.4166	3276.291	3216.954
4.4166	6996.267	7106.373	20.9166	2808.026	3026.962
4.9166	8363.531	8201.171	21.4166	3122.157	2836.678
5.4166	9327.633	9098.436	21.9166	2532.870	2645.092
5.9166	10594.406	10384.962	22.4166	2512.043	2486.401
6.4166	10454.495	10809.527	22.9166	2599.256	2301.942
6.9166	11340.553	11447.817	23.4166	2284.337	2183.174
7.4166	11316.872	11789.703	23.9166	2125.223	2033.652
7.9166	11518.268	11833.674	24.4166	1714.376	1909.009
8.4166	11525.707	11786.136	24.9166	1596.744	1791.937
8.9166	11695.786	11760.351	25.4166	1764.667	1677.174
9.4166	11075.764	11575.129	25.9166	1483.389	1581.493
9.9166	11458.934	11223.378	26.4166	1304.164	1472.694
10.4166	11336.561	10920.601	26.9166	1433.667	1388.597
10.9166	10537.854	10336.457	27.4166	1264.656	1294.035
11.4166	10436.030	9968.443	27.9166	1407.204	1208.910
11.9166	9807.700	9526.764	28.4166	1134.853	1127.060
12.4166	9394.073	9196.418	29.4166	1076.591	981.778
12.9166	9235.225	8716.648	30.4166	981.494	876.152
13.4166	8425.230	8237.215	31.4166	842.932	758.158
13.9166	7646.172	7728.679	32.4166	657.970	664.963
14.4166	7134.125	7291.027	33.4166	624.474	586.122
14.9166	7079.744	6821.024	34.4166	484.888	519.084
15.4166	6640.007	6392.481	35.4166	421.129	458.876
15.9166	5854.085	5886.645	36.4166	419.729	397.256
16.4166	5271.820	5562.637	37.4166	437.898	355.085
16.9166	5362.945	5187.899	38.4166	235.926	314.339
17.4166	4448.985	4788.629	39.4166	362.921	273.249
17.9166	4627.585	4560.188	40.4166	247.916	241.551

TABLE (A.T.7.2)
Parameter values for indium from programme 'PARSTA', (set 2).

Parameters		
Name	Value	Std. Dev.
'A_s'	.1292500E+04	.3554041E+02
'C_s'	.1497424E-01	.2098456E-03

TABLE (A.T.7.3)
Parameter values for indium from programme 'EVALPA', (set 2).

'A_m'	.3386137E+03	.7773694E+02
'B_m'	.6852681E+05	.8328140E+04
'C_m'	.1292693E-01	.6639482E-03
'f_m'	.1350567E+00	.6215191E-02

TABLE (A.T.7.4)
Parameter values for indium from programme 'PARLIN', (set 2).

'B_E'	.1152169E+06	.1407610E+05
'f_E'	.1519395E+00	.5351286E-02